FLUORESCENT MOLECULAR SENSORS BASED ON PHOTO-RESPONSIVE MODIFIED β-CYCLODEXTRIN AND CROWN ETHERS FOR DETECTING ORGANIC MOLECULES AND METAL IONS IN WATER

By

PHENDUKANI NCUBE

Thesis in fulfilment of the requirement for the degree

PHILOSOPHIAE DOCTOR

In

CHEMISTRY

In the

FACULTY OF SCIENCE

Of the

UNIVERSITY OF JOHANNESBURG

Supervisor	**:**	**PROF Rui W.M. KRAUSE**
Co-supervisor	**:**	**PROF Bhekie B. MAMBA**

DECLARATION

UNIVERSITY
OF
JOHANNESBURG

AFFIDAVIT: MASTER AND DOCTORAL STUDENTS
TO WHOM IT MAY CONCERN

This serves to confirm that I____
Full Name(s) and Surname

ID Number/
Passport____

Student number____________________________________ enrolled for the Qualification

____

in the Faculty of Science

Herewith declare that my academic work is in line with the Plagiarism Policy of the University of Johannesburg with which I am familiar.

I further declare that the work presented in the _______________________________(minor dissertation/dissertation/thesis) is authentic and original unless clearly indicated otherwise and in such instances full reference to the source is acknowledged and I do not pretend to receive any credit for such acknowledged quotations, and that there is no copyright infringement in my work. I declare that no unethical research practices were used or material gained through dishonesty. I understand that plagiarism is a serious offence and that should I contravene the Plagiarism Policy notwithstanding signing this affidavit, I may be found guilty of a serious criminal offence (perjury) that would amongst other consequences compel the University of Johannesburg to inform all other tertiary institutions of the offence and to issue a corresponding certificate of reprehensible academic conduct to whomever requests such a certificate from the institution.

Signed at Johannesburg _____________ on this _______ of ___________________2013

Signature _____________________________ Print name _____________________

STAMP: COMMISSIONER OF OATHS
Affidavit certified by a Commissioner of Oaths
This affidavit conforms with the requirements of the JUSTICES OF THE PEACE AND COMMISSIONERS OF OATHS ACT 16 OF 1963 and the applicable Regulations published in the GG GNR 1258 of 21 July 1972; GN 903 of 10 July 1998; GN 109 of 2 February 2001 as amended.

DEDICATION

This work is dedicated to my son Ndumiso, so that he may be inspired to excel not only academically but in life in general.

PUBLICATIONS AND PRESENTATIONS

The work presented in this thesis has been presented both as oral and poster presentations at the following conferences. The work has also been either published or submitted to peer-reviewed journals.

Conference Presentations

- Ncube P., Krause R.W., Ndinteh D.T. and Mamba B.B. *Fluorescent Sensing and Determination of Mercury (II) Ions in Water.* 13th WaterNet/WARFSA/GWP-SA International Symposium on Integrated Water Resource Management. **Oral Presentation**. The Birchwood Hotel and OR Tambo Conference Centre, Johannesburg, South Africa. 31 October 2012 – 2 November 2012.

- Ncube P. Mamba B.B and RW Krause. *Selective Recognition of* Hg^{2+} *and* Cu^{2+} *ions in Water by a Fluorescent Naphthyl-azo Modified Dibenzo-18-Crown-6-Ether*. **Poster Presentation**. 2nd Regional Conference of the Southern African Young Water Professionals (YWPs). CSIR International Conversion Centre (ICC), Pretoria, South Africa, 3 – 5 July 2011.

- Ncube P. Mamba B.B and RW Krause. *Fluorescent Sensing of Chlorophenols in Water Using an Azo Dye Modified β-Cyclodextrin Polymer.* **Oral Presentation**. Third Annual DST/Mintek/NIC “Nanotechnology for Life” Workshop and Conference, University of the Western Cape, Bellville, Cape Town, South Africa. 23 November 2010.

- Ncube P. Mamba B.B and RW Krause. *Chromophore Modified Cyclodextrin Polymers for the Sensing of Pollutants in Water*. **Oral Presentation**. NIC/MINTEK Conference, MINTEK, Johannesburg. 30 July 2010.

Peer-reviewed Publications

- Ncube, P., Krause, R.W. and Mamba, B.B. (2011). Fluorescent sensing of chlorophenols in water using an azo dye -modified β-cyclodextrin polymer. *Sensors,* **11**, 4598-4608.

- Ncube, P., Krause R.W., Ndinteh, D.T. and Mamba B.B. (2013). Fluorescent sensing and determination of mercury (II) ions in water. *Water SA;* (Accepted), **In Press**.

- Ncube, P., Krause R.W. and Mamba B.B. (2013). Detection of chloroform in water using an azo dye-modified β-cyclodextrin – epichlorohydrin copolymer as a fluorescent probe. *Physics and Chemistry of the Earth*; (Accepted), **In Press**.

ACKNOWLEDGEMENTS

I am most grateful to all who contributed to the successful completion of this work. Most notably I wish to thank:

- My supervisors Prof. Rui W. M. Krause and Prof. Bhekie B. Mamba for their invaluable advice and support throughout my research work.
- The National Research Foundation (NRF) for financial support.
- The Faculty of Science and Department of Applied Chemistry for financial support and for the facilities for carrying out this work.
- My colleagues and friends in the 3314 Laboratory and other research groups.
- Laboratory staff in the Department of Applied Chemistry
- Dr Derek Ndinteh for his assistance during part of my research.
- Dr Raquel Vico, Prof. Bruno Magio and Dr Alejandro of Departmento de Quimica Biologica and Departmento de Quimica Organica at Universidad National de Cordoba (UNC) Conicet, Argentina. I would also like to thank other staff members and postgraduate students in both departments for their help during my stay in Cordoba.
- My family for the moral support throughout my studies.

Finally I wish to thank the Almighty God, with whom all things are possible.

ABSTRACT

The problem of maintaining good quality of water for domestic use and for aquatic life remains a challenge. Water sources are often contaminated with pollutants from natural sources such as volcanic eruptions and by human activities such as manufacturing industries, mining, water-purification processes, agricultural activities and a vast number of other activities. Water-purification processes used by municipal authorities are designed to remove most of the pollutants but some trace amounts will always remain and have been detected in drinking water and treated waste water reservoirs. These trace amounts pose a threat to human health and the well-being of aquatic life. The detection of these trace amounts of pollutants is often carried out by laboratory-based techniques that require sophisticated, expensive instruments and often require extensive sample preparation and pre-concentration. Simple, quick and in-field detection methods are necessary especially for remote small communities with limited or no access to laboratories. Optical detection systems offer hope as a solution to this problem.

In this work newly developed fluorescence-based molecular sensors for the detection of pollutants in water were developed, characterised and tested for their sensing abilities towards organic and inorganic pollutants. The fluorescent probes for organic pollutants were designed based on the host-guest chemistry of the cyclodextrin molecule. Azo dye-modified β-cyclodextrins were synthesised and linked via ethylene glycol and epichlorohydrin to produce the sensors that were then tested for their sensing response towards chlorophenols and small aliphatic chlorinated alkanes which are often formed during the disinfection of water in the purification process. The sensor molecules were characterised by UV-Vis, FT-IR and 1D and 2D NMR spectroscopy. The amount of cyclodextrin in each sensor molecule was quantified using the anthrone method (67%) as well as by ^{1}H-NMR spectroscopy (72%). To demonstrate the host-guest interaction of the sensor molecules, isothermal titration calorimetry (ITC) was used. ITC measurements showed that modifying β-cyclodextrin and using linkers did not alter its host-guest interaction with guest molecules as demonstrated by the stoichiometry, *n*, stability (or binding or association) constant (*K*) and thermodynamic parameters of the interaction.

The sensor molecule linked via ethylene glycol showed selectivity towards 4-chlorophenol among the chlorophenols investigated and has the potential to be used in a sensor for the detection of 4-chlorophenol. The sensor molecule linked via epichlorohydrin showed sensitivity towards chloroform, a typical disinfection by-product. These experimental results showed that the sensor molecules could be used for quick on-field detection of chlorinated organic compounds in water.

Sensor molecules for inorganic pollutants were based on the complex formation of crown ethers with metal ions. The sensor was formed by modifying a dibenzo-18-crown-6 ether molecule with an azo dye. The sensor was then characterised using UV-Vis spectrophotmetry, FT-IR and NMR spectroscopies as well as mass spectrometry and CHNS elemental analysis. The sensor molecule was then subjected to different metal ions and the fluorescence change of the probe observed. Interestingly, the sensor was highly sensitive and selective to mercury (II) and Cu (II) ions in water. Mercury (II) is one of the most hazardous heavy metals among the heavy-metal ions found in environmental waters and its early detection in water sources is important. The synthesised molecular sensor can therefore be incorporated into a simple hand-held gadget with a light source and be used for on-field detection of mercury (II) ions in remote areas.

TABLE OF CONTENTS

Section ***Page***

CHAPTER 4B FLUOROMETRIC SENSING OF CHLOROFORM IN WATER USING AN AZO DYE-MODIFIED β-CD – EPICHLOROHYDRIN POLYMER 93

LIST OF FIGURES AND SCHEMES

LIST OF TABLES

LIST OF ABBREVIATIONS

ATR	attenuated total reflectance
^{13}C-NMR	carbon13 - nuclear magnetic resonance
α-CD	alpha-cyclodextrin
β-CD	beta-cyclodextrin
γ-CD	gamma-cyclodextrin
COSY	correlation spectroscopy
DB18C6	dibenzo-18-crown-6 ether
DBPs	disinfection by-products
DWA	Department of Water Affairs
DWAF	Department of Water Affairs and Forestry
ΔG	Gibbs free energy change
ΔH	enthalpy change
ΔS	entropy change
EPA	Environmental Protection Agency
EPC	epichlorohydrin
ESI-MS	electrospray ionisation – mass spectrometry
FT-IR	Fourier transform infrared
^{1}H-NMR	proton - nuclear magnetic resonance

ICP-OES	inductively coupled plasma optical emission spectroscopy
ITC	isothermal titration calorimetry
IWRM	integrated water resource management
K	binding constant
NMR	nuclear magnetic resonance
PEG	poly (ethylene glycol)
PET	photo-induced electron transfer
ppm	parts per million
p-TsCl	para-toluene sulphonyl chloride
Ts_2O	para-toluene sulphonic anhydride
THMs	trihalomethanes
UV-Vis	ultraviolet-visible
WHO	World Health Organization

CHAPTER 1

INTRODUCTION

1.1 BACKGROUND

Water sources are often contaminated with pollutants from both organic and inorganic sources. Organic pollutants are produced by natural sources, industrial activities as well as during the water-purification process where chlorine and its compounds used for the disinfection of water reacts with natural organic matter (NOM) to give toxic disinfection by-products such as trihalomethanes, haloacetic acids and nitrosamines (Xie, 2004) all of which are associated with serious health effects. Agricultural activities also introduce organic pollutants into water sources by the use of pesticides and other chemicals. Most of these pollutants are carcinogenic (Lawrence et al., 1984; King and Marret, 1996), can cause cardiac problems, liver, kidney and cell DNA damage (Cedergren et al., 2002; Komaki et al., 2009). Industrial processes like mining, burning of fossil fuels for power generation and municipal wastewater treatment and landfill leachates release toxic metal species such as mercury and other heavy metals into water sources. These pollutants are harmful to both human and aquatic life because they are non-biodegradable and can accumulate in plants, animals and in humans.

Detection of these pollutants in water sources is an important step as a quick means of knowing their presence in water before and after a purification process. Detection before the purification process is useful in deciding on whether an additional or more rigorous step is needed to remove the pollutant if present in very high levels. After the purification process it is also important to ascertain whether the purification process was successful.

The application of cyclodextrins in the removal of organic pollutants has received attention because of their ability to form host-guest complexes with organic molecules (Mhlanga et al., 2007). Crown ethers are capable of forming host-guest complexes with metal ions. These two macrocyclic molecules were therefore chosen as recognition agents in the design of chemo-sensing probes for organic and inorganic pollutants.

Methods often used in the detection of pollutants in water include chromatographic techniques (like GC, HPLC and GC-MS) for organics and spectroscopic techniques (like ICP-OES and AAS), as well as electro-analytical techniques, for metal species. While these methods are well established and accurate, they often require significant sample preparation and expensive laboratory-based instruments. Recent analytical interest has been focused on optical methods such as fluorescence spectroscopy which offer alternative, rapid methods for both organic and metal-ion screening in the field.

1.2 PROBLEM STATEMENT

The reported research work was intended to design, synthesise and characterise photo-responsive materials based on modified cyclodextrin and crown-ether compounds. Such materials find applications not only as chemo- and biosensors but also in drug-delivery systems, optical data storage and many other applications. Chemo-sensors are important and are used in fields like water treatment for the sensing and extraction of pollutants from water. Materials that can sense molecules of biological importance are also of importance to current research. There has been ongoing work in the department on the removal of organic pollutants from water using cyclodextrin-based polymers (Mhlanga et al., 2007). A similar approach was used in this research work, exploiting the ability of cyclodextrins to form host-guest complexes with many organic molecules. In this work, instead of using native cyclodextrin, the cyclodextrins were modified with a fluorophore as a signalling unit in the detection of organic molecules. In addition, fluorophore modified crown-ether compounds were used for the detection of metal ions. The crown part is capable of forming host-guest complexes with metal cations and amines (and ammonium ions) with the fluorophore providing a means of signalling.

Sensing systems are often prone to poor selectivity and sensitivity. Through variations of crown ring size and polymer backbone, the research work intended to produce molecular sensors that are selective and sensitive to particular species. The use of linkers; epichlorohydrin and ethylene glycol to bring together individual sensor molecules was used to give versatile systems, capable of selectively sensing inorganic and organic pollutants in water. In addition the design and synthesis of these materials is important as their applications are not restricted to sensor application since their photo-responsive nature can be exploited for other applications such as drug delivery systems, optical data storage (Wang et al., 2008) and in linear and non-linear optics among a variety of other applications.

1.3 OBJECTIVES OF THE STUDY

The main aim of this research work was to design, synthesise, characterise and test fluorescent chemo-sensing materials based on cyclodextrin and crown ethers for the detection of organic and inorganic pollutants in drinking water and wastewater.

To achieve the aim of this work the following specific objectives were set:

- Synthesis and characterisation of azo dye-modified β-cyclodextrin (β-CD) as well as an azo dye-modified dibenzo-18-crown-6-ether.

- Polymerisation of the modified β-CD via ethylene glycol and epichlorohydrin linkers to form azo dye-modified β-CD polymers.

- Testing of the polymers for sensing properties towards model organic chlorinated compounds using fluorescence spectroscopy.

- Investigating the thermodynamics of host-guest interaction of the modified β-CD sensor materials with organic guests in comparison to native β-CD using isothermal titration calorimetry (ITC).

- Testing of the modified crown ether for sensing properties towards toxic heavy metals, particularly mercury (II) amongst other metals.

- Investigating the interference from other metal-ions commonly found in water sources on the sensing properties of the sensor molecule.

- Testing the efficacy of the molecular sensors on actual drinking water and waste-water samples.

1.4 OUTLINE OF THE THESIS

The thesis is presented in the following outline:

Chapter 1: Introduction

This first chapter gives an introduction of the research reported in this thesis. The reason why the work was done, its relevance and importance and the aims and the objectives are given in this chapter.

Chapter 2: Literature review

This chapter gives the background on cyclodextrins and crown ethers and their use in the design of fluorescent molecular chemo-sensors. The chapter reviews the work that has been done previously and relates this to the reported work.

Chapter 3: Experimental

The synthetic methods and characterisation techniques, as well as all analytical methods used in this work are described in this chapter.

Chapter 4: Results and discussion

In this chapter, the results of the synthesis, characterisation, and sensing ability of the molecular sensors towards organic and inorganic pollutants are given in detail. The chapter is divided into three sub-chapters, namely 4A, 4B and 4C. Chapters 4A and 4B deal with the detection of organic pollutants using β-CD-based molecular sensors prepared by linking azo dye-modified β-CD with ethylene glycol units (Chapter 4A) and the other by using epichlorohydrin (Chapter 4B). Chapter 4C deals with the detection of metal ions in water using a crown-ether-based molecular sensor.

Chapter 4A: Fluorometric sensing of chlorophenols in water using an azo dye-modified β-cyclodextrin polymer

This chapter presents work on the detection of chlorinated aromatic pollutants in water using azo dye-modified β-cyclodextrin polyethylene glycol (PEG) polymer. The modified β-CD was polymerised with PEG and characterised by various spectroscopic techniques. Its sensing ability was investigated for different chlorinated aromatic molecules as model organic pollutants in water. A paper on the work described in this chapter was published in the peer-reviewed journal *Sensors* in 2011 (Ncube et al., 2011)

Chapter 4B: Fluorometric sensing of chloroform in water using an azo dye-modified β-cyclodextrin - epichlorohydrin polymer

The fluorometric detection of small chlorinated aliphatic compounds is presented in this chapter. These compounds like chloroform are formed during the disinfection of water using chlorination and are referred to as disinfection by-products (DBPs). These DBPs pose serious health risks to humans as they are carcinogenic when ingested for prolonged periods. The fluorescent probe used for the detection of the DBPs was an azo dye – modified β-CD – epichlorohydrin copolymer. The probe was synthesised, characterised and tested for its sensing ability on spiked and real water samples. A paper on the work described in this chapter has been submitted for publication in the journal; *Physics and Chemistry of the Earth*, 2013.

Chapter 4C: Fluorometric detection of heavy metal ions in water dye-modified crown ethers

The fluorometric sensing of metal ions using dye-modified crown ethers is presented in this chapter. The focus was on heavy metal detection and determination as these often have adverse health effects when released into water sources. An azo dye-modified dibenzo-18-crown-6 (DB18C6) ether was found to be sensitive and selective towards mercury (II) ions in water. The dye-modified crown ether can potentially be used as a sensing probe for the heavy metal. Its efficacy was tested on actual water samples collected from near a power-generating plant where extensive burning of coal can lead to the release of mercury into water sources nearby. A paper based on the work described in this chapter has been submitted for publication in the journal *Water SA*, 2013.

Chapter 5: General conclusion and recommendations

This chapter presents a comprehensive conclusion based on all the work reported in the thesis. The chapter ends with suggestions for possible further work that can be done as a follow-up to the work covered in the thesis.

Appendices: The appendices give spectra, figures and tables that are not shown in the main body of the thesis.

REFERENCES

Cedergren, M.I., Selbing, A.J. Lofman, O. and Kallen, B.A.J. (2002). Chlorination by-products and nitrate in drinking water and risk for congenital cardiac defects. *Environ. Res.* **89**(2), 124-130.

King, W.D. and Marrett L.D. (1996) Case-control study of bladder cancer and chlorination by-products in treated water (Ontario, Canada). *Cancer Causes and Control* **7**, 596 – 604.

Komaki, Y., Pals, J., Wagner, E.D., Marinas, B.J. and Plewa, M.J. (2009). Mammalian cell DNA damage and repair kinetics of monohaloacetic acid drinking water disinfection by-products. *Environ. Sci. Technol.* **43**, 8437 – 8442.

Lawrence, C.E.; Taylor, P.R.; Trock, B.J. and Reilly, A.A. (1984). Trihalomethanes in drinking water and colorectal cancer. *J. National Cancer Institute* **72**, 563 – 568.

Mhlanga, S.D., Mamba, B.B., Krause, R.W. and Malefetse, T.J. (2007). Removal of organic contaminants from water using nanosponge cyclodextrin polyurethanes. *J. Chem. Tech. Biotech.* **82**, 382 – 388.

Ncube, P., Krause, R.W. and Mamba B.B. (2011**).** Fluorescent sensing of chlorophenols in water using an azo dye modified β-cyclodextrin polymer. *Sensors* **11**, 4598-4608.

Wang, S., Choi, M.-S. and Kim, S.-H. (2008). Bistable photoswitching in poly(N-isopropylacrylamide) with spironaphthoxazine hydrogel for optical data storage. *J. Photochem. Photobio. A: Chem.* **198**(2–3), 150-155.

Xie, Y.F. (2004). *Disinfection By-Products in Drinking Water: Formation, Analysis and Control*. Lewis Publishers: Florida, USA. pp 1 – 10.

CHAPTER 2

LITERATURE REVIEW

2.1 INTRODUCTION

In this chapter the literature, terminology and background forming the thrust of this research are explored. The concept of photo-responsive materials is discussed along with the fluorescence technique. The use of cyclodextrin as a macromolecule in host-guest chemistry is assessed from the literature point of view. Cyclodextrin polymers formed with co-monomers or linkers are described with reference to the scope of this work. Also the use of crown ethers and their derivatives in ion recognition is described in this chapter, with a particular focus on their application in the detection of metal ions in water.

2.2 PHOTO-RESPONSIVE MATERIALS

Stimuli-responsive systems are those that show a reversible or irreversible change in physical properties and/or chemical properties as a result of an external stimulus such as pH, temperature, light irradiation, mechanical forces, electrical and magnetic forces and specific analytes like metal ions and organic pollutants (Hu and Liu, 2010). Of the external stimuli, light has been widely used because it can easily be accessed, can be quickly switched and focused onto specific areas (Ercole et al., 2010; Liu et al., 2010), as well as the fact that light is non-invasive (Wondraczek et al., 2011). Light irradiation of photo-responsive materials results in changes in properties like conformation, shape, phase, wettability, permeability and solubility (Ercole et al., 2010). Due to their versatility, photo-responsive materials have found application in wide-ranging areas like sensors, linear and non-linear optics, controlled drug and gene delivery, bio-separation, protein purification, personal care, industrial coatings, membrane science and water remediation (Hu and Liu, 2010).

A range of photo-responsive molecules have been employed in the aforementioned materials. They include simple organic molecules like naphthalene, organic and inorganic dyes and quantum dots. Of the organic dyes used, those that exhibit photochromism have been widely used.

2.2.1 Photochromism

Photochromism is defined as a reversible transformation of a chemical species, induced in one or both directions by electromagnetic radiation, between two states having observable light absorptions in different regions of the spectrum (Crano, 2001). Classes of organic photochromic compounds include azobenzenes, spiropyrans, benzo- and naphthopyrans, spirooxazines, fulgides and arylethenes (**Scheme 2.1**) (Bouas-Laurent and Durr, 2001).

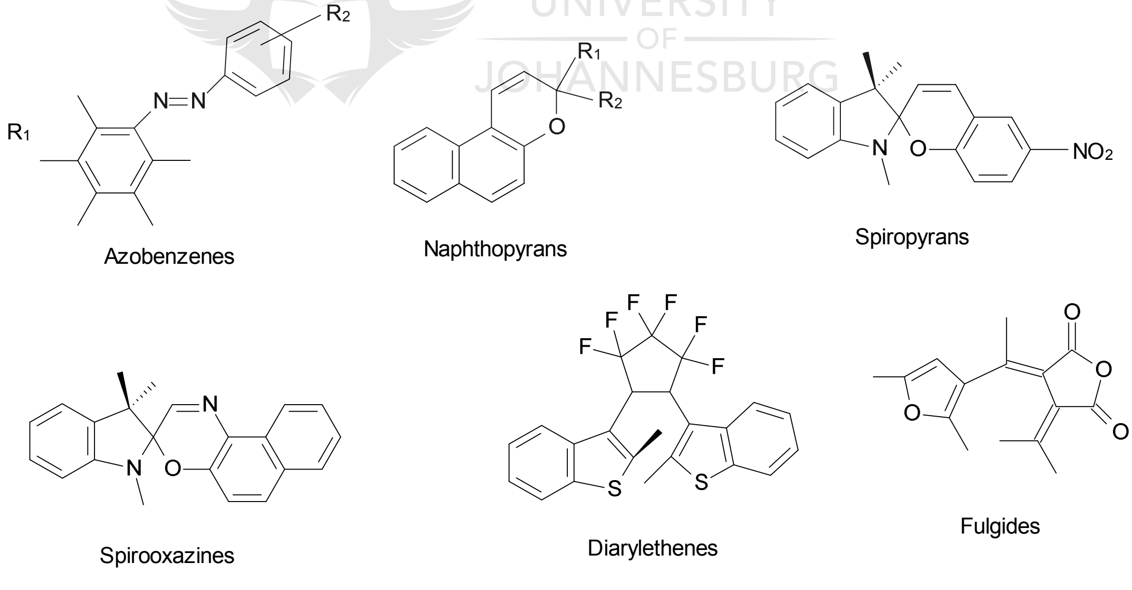

Scheme 2.1: Common classes of organic photochromic compounds

While classes like spiropyrans, spirooxazines and arylethenes have been widely investigated, not much work has been done on naphthopyrans. Azobenzene-containing systems are commonly used because of their ease of synthesis and remarkable conformational changes associated with their photochromic behaviour and have found useful applications in molecular machines, supramolecular polymers and drug-delivery materials (Liu et al., 2010).

Photochromism in naphthopyrans is due to the breaking of the carbon-oxygen bond of the pyran (**Scheme 2.2**). The trans-quinoidal open form (I) is the most stable and abundant species while the cis-quinoidal open form (II) is less stable. The zwitterionic open form (III) has been suggested but evidence of limited solvatochromism for the open form of the majority of naphthopyrans suggests this form not to be common (Van Gemert, 1999; Hepworth et al., 1999). Photochromism in azobenzenes is due to cis-trans isomerisation (Bouas-Laurent and Durr, 2001) (**Scheme 2.2**).

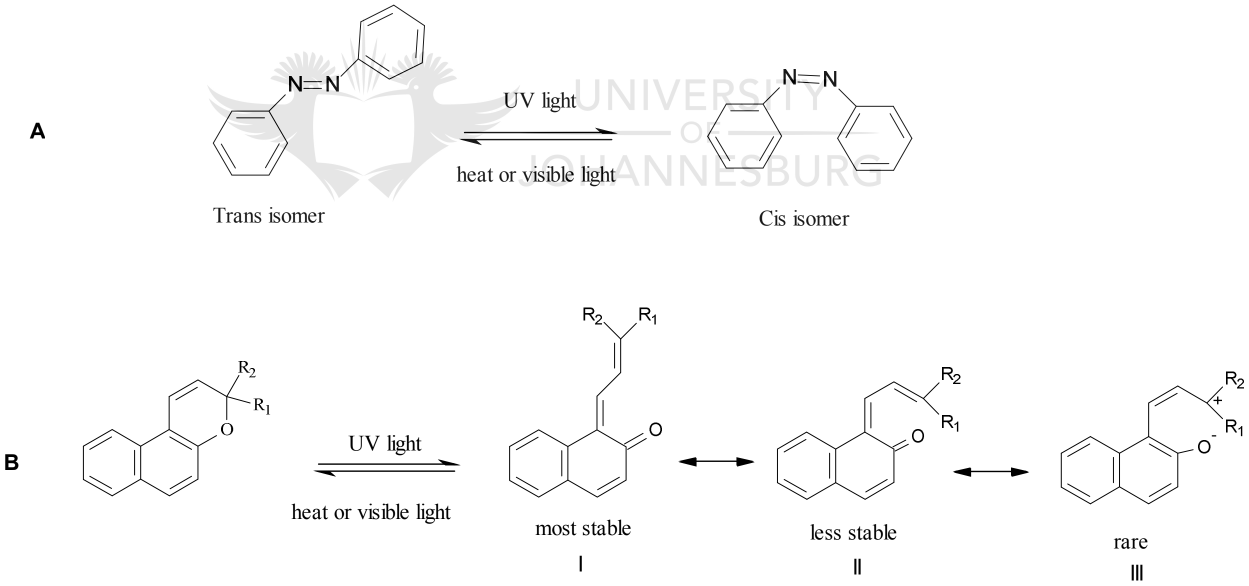

Scheme 2.2: Photochromic mechanism for azobenzenes (A) and naphthopyrans (B)

Applications of photochromic compounds are wide-ranging from ophthalmic lenses, camera filters, fluid flow visualisation, security printing inks and cosmetics to optoelectronic systems, reversible holographic systems, optical switches and sensors, photo-chemically switchable enzymatic systems and non-linear optical devices (Van Gemert, 1999). Recently, photochromic compounds responsive to organic and inorganic species have been investigated (Stauffer et al., 1997; Chernyshev et al., 2006; Han and Chen, 2011). These photo-responsive properties to external stimuli can be exploited for use in chemo-sensing materials.

For use in materials, photochromic compounds are often incorporated into polymer matrices (Nakao et al., 2002; Athanassiou et al., 2003) and recently, with the growing interest in nanotechnology, into nanoparticles (Allouche et al., 2010; Remy et al., 2011). Incorporation of these photochromic compounds into different materials alters their photochromic properties and the new properties can be exploited for different applications. Incorporation of these materials and investigating their properties for various applications is therefore important and was the scope of this work. The focus was on the synthesis of photo-responsive compounds containing cyclodextrins and crown ethers, incorporating these into polymeric matrices either covalently linked or physically embedded and then investigating the photo-responsive properties of these materials for applications in fluorescent molecular sensors.

2.3 FLUORESCENT MOLECULAR SENSORS

According to the International Union of Pure and Applied Chemistry (IUPAC) a molecular sensor is defined as ‘a device that transforms chemical information, ranging from the concentration of a specific sample to total composition analysis, into an analytically useful signal’ (Hulanicki et al., 1991). Chemical sensors are classified into optical, electrochemical, thermometric and gravimetric (mass sensitive). The focus of this study was on optical sensors as these have the advantages of being highly sensitive, selective, simple, low cost instruments and their fieldwork applicability (Valeur, 2001). These can further be divided into luminescence (fluorescence and phosphorescence), absorption, reflectance and light-scattering sensors (**Figure 2.1**).

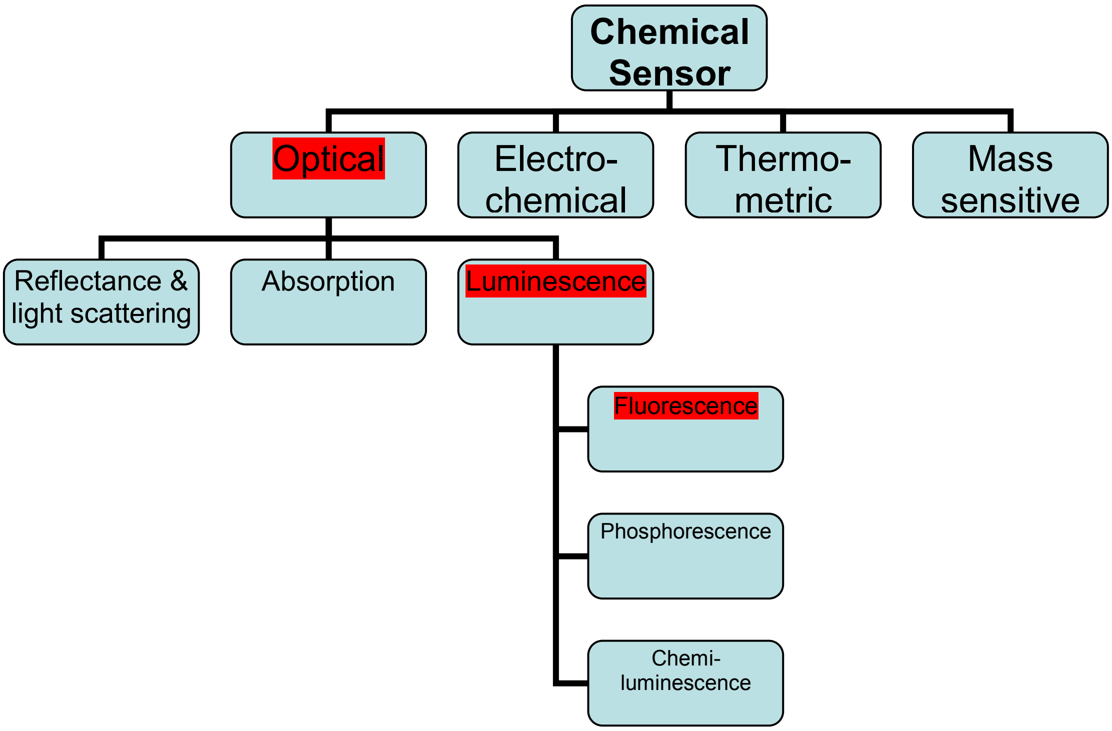

Figure 2.1: Classification of chemical sensors (Hulanicki et al., 1991)

The most widely used techniques in optical sensors are absorption and fluorescence. Analysis in optical sensors can be categorised as direct spectroscopic or reagent-mediated sensing. The latter is particularly important if an analyte has no optical property, for example a non-fluorescent analyte. In this case a change in optical response of an intermediate, usually an analyte-sensitive dye molecule, is used to monitor the analyte concentration (McDonagh et al., 2008).

Photo-responsive materials, including chemical sensing materials, often consist of a receptor part for molecular recognition of analyte and a signal unit, which could be a chromophore, fluorophore or a nanoparticle, for signalling the recognition event (**Figure 2.2**) (Basabe-Desmonts et al., 2007).

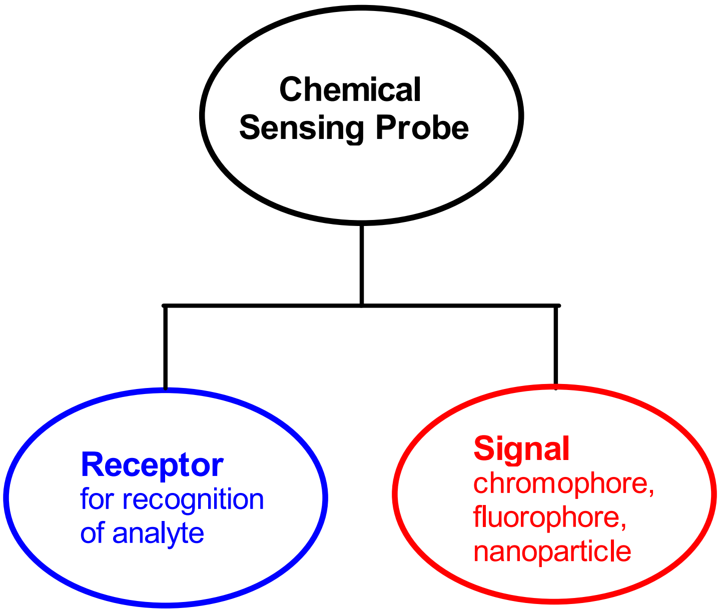

Figure 2.2: Components of a chemical sensing material (Basabe-Desmonts et al., 2007)

There are three ways in which fluorescent chemical sensors for ions and molecules are designed. The first case is when the fluorophore undergoes quenching upon collision with an analyte (**Figure 2.3 A**), the second is when the fluorophore has a receptor site where the analyte can reversibly bind (**Figure 2.3 B**), and the third case is when the fluorophore and the receptor part are linked either through a spacer **(Figure 2.3 C)** or integrated (**Figure 2.3 D**).

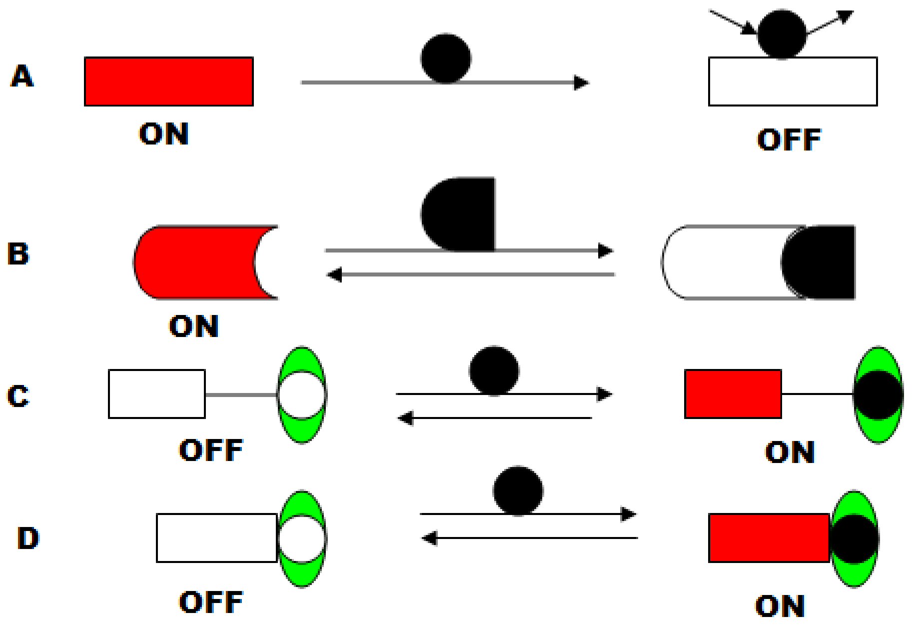

Figure 2.3: Illustration of different types of fluorescent probes

Changes in photo-physical properties of the fluorophore upon interaction with the bound analyte are due to the alteration of the photo-induced processes such as electron transfer or charge transport or energy transfer (Valeur, 2001).

2.3.1 The fluorescence technique: Theory

In luminescence sensing techniques, molecules are excited from the ground state to higher energy levels followed by release of the energy to lower levels by emitting radiation. Energy can also be released by non-radiative means via internal conversion (IC), intersystem crossing (ISC) and vibrational relaxations (**Figure 2.4**). Fluorescence is when the energy transition is between states of the same spin S1 → S0 (spin-allowed transition) and is therefore very fast while phosphorescence is a spin-forbidden transition (T1 → S0) and therefore, a slow process (Valeur, 2001).

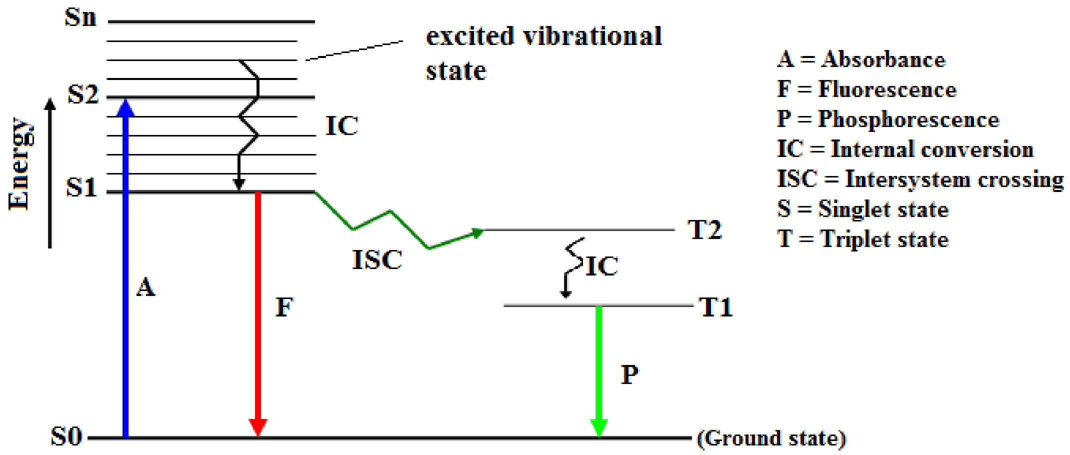

Figure 2.4: Jablonski diagram

Luminescence sensing techniques, particularly fluorescence, have received great attention (McDonaugh et al., 2008; Ogoshi and Harada, 2008) as analytical techniques because of various advantages. They are highly sensitive, fast, selective, and non-destructive to analyte, require no reference, are easily miniaturised and automated and are easily adapted for fieldwork analyses (Valeur, 2001). However, production of these fluorescent-based sensors has been limited because the implementation of the sensing probes into devices without loss of sensitivity is difficult. It therefore remains a challenge to design sensing probes that are incorporated into materials to avoid this loss of sensitivity. This work therefore sought to design such sensing materials by covalently attaching the photo-responsive dye onto β-CD and crown ethers as the receptor part.

By appropriate selection of the receptor part, sensing probes capable of selectively responding to particular molecules can be achieved. In our work we chose to use β-CD and crown ethers. Cyclodextrins can form inclusion complexes with various organic molecules and after modification can be specific to molecules of interest. Crown ethers, on the hand are known to complex with metal ions and can also be selective depending on the size and substituents. Photo-responsive materials were therefore designed based on β-cyclodextrin and crown ethers modified with azobenzenes and naphthopyrans as signalling units. These were then incorporated into various polymer matrices, characterised by appropriate techniques and tested for their photo-responsive properties for sensing properties

.

2.3.2 Stern-Volmer kinetics (Valeur, 2001)

The main photo-physical processes responsible for fluorescence quenching are summarised in **Scheme 2.3**. A molecule *M*, is excited to an excited-state *M**, by absorption of light (hv) and can be quenched by a quencher *Q*.

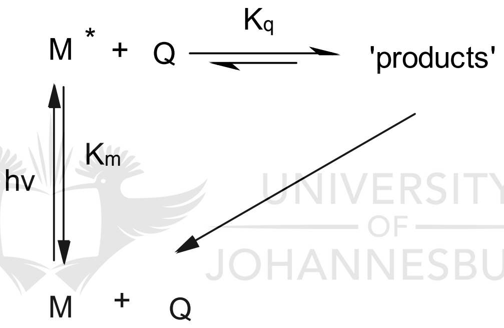

Scheme 2.3: Photo-physical properties responsible for fluorescence quenching

Where: $K_m = 1/\tau_o$, τ_o = excited-state lifetime, K_q = the Stern-Volmer rate constant.

The experimental quenching rate constant K_q is assumed to be time-independent. The time evolution of the concentration of the excited state obeys the following:

$$d[M^*] / dt = -(K_M + Kq[Q]) [M^*] = -(1/\tau_o + Kq[Q]) [M^*] \quad \textbf{1}$$

Integrating with [M*] = [M*] at t = 0 gives,

$$[M^*] = [M^*]_o\exp\{-(1/\tau_o + Kq[Q])t\} \quad \textbf{2}$$

The fluorescence intensity I α [M*] and is given by:

$$i(t) = K_r[M^*] \quad = K_r[M^*]_o \exp\{-(1/\tau_o + Kq[Q])t\}$$
$$= i(0) \exp\{-(1/\tau_o + Kq[Q])t\} \text{ ……….……………… } \mathbf{3}$$

Where:

K_r is the radiative rate constant of M^*

The fluorescence decay is thus a single exponential whose time constant τ is:

$$\tau = 1 / 1/\tau_o + Kq[Q] = \tau_o / \{1 + Kq\tau_o[Q]\}, \text{ then}$$

$$\tau_o / \tau = 1 + Kq\tau_o[Q] \text{ ………..…………………………. } \mathbf{4}$$

Time resolved experiments in the absence and presence of a quencher can then be used to check whether the fluorescence decay is a single exponential and provide directly the value of K_q. The fluorescence quantum yield Φ in the presence of a quencher is given by:

$$\Phi = K_r / \{1/\tau_o + Kq[Q]\} \text{ ……………………………….. } \mathbf{5}$$

In the absence of a quencher the quantum yield is given by:

$$\Phi_o = K_r\tau o \text{ ……………………………………………. } \mathbf{6}$$

This gives the Stern-Volmer relation:

$$\Phi_o / \Phi = I_o / I = 1 + Kq\tau_o[Q] = K_{sv}[Q] \text{ …………….. } \mathbf{7}$$

where:

I_o and I are the steady-state fluorescence intensities in the absence and presence of quencher, respectively

$K_{sv} = Kq\tau_o$ is the Stern-Volmer constant

A plot of I_o/I vs. $[Q]$ is the Stern-Volmer plot, and if linear, the slope gives K_{sv} and K_q can then be calculated if the excited-state lifetime in the absence of quencher is known.

Fluorescence quenching is often due to photo-induced electron transfer (PET) which is involved in many organic photochemical reactions. PET plays a role in photosynthesis and in artificial systems for conversion of solar energy based on photo-induced charge separation.

2.3.3 Photo-induced electron transfer (PET) systems

The application of photo-induced electron transfer (PET) systems in the development of fluorescence sensors and switches was only started about three decades ago. Fluorescence PET signalling systems have a natural 'all or none' switchability which results in guest-induced 'off-on' and 'on-off' fluorescence switching (De Silva et al., 1997). In 'on-off systems', such as those reported in this work, binding of guest molecules triggers electron transfer to or away from it or both depending upon its redox potentials as compared to those of the fluorophore, with both transfers resulting in 'on-off' switching of fluorescence (**Figure 2.5**).

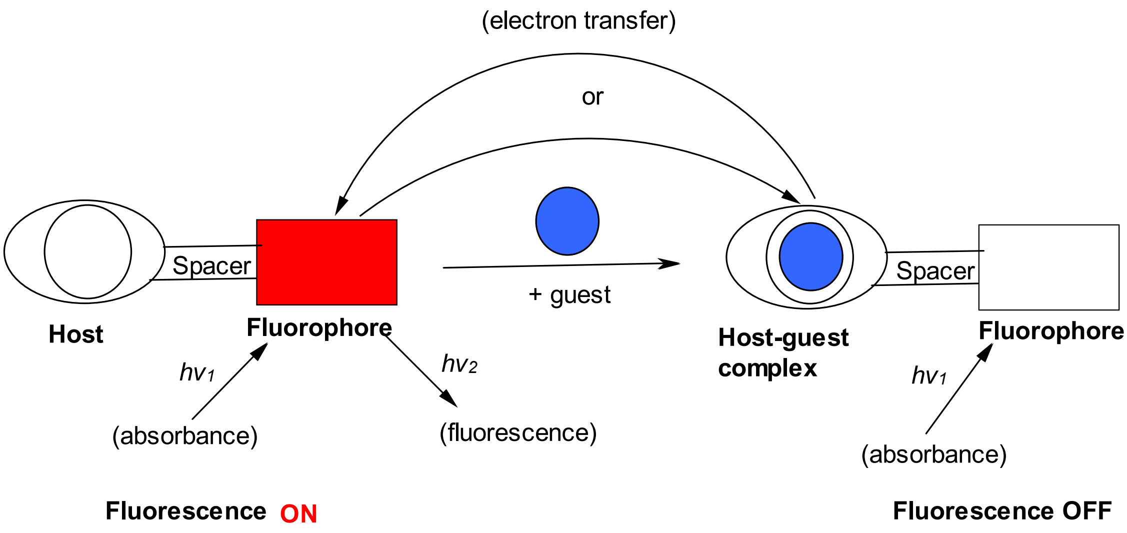

Figure 2.5: Fluorescent PET 'on-off' switching of fluorophore (De Silva et al., 1997)

The selection of the host depends on the target analyte guest molecule and the effect on the behaviour of the fluorophore will depend on a number of factors including the nature of guest, pH, and solvent used. In this work two host molecules where chosen, namely β-cyclodextrin (**Section 2.4**) for organic guests and crown ethers (**Section 2.5**) for metal-ion guests. The fluorophore chosen for both was the naphthyl azo group because of the versatility of azo derivatives, discussed in **Sections 2.2.1, 2.4.2.1 and 2.5.2**.

2.4 CYCLODEXTRINS

Cyclodextrins (CDs) are cyclic oligosaccharides made up of D-glucopyranose units linked by α (1 → 4) bond. They are naturally occurring being produced by the enzymatic action on starch. The most common have six, seven, and eight repeat glucose units and are named α, β and γ cyclodextrins, respectively (Ogoshi and Harada, 2008). Cyclodextrins have been widely used as macrocyclic hosts in various applications because they are inexpensive, commercially available, and non-toxic, easily functionalised and are water-soluble natural products. They have bucket-like structures with a hydrophobic interior and free primary hydroxyl groups on the narrow cavity side and secondary hydroxyl groups on the wider cavity side (**Figure 2.6**). The hydrophobic micro-environment in the cavity enables CDs to form host-guest inclusion complexes with hydrophobic guest molecules in aqueous media. β-CD was used for this research work and its structure is shown in **Figure 2.6**.

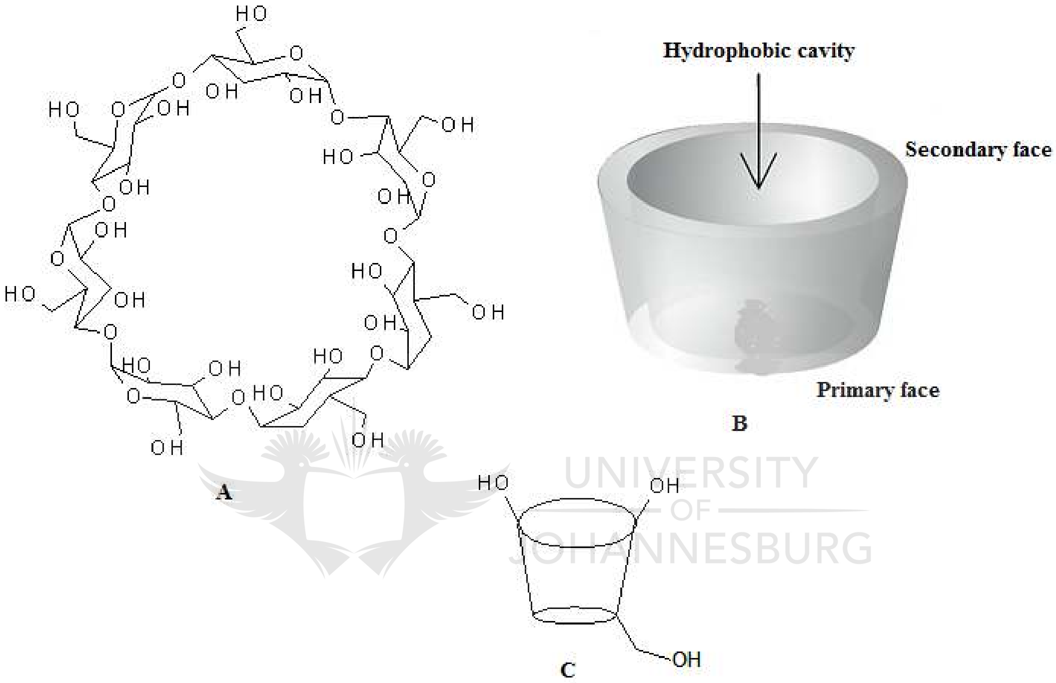

Figure 2.6: Structure of β-cyclodextrin (A), its representation showing the bucket-like structure (B) and a simplified representation (C)

The diameter of the CD cavity increases with the increase in number of glucose units, therefore, α-CD has the smallest diameter (4.7 Å to 5.2 Å), then β-CD (6.0 Å to 6.4 Å), and the largest is γ-CD (7.5 Å to 8.3 Å). Table 2.1 below summarises some properties of cyclodextrins. The size of β-CD makes it suitable to accommodate benzene and naphthyl groups (Ogoshi and Harada, 2008).

Table 2.1: Selected properties of cyclodextrins (Ogoshi and Harada, 2008)

	α-CD	β-CD	γ-CD
Glucose units	6	7	8
Molecular weight	972.86	1 135.01	1 297.15
Water solubility (g/ℓ)	145	18.5	232
Internal diameter (Å)	4.7 – 5.2	6.0 – 6.4	7.5 – 8.3
Depth of cavity (Å)	6.7	7.0	7.0
Cavity volume ($Å^3$)	176	346	510

The ability of cyclodextrins to form host-guest inclusion complexes is the basis for their application. They are able to pick up hydrophobic molecules from solution to form these inclusion complexes. The binding of guests in these inclusion complexes can be evaluated in terms of binding constants and thermodynamic parameters. One technique that is capable of directly measuring all these quantities, including the stoichiometry of the inclusion complex, is isothermal titration calorimetry (ITC).

2.4.1 Studies of binding of guest molecules to CDs by ITC

Isothermal titration calorimetry (ITC) is a technique based on the measurement of the heat generated or absorbed when two molecules interact (Bouchemal and Mazzaferro, 2012). ITC is used to show whether an interaction process occurs between the molecules involved and allows the evaluation of stability (or binding or association) constant (*K*) and thermodynamic parameters as well as the stoichiometry (*n*) of the interaction. Among other methods used to determine these parameters like NMR, fluorescence, potentiometry, and chromatographic techniques, ITC is the most sensitive, capable of determining low and high affinity associations.

ITC has been widely used for the characterisation of interactions between cyclodextrins (CD) and various guests. The parameters determined by ITC are important in understanding the phenomena of molecular recognition in CD-based systems like sensors. In ITC measurements the raw data obtained are processed by fitting into an appropriate non-linear curve fitting model which gives directly the stoichiometry (n), binding constant (K), the enthalpy change (ΔH) and the entropy change (ΔS) of the interaction. The Gibbs free energy, ΔG is then calculated from:

$$\Delta G = \Delta H - T\Delta S \quad \textbf{8}$$

where:

T is the reaction temperature

For cyclodextrins to be specific and more selective towards particular guests, they are often modified with various groups. These groups can be photo-active thereby giving photo-responsive cyclodextrins.

2.4.2 Modification of cyclodextrins

Since CDs have free hydroxyl groups both on the primary and secondary faces, they can easily be functionalised. A common approach is to first replace the hydroxyl group with a good leaving group like a tosylate, followed by displacement with a group of interest (Casas-Solvas et al., 2008) (**Scheme 2.4**).

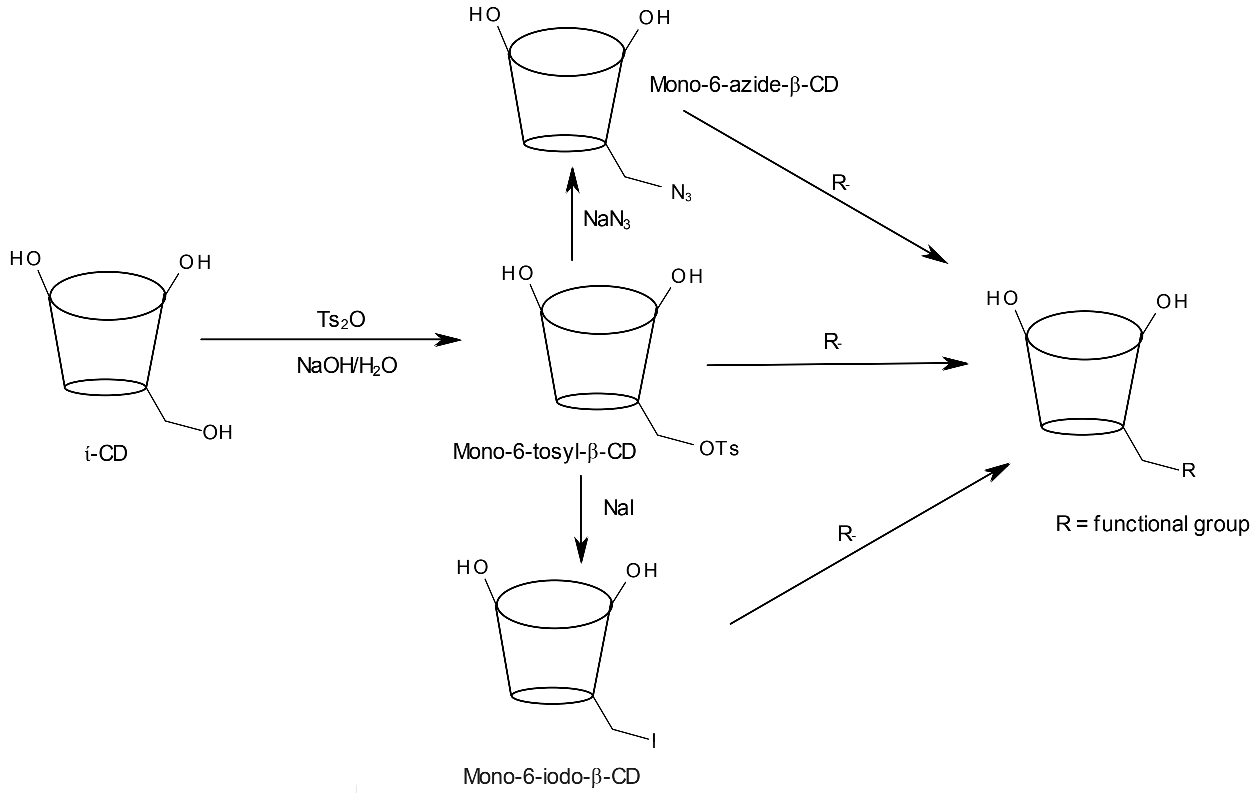

Scheme 2.4: Modification of cyclodextrins

The R group can be chosen such that inclusion of a guest is controlled through external stimuli. The attached R group responds to the external stimulus like pH, metallic cations, electrochemical signals or light. Those that respond to light give rise to photo-responsive materials for use in various applications including pharmaceutical and biomedical areas (Van de Manakker et al., 2009), sensors (Ogoshi and Harada, 2008), as well as in liquid crystal displays (Petr and Hammond, 2011), among various other applications.

2.4.3 Cyclodextrin polymers

Cyclodextrins and their derivatives are easily co-polymerised with bi-functional linkers to give a variety of polymers. Most commonly used linkers to obtain insoluble polymers are the diisocyanates. Hexamethylene diisocyanate (HMDI)

(Salipira, 2008), tolylene-2,4-diisocyanate (TDI) (Kyzas, 2013), phenylene diisocyanates (PDI) and methylene diisocyanate are a few examples of compounds that have been used to give polyurethane CD polymers.

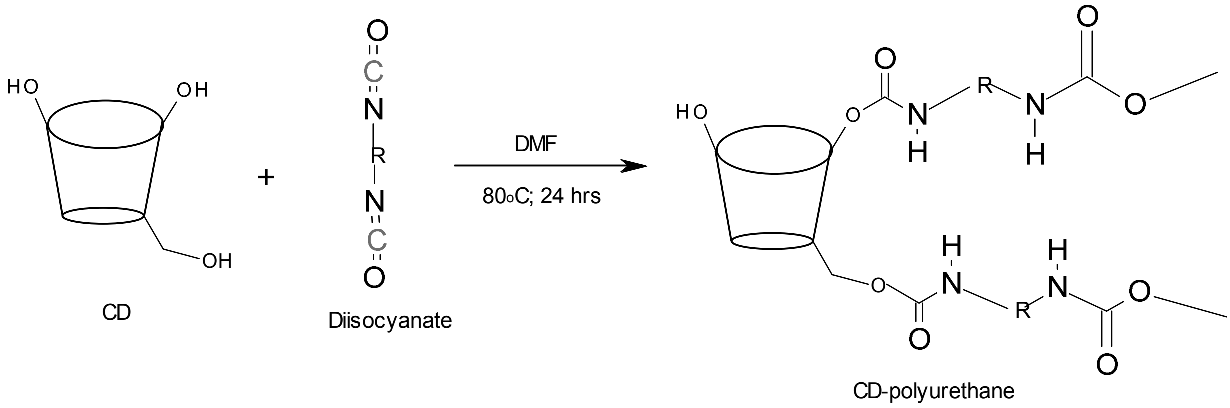

Scheme 2.5: Polymerisation of CDs with diisocyanates

Other linkers that have been used include acid anhydrides like maleic and succinic anhydrides (Girek, 2000; 2005), as well as dichlorides (Guan et al., 2009) and epichlorohydrin (Renard et al., 1997; Morin-Crini and Crini, 2013).

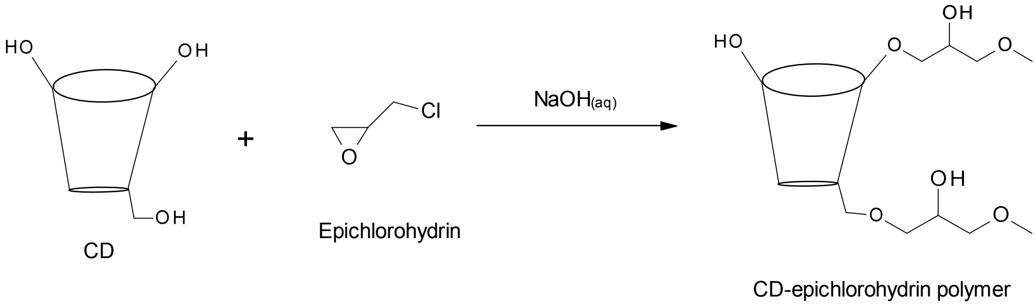

Scheme 2.6: Polymerisation of CDs with epichlorohydrin

The properties of the polymers formed often depend on the ratio of CD to the linker used. More of the linker results in extensive cross-linking giving rigid, insoluble polymers while less of the linker results in less cross-linking and more soluble polymers.

2.4.3.1 Photo-responsive cyclodextrin polymers

Using linkers mentioned in **Section 2.4.2** above and other strategies, CDs and their derivatives have been used as building blocks for the development of a wide variety of polymeric networks and assemblies. In these polymeric materials the CDs are either chemically cross-linked, as in examples above, or physically assembled. The resulting materials have unique mechanical properties, controllable drug-release characteristics as well as stimuli-responsiveness, which was the focus of this research work.

The azobenzene unit (**Section 2.2.1** and **Scheme 2.2**) is one of the most popularly used photo-active moieties in cyclodextrin-based photo-responsive materials (Hamon et al., 2009). The reason for this is the photochromic properties of the azobenzene, and the fact that the trans-isomer binds strongly to α- and β-CD, while the cis-isomer cannot bind or binds very weakly (Chen and Jiang, 2011). As a result of this phenomenon, many photo-responsive materials based on the azobenzene-CD system have been designed. Zou et al. (2007) prepared an inclusion complex of CDs with azobenzene which was photo-switchable from being hydrophobic to being amphiphilic by UV irradiation. The same workers again synthesised a polymeric amphiphile made of β-CD-PNIPAM as the hydrophobic part and azobenzene dendron as the hydrophilic part. Vesicles formed in aqueous solution were changed into solid spheres under UV irradiation and switched back to vesicles under visible light (Zou et al., 2009). Similar photo-switching was observed by Wang et al. (2007) in an amphiphile with a hydrocarbon chain and azobenzene ends. On making thin films containing azobenzene derivatives intercalated with a hydroxide, the films again showed photo-responsive properties (Wang et al., 2010). This allows for application of these materials in the desired areas, as they show the same photo-responsiveness in various environments and forms.

Photo-responsive sol-gel and gel-sol transitions have also been widely exploited using a variety of materials (Liao et al., 2010). A photo-responsive hydrogel system consisting of CD, dodecyl modified poly(acrylic acid) and an azobenzene guest was prepared by Tomatsu and co-workers (2005). On UV irradiation the azobenzene changed from trans- to cis-form and the mixture changed from gel to sol and this transition was reversed by visible light irradiation. A variety of other classes of photochromic dyes have been used in photo-responsive materials in conjunction with cyclodextrins. Stilbene-modified cyclodextrins were synthesised and their photo-stimuli responsiveness investigated by Kanaya and co-workers (2010).

2.4.3.2 Cyclodextrin-based fluorescent sensors for organic compounds

Molecular fluorescence-based detection of non-fluorescent organics has been achieved by using host-guest chemistry (Valeur, 2002) with cyclodextrin (CD)-based sensing systems having the CD act as a host for organic guest molecules (Nakashima and Yoshida, 2006; Wang and Ueno, 2000). The CD molecule is often modified with a fluorescent moiety whose fluorescence is either enhanced (Voronina et al., 2011) or quenched (Zohrehvand and Evans, 2005; Becuwe et al., 2008) depending on the nature of the guest organic molecule in the CD.

Analysis of these chlorinated organic compounds has been traditionally done by gas chromatography (GC) either by direct injection or adsorption on an activated adsorbent followed by desorption by solvent extraction prior to injection into the GC (WHO, 2004). Other methods, for example, electrochemical impedance spectroscopy, have also been employed in their detection (Carvalho et al., 2007). These methods, although well established and accurate, are often tedious and require expensive laboratory-based instruments. It is therefore important to design simple and direct methods for the detection and quantification of chlorinated organics; fluorescence spectrometry offers a simpler method in this regard.

2.5 CROWN-ETHER CONTAINING MATERIALS

2.5.1 Crown ethers

Crown ethers are cyclic chemical compounds consisting of several ether groups, which were discovered by Pederson (1967). Since their discovery several forms have been synthesised to give a variety of crowned compounds like azacrown and thiacrown ethers (**Scheme 2.7**).

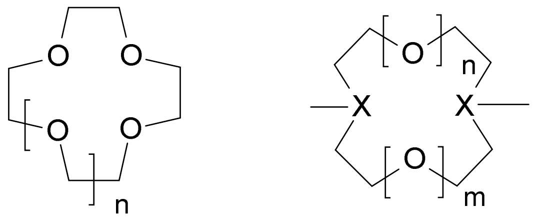

1 **2**

n and m = 1 to 10

X = N, S

Figure 2.7: Crown-ether compounds

Crown-ether compounds are known to be the most effective chelating ligands for metal cations and cationic organic species like amines (Shinkai, 2001). This complex-forming ability is a result of the fact that the cavity of crown ethers is electron rich because of the lone pairs of electron on oxygen, nitrogen and sulphur atoms. Depending on the cavity size and ion size, crown ethers can selectively complex with particular species. A system of naming crown ethers that is widely accepted is in the form; x-crown-y ether, where x is the ring size and y is the number of oxygen atoms. Examples are given in **Scheme 2.8**.

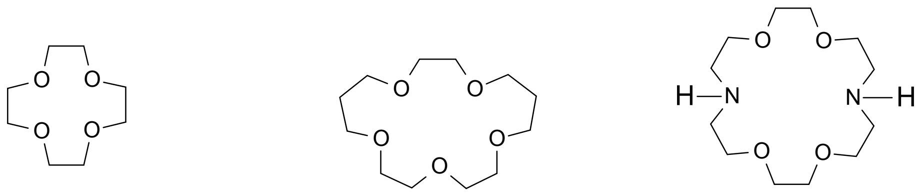

12-crown-4 ether 17-crown-5 ether diaza-18-crown-6

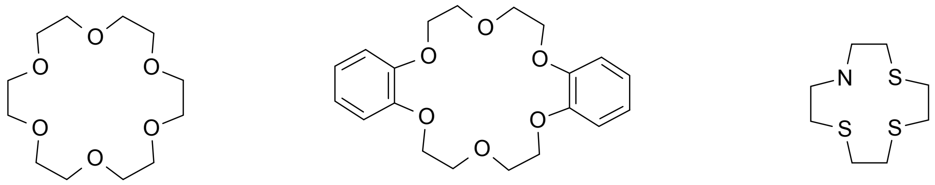

18-crown-6 ether Dibenzo-18-crown-6 ether monoazatrithia-12-crown-4 ether

Figure 2.8: Examples of crown-ether compounds

2.5.2 Photo-responsive crown ethers

Crown-ether containing materials that are photo-responsive have received much attention for a long time now because of their versatility in terms of application. In their series of work dating back to the 1980s Shinkai and co-workers (1980) synthesised several photo-responsive crown ethers. Examples are given in **Scheme 2.9**.

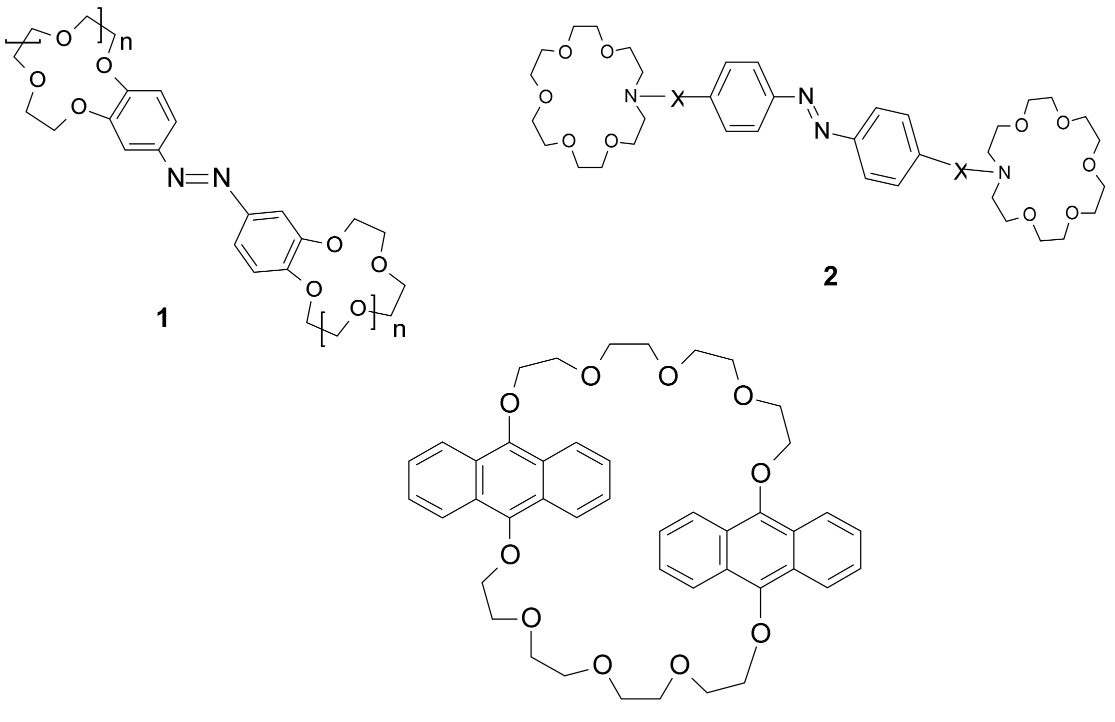

1

2

3

Figure 2.9: Examples of photo-responsive crown-ether compounds

As with cyclodextrin-based photo-responsive materials (**Section 2.4**), the azobenzene moiety finds great use in crown-ether-based materials, as seen in example compounds 1 and 2 (**Scheme 2.9**). Azobenzene derivatives exhibit photo-induced cis-trans isomerism followed by a considerable structural change. As a result azobenzene-containing compounds are controlled by these photo-induced configurational changes resulting in varying chemical applications (Shinkai et al., 1980).

Azo dye-modified photo-responsive compounds include a bis(crown ether) (Shinkai et al., 1981), an azo bis(benzocrown ether) (Shinkai et al., 1982a) and a benzo-18-crown-6 ether (Shinkai et al., 1982b). All these compounds were ionophores, responsive to the presence of alkali metal cations, and all showing enhancement of the cis-isomer. Incorporation of these compounds in polymers has also been investigated. Solution properties of complexes of an azo(benzo-18-

crown-6 ether) and polymethylene diammonio cations [$H_3N^+(CH_2)NH_3^+$] have been investigated and the results showed the complex formation through various techniques (Shinkai et al., 1988). The crown moiety has also been made part of a polymer chain as in the work done by Shinkai et al. (1983) where azobenzenophane-type crown ethers were linked by a polyoxyethylene chain. Polymers containing crown ethers formed by self-assembly have also been reported in the literature recently (Niu et al., 2011). The crown ethers also showed the reversible trans-cis isomerisation on irradiation with UV light and also alkali metal cations interacted with the cis-isomer.

2.5.2.1 Photo-responsive crown ethers as fluorescence sensors

Crown-ether-based ionophores have been used extensively in fluorescence sensing of metal ions and other positively charged species of biological importance (Gokel, 2004). These ionophores where initially used for the signalling of alkali metal ions (De Silva and De Silva, 1986; De Beer and Dent, 1988) and for signalling the brain neurotransmitter [gamma]-aminobutyric acid (GABA) (De Silva et al., 1996). Over the years, variation of the crown-ether moiety, spacer and fluorophore has resulted in fluorescence sensors for various metal ions, including the heavy metals which are hazardous to the health of humans, animals and the environment.

Fluorescent sensors for Cu^{2+} (Chen et al., 2009; Hsieh et al., 2009), for Hg^{2+} (Yari and Papi, 2009; Du et al., 2012; Lee et al., 2012; Ermakova et al., 2013) for Pb^{2+} (Thakur et al., 2013; Neupane et al., 2013), for Zn^{2+} (Basa and Sykes, 2012) and for inorganic As(III) (Ezeh and Harrop, 2013) have been designed and used to detect these heavy metals at levels comparable to well-established methods of metal-ion determination like inductively coupled plasma optical emission spectroscopy (ICP-OES) and atomic absorption spectroscopy (AAS). The continued research into these new fluorescent molecular sensors remains essential to improve on their efficacy, selectivity and ease of incorporation into gadgets for field-work applications.

2.6 REFERENCES

Allouche, J., Beulze A.L., Dupin J.-C., Ledeuil, J.-L., Blanc, S. and Gonbeau, D. (2010). Hybrid spiropyran-silica nanoparticles with a core shell structure: sol-gel synthesis and photochromic properties. *J. Mater. Chem*. **20**, 9370-9378.

Athanassiou, A., Lakiotaki, K.; Tornari, V.; Georgiou, S. and Fotakis, C. (2003) Photocontrolled mechanical phenomena in photochromic doped polymeric systems. *Appl. Phys. A.* **76**, 97-100.

Basa, P.N. and Sykes, A.G. (2012). Differential sensing of Zn(II) and Cu(II) via two independent mechanisms. *J. Org. Chem.* **77**(19), 8428-8434.

Basabe-Desmonts, L., Reinhoudt, D.N. and Crego-Calama, M. (2007). Design of fluorescent materials for chemical sensing. *Chem. Soc. Rev.* **36**(6), 993-1017.

Becuwe, M., Landy, D., Delattre, F., Czier, F. and Fourmentin, S. (2008). Fluorescent indolizine-β-cyclodextrin derivatives for the detection of volatile organic compounds. *Sensors* **8**, 3689-3705.

Bouas-Laurent, H. and Dürr**,** H. (2001). Organic photochromism (IUPAC Technical Report). *Pure Appl. Chem*. **73**(4), 639-665**.**

Bouchemal, K. and Mazzaferro, S. (2012). How to conduct and interpret ITC experiments accurately for cyclodextrin-guest interactions. *Drug Discovery Today*, **17**(11-12), 1 - 7.

Casas-Solvas, J.M., Martos-Maldonado, M.C. and Vargas-Berenguel, A. (2008). Synthesis of [beta]-cyclodextrin derivatives functionalized with azobenzene. *Tetrahedron* **64**(48), 10919-10923.

Carvalho, E., Filho, N.C., Venancio, E.C., Jr, O.N.O., Mattoso, L.H.C. and Martin-Neto, L. (2007). Detection of brominated by-products using a sensor array based on nanostructured thin films of conducting polymers. *Sensors* **7**(12), 3258-3271.

Chen, G. and Jiang, M. (2011). Cyclodextrin-based inclusion complexation bridging supramolecular chemistry and macromolecular self-assembly. *Chem. Soc. Rev.* **40**(5), 2254-2266.

Chen, X., Jou, M.J., Lee, H., Kou, S. Lim, J., Nam, S.-W., Park, S., Kim, K.-M., and Yoon, M. (2009). New fluorescent and colorimetric chemosensors bearing rhodamine and binaphthyl groups for the detection of Cu^{2+}. *Sensors Act. B: Chem.* **137**(2), 597-602.

Chernyshev, A.V., Voloshin, N.A., Raskita, I.G., Metelitsa, A.V. and Minkin, V.I. (2006) Photo- and ionochromism of 5’-(4,5-diphenyl-1,3-oxazol-2-yl) substituted spiro[indoline-naphthopyrans]. *J. Photochem. & Photobiol. A: Chem.* **184**, 289-297.

Ciardelli, F. and Pieroni, O. (2001) Photoswitchable peptides. In*:* Feringa, B.L. (ed.) *Molecular Switches*. Wiley-VCH Verlag GmbH, Weinheim, Germany. Pp 399 – 441.

Crano, J.C. (1999). Introduction. In: Crano, J.C. and Guglielmeltti, R. (eds.) *Organic Photochromic and Thermochromic Compounds.* **Vol. 1**. Plenum Press, New York, USA. pp 1 – 9.

De Beer, P. and Dent, S.W. (1998). Potassium cation induced switch in anion selectivity exhibited by heteroditopic ruthenium(II) and rhenium(I) bipyridyl bis(benzo-15-crown-5) ion pair receptors. *Chem. Comm.* **0**(7), 825-826.

De Silva, A.P. and de Silva, S.A. (1986). Fluorescent signalling crown ethers; 'switching on' of fluorescence by alkali metal ion recognition and binding in situ. *J. Chem. Soc., Chem. Comm.* **0**(23), 1709-1710.

De Silva, A.P., Gunaratne, H.Q.N., Gunnlaugsson, T., Huxley, A.J.M., McCoy, C.P., Rademacher, J.T. and E. Rice T.E. (1997). Signaling recognition events with fluorescent sensors and switches. *Chem. Rev.* **97**(5), 1515-1566.

De Silva, A.P., Gunaratne, H.Q.N., et al. (1996). Fluorescent signalling of the brain neurotransmitter [gamma]-aminobutyric acid and related amino acid zwitterions. *Chem. Comm.* **0**(18), 2191-2192.

Du, J., Liu, M., Lou, X., Wang, Z., Xue, Y., Zhao, J. and Xu, Y. (2012). Highly sensitive and selective chip-based fluorescent sensor for mercuric ion: Development and comparison of turn-on and turn-off systems. *Anal. Chem.* **84**(18), 8060-8066.

Ercole, F., Davis, T.P. and Evans, R.A. (2010). Photo-responsive systems and biomaterials: photochromic polymers, light-triggered self-assembly, surface modification, fluorescence modulation and beyond. *Polym. Chem.* **1**(1), 37 – 54.

Ermakova, E., Michalak, J., Meyer, M., Arslanov, V., Tsivadze, A., Guilard, R. and Bessmertnykh-Lemeune, A. (2013). Colorimetric Hg^{2+} sensing in water: From molecules toward low-cost solid devices. *Org. Lett.* **15**(3), 662-665.

Ezeh, V.C. and Harrop, T.C. (2013). Synthesis and properties of arsenic (III)-reactive coumarin-appended benzothiazolines: A new approach for inorganic arsenic detection. *Inorg. Chem.* **52**(2), 2323-2334.

Girek, T., Kozlowski, C.A., et al. (2005). Polymerisation of β-cyclodextrin with succinic anhydride. Synthesis, characterisation, and ion flotation of transition metals. *Carbohydrate Polymers* **59**(2), 211-215.

Girek, T., Shin, D.-H. and Lim, S.-T. (2000). Polymerization of β-cyclodextrin with maleic anhydride and structural characterization of the polymers. *Carbohydr. Polym.* **42**(1), 59-63.

Gokel, G. W., Leevy, W.M., and Weber, M.E. (2004). Crown ethers: sensors for ions and molecular scaffolds for materials and biological models. *Chem. Rev.* **104**(5), 2723-2750.

Guan, Z., Wang, Y., Chen, Y., Zhang, L. and Zhang, Y. (2009). Novel approach for synthesis of 2:1 permethylated β-cyclodextrin–C60 conjugate. *Tetrahedron* **65**(6), 1125-1129.

Hamon, F., Djedaini-Pilard, F., Barbot, F. and Len, C. (2009). Azobenzenes — synthesis and carbohydrate applications. *Tetrahedron* **65**(49), 10105-10123.

Han, S. and Chen, Y. (2011). Mercury ion induced activation of the C – O bond in a photoresponsive spiropyran. *Dyes and Pigments* **88**, 235-239.

Hepworth, J.D., Gabbutt, C.D. and Heron, B.M. (1999). Photochromism of naphthopyrans. *Proceedings of the Colour Science ’98 Conference* **1**, 161-173.

Hsieh, Y.-C., Chir, J.-L.,Wu, H.-H., Chang, P.-S. and Wu, A.T. (2009). A sugar-aza-crown ether-based fluorescent sensor for Hg^{2+} and Cu^{2+}. *Carbohydr. Res.* **344**(16), 2236-2239.

Hu, J., and Liu, S. (2010). Responsive polymers for detection and sensing applications: Current status and future developments. *Macromolecules* **43**(20), 8315-8330.

Hulanicki, A., Geab, S. and Ingman, F. (1991). IUPAC chemical sensors: definitions and classification. *Pure & Appl. Chem.* **63**(9), 1247-1250.

Kanaya, A., Takashima, Y. and Harada, A. (2010). Double-threaded dimer and supramolecular oligomer formed by stilbene modified cyclodextrin: Effect of acyl migration and photostimuli. *J. Org. Chem.* **76**(2), 492-499.

Kim, I. W., Choi, H.M., Yoon, H.J. and Park, J.H. (2006). β-Cyclodextrin-hexamethylene diisocyanate copolymer-coated zirconia for separation of racemic 2,4-dinitrophenyl amino acids in reversed-phase liquid chromatography. *Anal. Chim. Acta* **569**(1–2), 151-156.

Kyzas, G. Z., Lazaridis, N.K., and Bikiaris, D.N. (2013). Optimization of chitosan and β-cyclodextrin molecularly imprinted polymer synthesis for dye adsorption. *Carbohydr. Polym.* **91**(1), 198-208.

Lee, H., Lee, H.-S., Reibenspies, J.H. and Hancock, R.D. (2012). Mechanism of “turn-on” fluorescent sensors for mercury (II) in solution and its implications for ligand design. *Inorg. Chem.* **51**(20), 10904-10915.

Liao, X., Chen, G., Liu, X., Chen, W., Chen, F. and Jiang, M. (2010). Photoresponsive pseudopolyrotaxane hydrogels based on competition of host–guest interactions. *Angew. Chem. Int. Ed.* **49**(26), 4409-4413.

Liu, M., Yan, X., Hu, M., Chen, X., Zhang, M., Zheng, B., Hu, X., Shao, S. and Huang, F. (2010). Photoresponsive host-guest systems based on a new azobenzene-containing cryptand. *Org. Lett.* **12**(11), 2558-2561.

McDonagh, C., Burke, C.S. and MacCraith, B.D. (2008). Optical chemical sensors. *Chem. Rev.* **108**, 400-422.

Mohamed, M. H., Wilson, L.D., and Headley, J.V. (2011). Design and characterization of novel β-cyclodextrin based copolymer materials. *Carbohydr. Res.* **346**(2), 219-229.

Morin-Crini, N. and Crini, G. (2013). Environmental applications of water-insoluble β-cyclodextrin–epichlorohydrin polymers. *Prog. Polym. Sci.* **38**(2), 344 – 368.

Muderawan, I.W., Ong, T.T., Lee, T.C., Young, D.J., Ching, C.B. and Ng, S.C. (2005). A reliable synthesis of 2- and 6-amino-β-cyclodextrin and permethylated-β-cyclodextrin. *Tetrahedron Lett.* **46**, 7905-7907.

Nakao, R., Noda, F., Horii, T. and Abe, Y. (2002) Thermal stability of the spironaphthoxazine colored form in polymeric siloxanes. *Polym. Adv. Tech.* **13**, 81-86.

Nakashima, H. and Yoshida N. (2006). Fluorescent detection for cyclic and acyclic alcohol guests by naphthalene-appended amino-β-cyclodextrins. *Org. Lett.* **8**(22), 4997-5000.

Neupane, L. N., Park, J.-Y., Park, J.H. and Lee, K.-H. (2013). Turn-on fluorescent chemosensor based on an amino acid for Pb(II) and Hg(II) ions in aqueous solutions and role of tryptophan for sensing. *Org. Lett.* **15**(2), 254-257.

Niu, Z., Huang, F., and Gibson, H.W. (2011). Supramolecular AA−BB-type linear polymers with relatively high molecular weights via the self-assembly of bis(m-phenylene)-32-crown-10 cryptands and a bisparaquat derivative. *J. Am. Chem. Soc.* **133**(9), 2836-2839.

Ogoshi, T. and Harada, A. (2008). Chemical sensors based on cyclodextrin derivatives. *Sensors* **8**(8), 4961-4982.

Petr, M. and Hammond, P.T. (2011). Room temperature rapid photoresponsive azobenzene side chain liquid crystal polymer. *Macromolecules* **44**(22), 8880-8885.

Remy, S., Shah, S.M., Martini, C. Poize, G., Margeat, O., Heynderickx, A., Ackerman, J. and Fages, F. (2011). Functionalization of zinc oxide nanorods with diarylethene-based photochromic compounds. *Dyes and Pigments*, **89**, 266-270.

Renard, E., Deratani, A., Volet, G. and Sebille, B. (1997). Preparation and characterization of water soluble high molecular weight β-cyclodextrin-epichlorohydrin polymers. *Eur. Polym. J.* **33**(1), 49-57.

Salipira, K. L., Krause, R.W., Mamba, B.B., Malefetse, T.J., Cele, L.M. and Durbach, S.H. (2008). Cyclodextrin polyurethanes polymerized with multi-walled carbon nanotubes: Synthesis and characterization. *Mater. Chem. Phys.* **111**(2–3), 218-224.

Shinkai, S. (2001). Switchable molecular receptors and recognition processes: From photoresponsive crown ethers to allosteric sugar sensing system. In*:* Feringa, B.L. (ed.) *Molecular Switches*. Wiley-VCH Verlag GmbH, Weinheim, Germany. pp 281-307.

Shinkai, S., Nakaji, T., Ogawa, T., Shigematsu, K. and Manabe, O. (1981). Photoresponsive crown ethers. 2. Photocontrol of ion extraction and ion transport by a bis(crown ether) with a butterfly-like motion. *J. Am. Chem. Soc.* **103**(1), 111-115.

Shinkai, S., Nakaji, T., Nishida, Y., Ogawa, T. and Manabe, O. (1980). Photoresponsive crown ethers. 1. Cis-trans isomerism of azobenzene as a tool to enforce conformational changes of crown ethers and polymers. *J. Am. Chem. Soc.* **102**(18), 5860-5865.

Shinkai, S., Shigematsu, K. , Sato, M. and Manabe, O. (1982a). Photoresponsive crown ethers. Part 6. Ion transport mediated by photoinduced cis-trans interconversion of azobis(benzocrown ethers). *J. Chem. Soc., Perkin Trans.***1**, 2735-2739.

Shinkai, S., Ogawa, T., Kusano, Y., Manabe, O., Kikukawa, K., Goto, T. and Matsuda, T. (1982b). Photoresponsive crown ethers. Part 4. Influence of alkali metal cations on photoisomerization and thermal isomerization of azobis(benzocrown ethers). *J. Am. Chem. Soc.* **104**(7), 1960-1967.

Shinkai, S., Minami, T., Kusano, Y. and Manabe, O. (1983). Photoresponsive crown ethers. 8. Azobenzenophane-type switched-on crown ethers which exhibit an all-or-nothing change in ion-binding ability. *J. Am. Chem. Soc.* **105**(7), 1851-1856.

Shinkai, S., Yoshida, T., Manabe, O., and Fuchita, T. (1988). Photoresponsive crown ethers. Part 20. Reversible photocontrol of association-dissociation equilibria between azobis(benzo-18-crown-6) and diammonium cations. *J. Chem. Soc., Perkin Trans.* **1**(6), 1431-1437.

Stauffer, M.K., Knowles, D.B., Brennan, C., Funderburk, L., Lin, F.-T. and Weber, S.G. (1997). Optical control over Pb^{2+} binding to a crown ether containing chromene. *Chem. Commun.*, **1997**, 287 – 288.

Takahashi, K. and Hattori, K. (1984). Synthesis of two regiospecific isomers of monotosyl-γ-cyclodextrin. *J. Incl. Phenom.* **2**, 661 – 667.

Thakur, A., Mandal, D., and Ghosh, S. (2013). Sensitive and selective redox, chromogenic, and "turn-on" fluorescent probe for Pb(II) in aqueous environment. *Anal. Chem.* **85**(3), 1665-1674.

Tomatsu, I., Hashidzume, A., and Harada, A. (2005). Photoresponsive hydrogel system using molecular recognition of α-cyclodextrin. *Macromolecules* **38**(12), 5223-5227.

Uekama, K., Otagiri, M., Irie, T., Seo, H. and Tsuruoka, M. (1985). Improvement of dissolution and absorption characteristics of phenytoin by a water-soluble β-cyclodextrin-epichlorohydrin polymer. *Int. J. Pharm.* **23**(1), 35-42.

Valeur, B. (2001). *Molecular Fluorescence: Principles and Applications*. Chapter 1: Introduction. Wiley-VCH Verlag GmbH, Weinheim, Germany. pp 3-19.

Valeur, B., Berberan-Santos, M.N. and Martin, M.M. (2007). Photophysics and photochemistry of supramolecular systems. In: Schalley, C.A. (ed.) *Analytical Methods in Supramolecular Chemistry*. Wiley-VCH Verlag, Weinheim, Germany, pp 220-262.

Van de Manakker, F., Vermonden, T., Van Nostrum, C.F. and Hennink, W.E. (2009). Cyclodextrin-based polymeric materials: Synthesis, properties, and pharmaceutical/biomedical applications. *Biomacromol.* **10**(12), 3157-3175.

Van Gemert, B. (1999). Benzo and naphthopyrans (chromenes). In: Crano, J.C. and Guglielmeltti, R. (eds.) *Organic Photochromic and Thermochromic Compounds.* **Vol. 1**. Plenum Press, New York, USA. pp 111 – 140.

Voronina, L., Livshits, V., et al. (2011). Studies of possibility of detecting aromatic hydrocarbons in gas phase on the basis of fluorescence of host-guest complexes with cyclodextrins immobilized on silica microspheres. *Nanotechnologies in Russia* **6**(7), 444-455.

Wang, J. and Ueno, A. (2000). Naphthol-modified β-cyclodextrins as fluorescent sensors for detecting contaminants in drinking water. *Macromol. Rapid Comm.* **21**(13), 887-890.

Wang, S., Choi, M-S. and Kim, S-H. (2008). Multiple switching photochromic poly(N-isopropylacrylamide) with a spironaphthoxazine hydrogel. *Dyes and Pigments.* **78**, 8 – 14.

Wang, X. R, Lu, J., Wei, M. and Duan, X. (2010). Photoresponsive thin films containing an azobenzene derivative intercalated with a layered double hydroxide. *Chin. Sci. Bull.* **55**(34), 3894-3900.

Wang, Y., Ma, N., Wang, Z. and Zhang, X. (2007). Photocontrolled reversible supramolecular assemblies of an azobenzene-containing surfactant with α-cyclodextrin. *Ang. Chem. Int. Ed.* **46**(16), 2823-2826.

Wondraczek, H. and Kotiaho, A., Fardim, P. and Heinze, T. (2011). Photoactive polysaccharides. *Carbohydr. Polym.* **83**(3), 1048-1061.

WHO (2004). *Trihalomethanes in Drinking Water*. WHO/SDE/WSH/03.04/64. Background document for development of WHO *Guidelines for Drinking Water Quality,* World Health Organization, Geneva, Switzerland. pp. 1-39.

Yari, A. and Papi F. (2009). Highly selective sensing of mercury (II) by development and characterization of a PVC-based optical sensor. *Sensors Act. B: Chem*. **138**(2), 467-473.

Yuan, C., Zhang, K., Zhang, Z. and Wang, S. (2012). Highly selective and sensitive detection of mercuric ion based on a visual fluorescence method. *Anal. Chem.* **84**(22), 9792-9801.

Zha, F., Li, S., and Chang, Y. (2008). Preparation and adsorption property of chitosan beads bearing β-cyclodextrin cross-linked by 1,6-hexamethylene diisocyanate. *Carbohydr. Polym.* **72**(3), 456-461.

Zohrehvand, S. and Evans C.H. (2005). 2-Naphthol-containing β-cyclodextrin–epichlorohydrin copolymers: synthesis, characterization and fluorescence studies. *Polym. Int.* **54**(5), 744-753.

Zou, J., Guan, B., Liao, X., Jiang, M. and Tao, F. (2009). Dual reversible self-assembly of PNIPAM-based amphiphiles formed by inclusion complexation. *Macromolecules* **42**(19), 7465-7473.

Zou, J., Tao, F., and Jiang, M. (2007). Optical switching of self-assembly and disassembly of noncovalently connected amphiphiles. *Langmuir* **23**(26), 12791-12794.

CHAPTER 3

EXPERIMENTAL: SYNTHESIS AND CHARACTERISATION OF SENSOR MOLECULES

3.1 INTRODUCTION

This chapter gives an account of the experimental procedures followed in achieving the objectives of this study. The methods for the synthesis and characterisation of the sensor molecules are given in this chapter. All experimental and analytical procedures that were used in this study are described in this chapter.

3.2 SYNTHESIS OF PEG-LINKED AZO DYE-MODIFIED β-CD SENSOR

3.2.1 Materials and equipment

All chemicals, unless otherwise stated, were purchased from Sigma-Aldrich and were used without further purification. Solvents were distilled before use.

3.2.2 Azo dye synthesis

An aqueous NaOH solution (10%) was prepared by dissolving NaOH (6 g) in 54 mℓ of water in a 250 mℓ conical flask. β-naphthol (2.884 g, 0.020 mol) was then added to the NaOH solution and the mixture was stirred until all the β-naphthol had dissolved. The resulting β-naphthol solution was then left standing in an ice-bath while carrying out the next step.

$NaNO_2$ (1.475 g, 0.021 mol) was dissolved in 10 mℓ of water in a 100 mℓ conical flask and also placed in an ice-bath. Into a 250 mℓ conical flask was placed 4-aminophenol (2.445 g, 0.022 mol) and 90 mℓ of water. Concentrated HCl (20.0 mℓ) was then added slowly to this solution while stirring until all the aminophenol had dissolved completely. The resulting solution was then cooled in an ice-bath to 3^{o}C. The previously prepared $NaNO_2$ solution was then added slowly with a dropper while stirring. After all of the solution had been added, the resulting turbid greyish solution was stirred for a further 5 min.

The turbid solution was then added drop-by-drop to the previously prepared β-naphthol solution. When the addition was complete, the mixture was stirred for a further 15 min. The resulting precipitate was filtered and washed on the Buchner funnel with cold water. When the solid was sufficiently dry on the pump, the product was left to dry in air to give a brick-red solid (yield: 3.568 g, 82.6%).

3.2.3 Tosylation of β-CD

The procedure used was based on the method described by Zhong et al. (1998).

A mixture of β-CD (11.501 g, 10.13 mmol) and Ts_2O (4.925 g, 15 mmol) in 200 mℓ water was stirred for 2 h at room temperature under an inert $N_2(g)$ atmosphere. A solution of NaOH (5 g in 50 mℓ, 10%) was then added and the mixture stirred for a further 10 min. The excess Ts_2O remaining was filtered off through silica gel. The pH of the filtrate was then adjusted by adding $NH_4Cl(s)$ until the pH was 8 (on Universal Indicator-Merck). The white precipitate formed was thereafter left in the refrigerator (~ 4^{o}C) overnight. The white precipitate was then collected under suction filtration and dried in air (yield: 6.980 g, 53.5%).

3.2.4 Azo dye-modified β-CD

The previously synthesised azo dye (**Section 3.2.2**) was stirred in DMF under a nitrogen atmosphere for 1 h. The previously synthesised monotosylated β-CD (**Section 3.2.3**) was then added and the reaction mixture heated at 80°C under a nitrogen atmosphere for 12 h. The reaction mixture was then poured into acetone and the resulting precipitate filtered off, washed with copious amounts of acetone and dried to give an orange powder (yield: 75%). FT-IR: 3 292 cm^{-1} (broad) O-H stretch; 1 219 cm^{-1}and 1 025 cm^{-1} (sharp) due to the C–O–C bond stretch. ^{1}H-NMR: Dye protons; d, δ = 7.17–7.19 and d, δ= 7.51–7.53; and s, δ= 7.75.

3.2.5 Synthesis of PEG linked azo dye-modified β-CD sensor

β-CD (2.515 g, 1.90 mmol) and β-CD-dye (0.253 g, 0.185 mmol) were stirred in DMF (30 mℓ) under a nitrogen atmosphere for 5 min. Ethylene glycol ditosylate (0.790 g, 1.90 mmol) dissolved in DMF (5 mℓ) was added drop-wise with continued stirring. Three drops of dibutyltin dilaurate (DBTDL) catalyst were added and the mixture was stirred for a further hour. The resulting mixture was added drop wise to acetone (200 mℓ) and the solid formed filtered off, washed with acetone and dried in a desiccator to give an orange powder (2.340 g, 93% m/m yield of β-CD). FT-IR: 3 331 cm^{-1} (broad) O-H stretch; 1 654 cm^{-1} and 1 081 cm^{-1} (sharp) due to the C-O-C bond stretch. ^{1}H-NMR: Dye protons; d, δ = 7.16–7.18 and d, δ = 7.49–7.52; and s, δ = 7.75; CH_2 (O) m δ = 3.38–3.48.

3.2.6 Characterisation

Absorption spectra were recorded on a Shimadzu UV-2450 UV-Vis Spectrophotometer at room temperature in quartz cuvettes. Fluorescence measurements were done on a Perkin Elmer LS45 Fluorescence Spectrometer whereas infrared spectra were recorded on a Perkin Elmer Spectrum 100 FT-IR Spectrometer in the attenuated total reflectance (ATR) mode. ^{1}H-NMR spectra were obtained on a 400 MHz Bruker Avance NMR spectrometer in deuterated water (D_2O).

3.3 SYNTHESIS OF EPC-LINKED AZO DYE-MODIFIED Β-CD SENSOR

3.3.1 Materials and equipment

3.3.2 Method

The method used for the polymerisation with epichlorohydrin (EPC) was adopted from the work done by Renard et al. (1997). Both native β-CD and the azo dye-modified β-CD were polymerised with EPC for comparison.

3.3.2.1 Polymerisation with EPC

To β-CD (5.055 g, 4.45 mmol) was added a 10% NaOH solution (5 mℓ) and the mixture was stirred overnight at room temperature. The mixture was then heated to 30°C and EPC (3.5 mℓ, 44.60 mmol) added all at once. The reaction was stopped after 4 h by adding acetone. The solid formed was decanted off and the acetone evaporated. The remaining solution was adjusted to pH 12 by addition of a few drops of HCl (32%). The reaction mixture was then heated to 60°C and stirred overnight. The resulting solution was thereafter neutralised with more HCl and acetone added to form a precipitate, which was dried to give a white powder (yield; 5.650g).

3.3.3 Quantification of cyclodextrin in EPC-βCD polymer

The amount of cyclodextrin incorporated into the sensor material was quantified using two methods, namely NMR spectroscopy and the anthrone method.

3.3.3.1 NMR quantification

The polymer material (0.1175 g) and p-nitrophenol (0.0076 g, 5.46×10^{-5} mol) were dissolved in a total of 1 mℓ D_2O to give a solution which was 0.0546 M in PNP and 0.1175 g/mℓ in the polymer material. NMR spectra were recorded on a Bruker Avance II 400 NMR spectrometer with broad band inverse (BBI) magnet.

3.3.3.2 Anthrone reaction quantification

Solutions were prepared as follows:

Anthrone solution: Anthrone (0.0998 g, 5.138 x 10^{-4} mol) was dissolved in an H_2SO_4: H_2O (5:2) solution in a 50 mℓ volumetric flask to give a yellow solution. The flask was ultrasonicated until all anthrone was completely dissolved.

Standard stock solution: β-CD (0.0066 g, 5.815 x 10^{-6} mol) was dissolved in Milli-Q water in a 50 mℓ volumetric flask and the flask filled to the mark to give a stock solution of β-CD of concentration 1.163 x 10^{-4} mol.

Sample solution: The polymer sample (EPC-CD polymer) (0.0068 g) was weighed into a 50 mℓ volumetric flask, dissolved in Milli-Q water and the flask made up to the mark with the water.

Procedure

Solutions for the calibration curve were prepared from the standard stock solution by serial dilution. Into each of five test tubes was first added water, then stock solution to give a total of 4.8 mℓ. A blank was prepared in which no β-CD was added. Three replicate sample solutions were also prepared in which 0.2 mℓ and 0.6 mℓ water were placed in three separate test tubes. The nine test tubes were then placed in an ice/water bath for 5 min. The anthrone solution was thereafter added to each test tube; 8 mℓ for the blank and 4 mℓ each for the rest of the tubes. All the test tubes were then heated in a pre-set water bath (ca. 90°C) for 10 min. The solutions with cyclodextrin turned green. The tubes were then placed back into an ice/water bath to stop the reaction and the absorbance of each solution at 620 nm measured, starting with the least concentrated standard solution and ending with sample solutions.

3.3.4 Thermodynamics of binding of guest molecules to EPC-CD polymer by ITC

3.3.4.1 Materials and methods

Solutions were prepared as follows:

Adamantylamine solution: Adamantylamine hydrochloride (amantadine hydrochloride) (0.0681 g, 3.628 x 10^{-4} mol) was dissolved in Milli-Q water (5 mℓ) to give a 0.0725 M stock solution. For ITC measurements, 0.5 mℓ of stock solution was diluted to 5.0 mℓ buffer solution to give a 7.25 mM solution.

Buffer solution (phosphate **buffer; pH ~ 7)**

NaH_2PO_4 (0.1284 g), Na_2HPO_4 (0.2152 g) and NaCl (0.0585 g) were dissolved in Milli-Q water in a 50 mℓ volumetric flask and the volume made up to the mark. The pH was measured on a pH meter. The measured pH was 6.932. The pH of all other subsequently prepared buffer solutions was measured.

β-Cyclodextrin solution

β-CD (0.0089 g; 7.8414 x 10^{-6} mol) was dissolved in phosphate buffer (5.0 mℓ, pH = 6.932) in a 5 mℓ volumetric flask.

Polymer solution

EPC-β-CD polymer sample (0.0091 g) was dissolved in phosphate buffer (10.0 mℓ, pH = 6.932) in a 10 mℓ volumetric flask. From the ^{1}H-NMR estimation of CD concentration in the polymer of 72%, the concentration of CD cavity sites for use in the ITC was calculated to be 5.773 x 10^{-4} M (~ 0.58 mM).

p-Chlorophenol: The p-chlorophenol (0.0095 g, 7.389 x 10^{-5} mol) was dissolved in the buffer solution in a 5 mℓ volumetric flask and the volume made up to 5 mℓ with the buffer solution (to give a 15 mM solution).

1-Chloronaphthalene: The 1-chloronaphthalene (M_r = 162.62 g/mol) is not soluble in water. A 0.7 M stock solution was prepared in acetonitrile (0.48 mℓ, 1.192 g/mℓ). The phosphate buffer solution was prepared (pH = 6.984) in a 1% AcN solution. From the stock solution 0.10 mℓ was diluted to 10.00 mℓ in the 1% AcN buffer solution to give a 7 mM solution of 1-chloronaphthalene [NB: A few bubbles were seen that may mean that some of the 1-chloronaphthalene did not dissolve and so the concentration of 1-chloronapthalene may be less than 7 mM]. The EPC-CD polymer (0.0091 g) was dissolved in the 1% buffer solution.

3.3.5 Characterisation

Absorption spectra were recorded on a Shimadzu UV-2450 UV-Vis Spectrophotometer at room temperature in quartz cuvettes. Fluorescence measurements were carried out on a Perkin Elmer LS45 Fluorescence Spectrometer whereas infrared spectra were recorded on a Perkin Elmer Spectrum 100 FT-IR Spectrometer operating in the attenuated total reflectance (ATR) mode. ^{1}H-NMR spectra were obtained from a 400 MHz Bruker Avance NMR spectrometer in deuterated water (D_2O).

3.4 SYNTHESIS OF AZO DYE-MODIFIED DB18C6 ETHER SENSOR

3.4.1 Materials and equipment

3.4.2 Method

The crown-ethers were synthesised based on methods reported by Grebenyuk et al. (2000) and by Pandya and Agrawal (2002) with modifications as follows. Dibenzo-18-crown-6-ether **1** (5.058g, 14 mmol) was dissolved in acetic acid (50 mℓ) and nitric acid (0.65 mℓ, d = 1.37 g/cm^3, 14 mmol) added. The mixture was stirred at room temperature for 18 h. The reaction mixture, which had turned yellow, was poured into an ice/water mixture (200 mℓ). The resulting precipitate was filtered off and washed with cold water until neutral to give yellow crystals **2** [yield: 4.264 g, 74.6%; mp: 176 – 179°C (Lit. mp. 173°C to 177°C)].

(a) Reduction

A mixture of **2** (2.530 g, 6.3 mmol) and Raney nickel (5 g) was stirred under reflux in 2-propanol (100 mℓ) for 5 min. Hydrazine monohydrate (0.50 mℓ, 10.4 mmol) was then added drop-wise and the mixture was refluxed for a further 6 h. The catalyst was removed by filtering the reaction mixture while hot. The solvent was then reduced on the rotary evaporator to around 20 mℓ. A white solid was formed on cooling, which was filtered off and dried to give **3** [yield: 1.205 g, 51.3%; mp: 200°C to 204°C (Lit. mp. 197°C to 203°C)].

(b) Diazo coupling

A slurry of **3** (0.935 g, 2.5 mmol) in HCl (conc. 32%; 10 mℓ) was cooled to -6°C in ice/water with continued stirring. An aqueous solution of $NaNO_2$ (5 mℓ) was added drop-wise and the reaction mixture was stirred for 10 min in ice water. In the meantime, β-naphthol **4** (0.362 g, 2.5 mmol) was dissolved in NaOH solution (10%) and cooled in ice water to -6°C. The previously prepared solution (**3**) was then added drop-wise to the β-naphthol solution with continued stirring in ice water. After complete addition, the mixture was stirred for a further 20 min. The resulting precipitate was collected by filtration, washed with cold water and dried to give a deep red solid [yield: 0.734 g, 55.1%; mp: 261°C to 263°C (Lit. mp. 260°C)].

3.4.3 Characterisation

Absorption spectra were recorded on a Shimadzu UV-2450 UV-Vis Spectrophotometer at room temperature in quartz cuvettes. Fluorescence measurements were done on a Perkin Elmer LS45 Fluorescence Spectrometer whereas infrared spectra were recorded on a Perkin Elmer Spectrum 100 FT-IR Spectrometer operating in the attenuated total reflectance (ATR) mode. ^{1}H-NMR spectra were obtained from a 400 MHz Bruker Avance NMR spectrometer in deuterated water ($CDCl_3$).

3.5 REFERENCES

Zhong, N., Byun, H.-S., and Bittman, R. (1998). An improved synthesis of 6-O-monotosyl-6-deoxy-[beta]-cyclodextrin. *Tetrahedron Lett.* **39**(19), 2919-2920.

Renard, E., Deratani, A., Volet, G. and Sebille, B. (1997). Preparation and characterization of water soluble high molecular weight β-cyclodextrin-epichlorohydrin polymers. *Eur. Polym. J.* **33**(1), 49-57.

Grebenyuk, A.D., Andreev, S.A., Stempnevskaya, I.A., Levkovich, M.G. and Tashmukhamedova, A.K. (2000) Nitration of benzo crown ethers with potassium nitrate in polyphosphoric acid. *Chem. Heterocycl. Comp.* **36**, 1449-1456.

Pandya, B.R. and Agrawal, Y.K. (2002). Synthesis and characterization of crown ether based azo dyes. *Dyes and Pigments* **52**, 161-168.

CHAPTER 4

RESULTS AND DISCUSSION

This chapter presents the results of the fluorescent detection of chlorinated organic compounds (Chapters 4A and 4B) as well as the detection of mercury (Chapter 4C), a representative heavy-metal pollutant. Each sub-chapter begins with a discussion of the synthesis of the sensor materials used in the detection of the respective pollutants. The discussion of the results is given along with the obtained results.

CHAPTER 4A

FLUOROMETRIC SENSING OF CHLOROPHENOLS IN WATER USING AN AZO DYE-MODIFIED β-CYCLODEXTRIN POLYMER

4.1 INTRODUCTION

Chlorophenols are typical organic pollutants found in water sources and were used in this chapter as representative aromatic compounds. These pose serious health threats and their levels in water are regulated by various organisations such as the World Health Organization (WHO), Environmental Protection Agency (EPA), and locally by the South African Department of Water Affairs and Forestry (DWAF), now the Department of Water Affairs (DWA). The detection of these compounds has been traditionally done by chromatographic techniques. Of interest is the use of cyclodextrins in columns for these chromatographic determinations. It was therefore appropriate to use cyclodextrins in the reported work for the same compounds.

In this chapter, therefore, we report on the detection of selected chlorophenols using a fluorescent azo dye-modified β-CD copolymer. The synthesis of the dye-modified cyclodextrin and of the polymer was carried out using the protocol found in the literature (Casas-Solvas, 2008; Hamon et al., 2009) and the characterisation was done by UV/Vis Spectrophotometry, FT-IR and ^{1}H-NMR spectroscopy. The detection of chlorophenols in water was then done using fluorescence spectroscopy.

The work presented in this chapter was published as: Ncube et al. (2011). *Sensors*, **11,** 4598 – 4608.

4.2 EXPERIMENTAL

The synthesis, characterisation techniques and testing of materials is described in **Chapter 3.**

4.3 RESULTS AND DISCUSSION

4.3.1 Synthesis of PEG-CD-dye polymer

The dye-modified β-CD polymer **4** was synthesised as outlined in **Scheme 4A.1**, based on methods described in the literature (Casas-Solvas, 2008; Hamon et al., 2009).

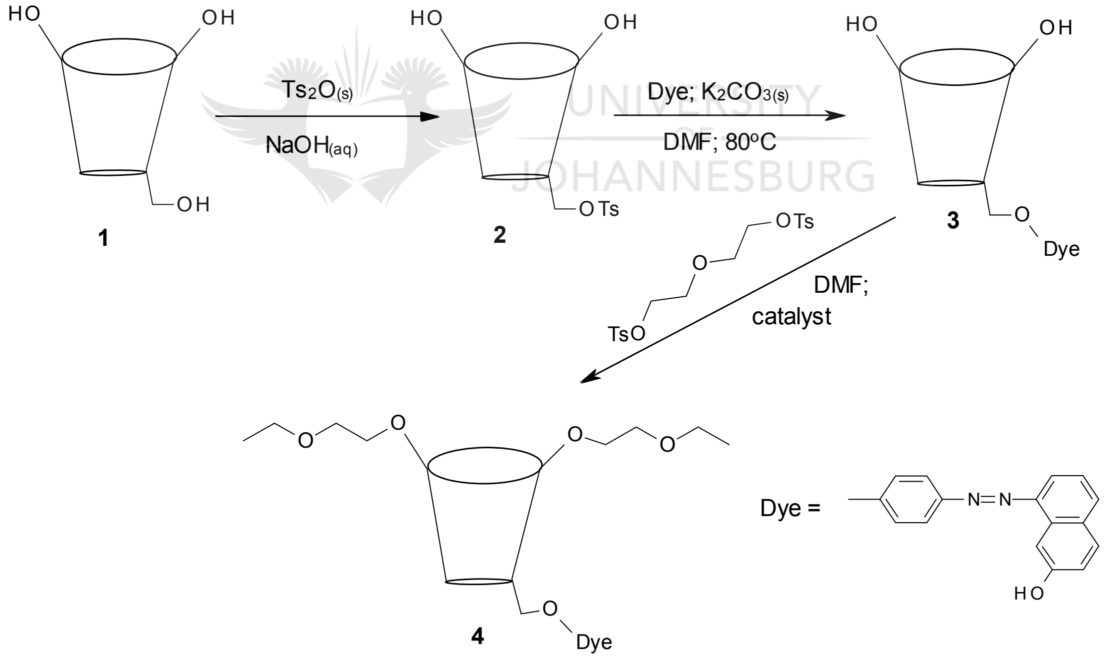

Scheme 4A.1: Synthetic pathway to sensor polymer 4

Starting from β-CD **1**, a tosyl group was introduced at C-6 by the use of Ts_2O as described in **Section 3.2.3**. Previous tosylation of β-CD has been achieved by the use of para-tosyl chloride (p-TsCl) but this reaction is prone to deliver low yields (Muderawan et al., 2005). An improved method using Ts_2O under alkaline conditions (Zhong et al., 1998) was used for this synthesis, and fair yields were obtained, ranging from 53% to as high as 70% on repeating the procedure.

4.3.2 Characterisation

4.3.2.1 Ultraviolet (UV) spectrophotometric analysis

The UV/Vis spectrum of **3** showed a λ_{max} of 480 nm characteristic of the azo dye, suggesting that the attachment of the dye does not alter its absorption properties.

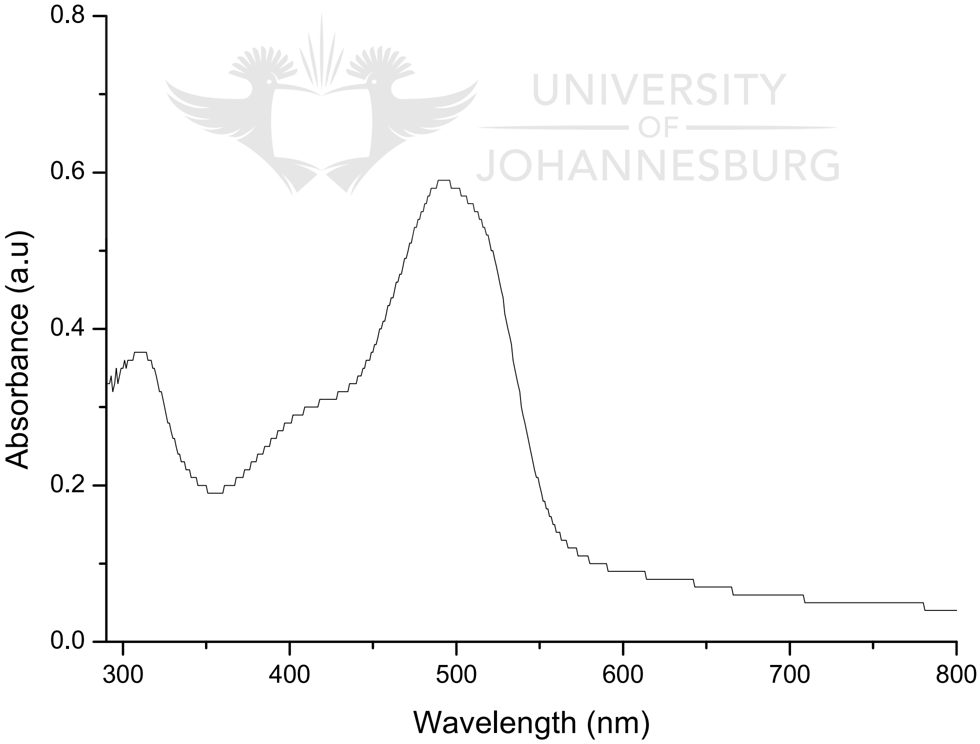

Figure 4A.1: UV-Vis spectrum of CD-dye only

To gain some insight into the conformational structure of the azo dye β-CD polymer, the effect of pH on the absorbance of the dye was investigated. The pH dependence of the absorption of azo dye-modified β-CD is shown in **Figure 4A.2** and that for the azo dye-modified β-CD polymer is shown in **Figure 4A.3**.

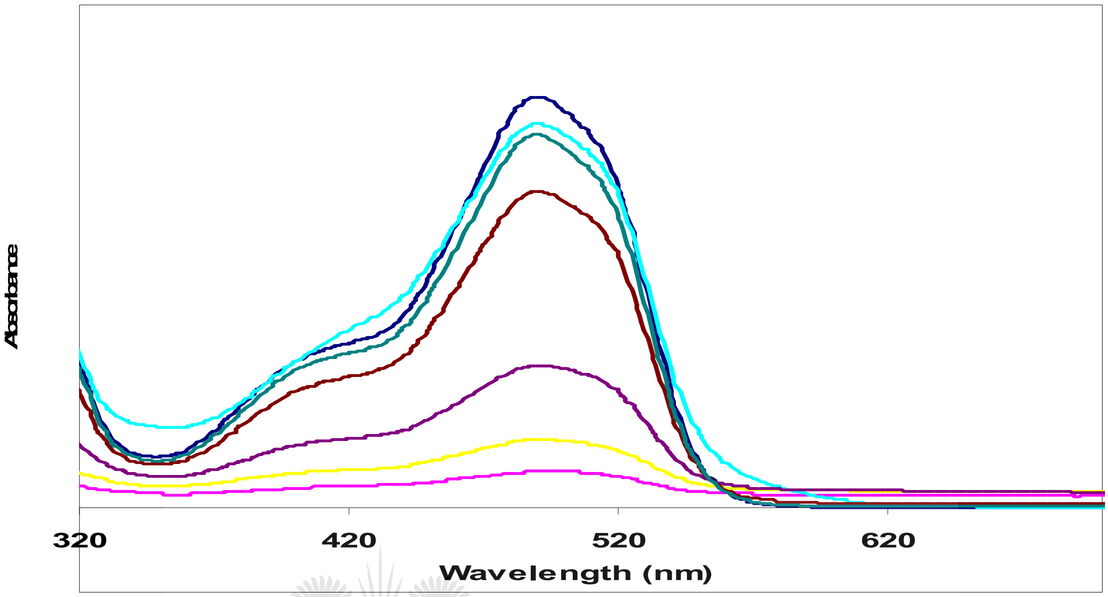

Figure 4A.2: Effect of pH on azo dye-modified β-CD

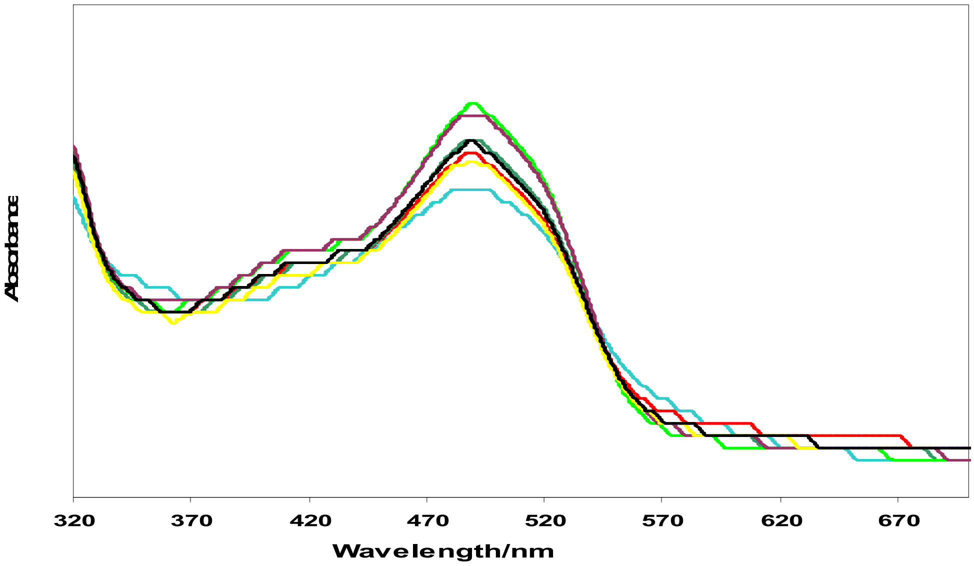

Figure 4A.3: Effect of pH on azo dye-modified β-CD polymer

As the pH was increased (pH 6 to pH 13) the absorption of **3** was greatly reduced when compared to that of **4**. This suggests that the polymer matrix acts as a form of protection to the dye moiety, making it more stable even in very alkaline conditions. This stability in the polymer matrix is important in investigating the guest-induced response properties of the polymer as different solutions may have different pH values.

These observations suggest that the dye moiety is encapsulated inside the β-CD cavity under neutral conditions and lies outside the cavity under alkaline conditions.

On polymerisation of the dye-modified β-CD, the λ_{max} was again not altered, confirming that the process of polymerisation does not alter the dye structure.

4.3.2.2 FT-IR spectroscopic characterisation

The FT-IR spectra of native β-CD, azo dye-modified β-CD and the sensor material are shown in **Figure 4A.4**. The broad peak around 3 300 cm^{-1} due to the O-H stretch is seen in all the three spectra along with the peak at 2 950 cm^{-1} due to C – H stretch and the sharp peaks at 1 654 cm$^{−1}$ and 1 081 cm$^{−1}$ due to the C–O–C bond stretch since all these are all present in all three molecules. The appearance of overtone peaks due to the aromatic rings in the dye, in the spectrum of the azo dye-modified β-CD, is confirmation of the introduction of these aromatic groups.

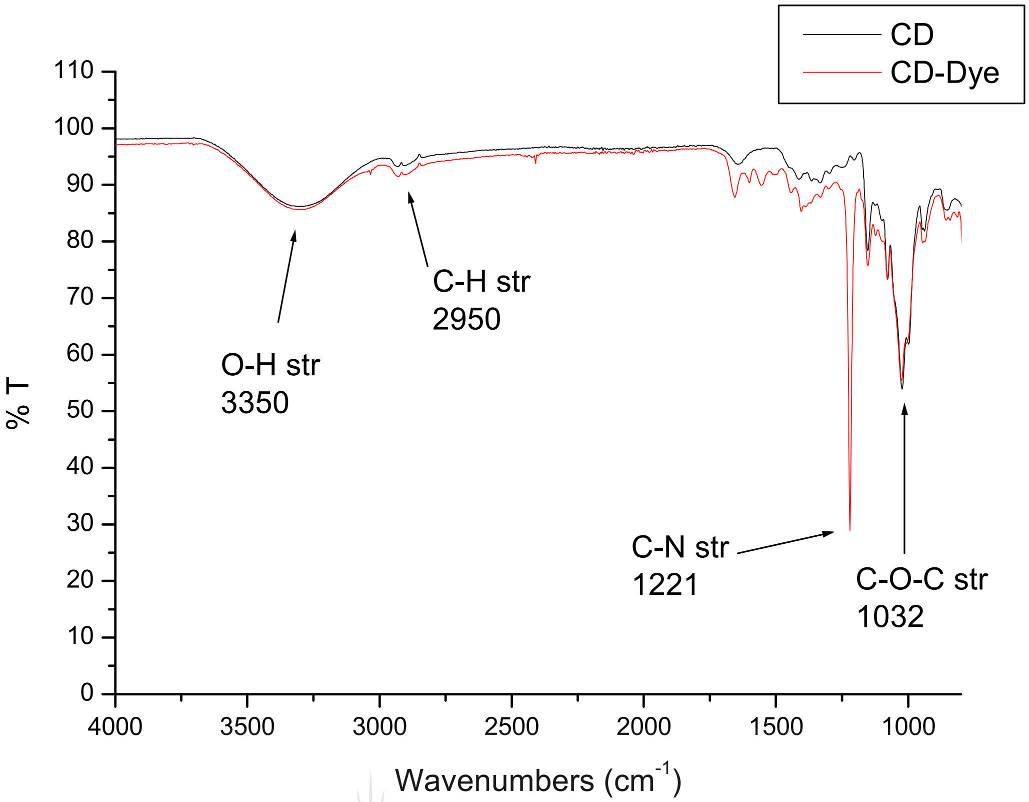

Figure 4A.4: IR spectra of the sensor polymer material compared to native and dye-modified CD

4.3.2.3 NMR spectroscopic characterisation

To further characterise the synthesised sensor material, ^{1}H-NMR spectroscopy was employed. The ^{1}H-NMR spectrum of native β-CD as shown in **Figure 4A.5** consists of a peak due to the hydroxyl (OH) group at δ = 4.90 – 4.91 as well as the aliphatic peaks due to H1 to H6 as shown on the structure.

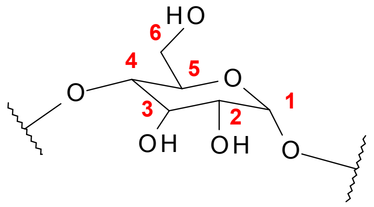

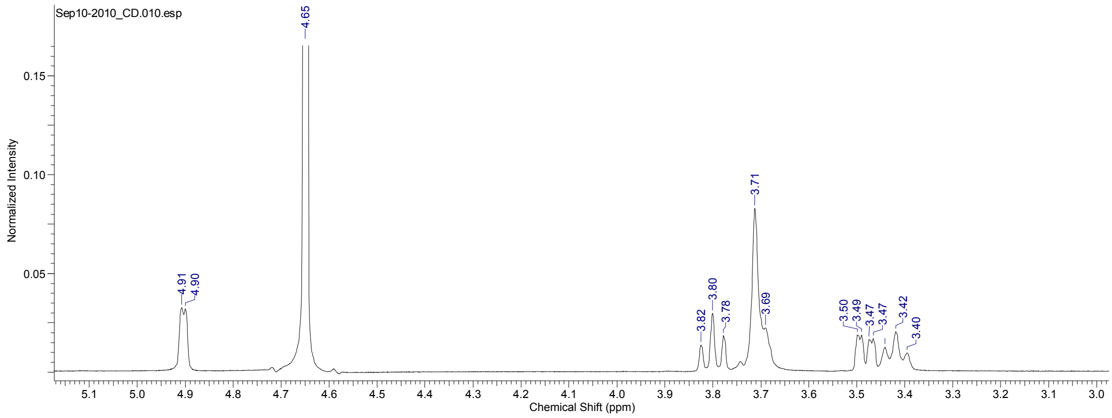

Figure 4A.5: NMR spectrum of native β-CD

The protons of the dye are seen in the aromatic region (δ = 6 – 8), as expected (see **Figure 4A.6**).

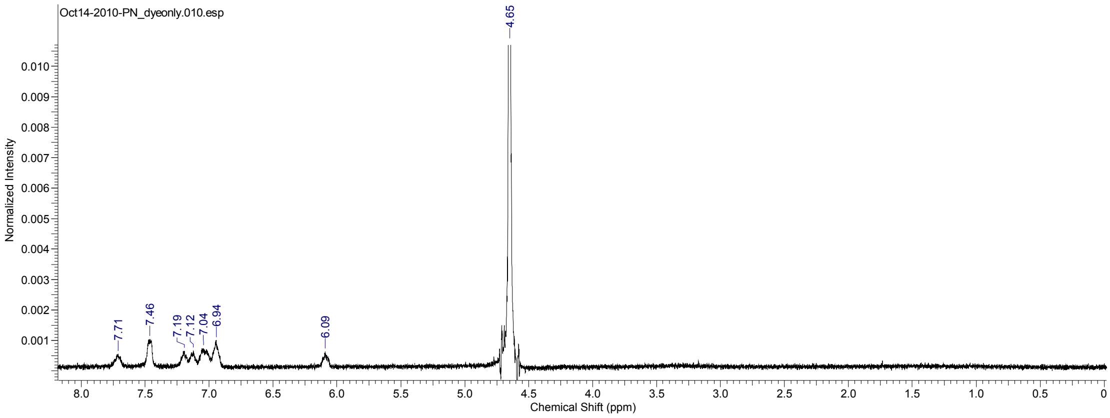

Figure 4A.6: NMR spectrum of azo dye

After polymerisation with the ethylene glycol linker the appearance of the alkyl protons (CH_2) between δ = 2.0 and δ = 3.0 confirmed the linkage of CD units. The spectrum of the product formed by polymerisation of native CD with the PEG linker is shown in **Figure 4A.7**. Three peaks at δ = 2.05, δ = 2.6 to 2.7 and at δ = 2.8 are observed. These are due to the CH_2 protons that are in a CD chain, in unreacted PEG and in the terminal PEG units in the final product, respectively.

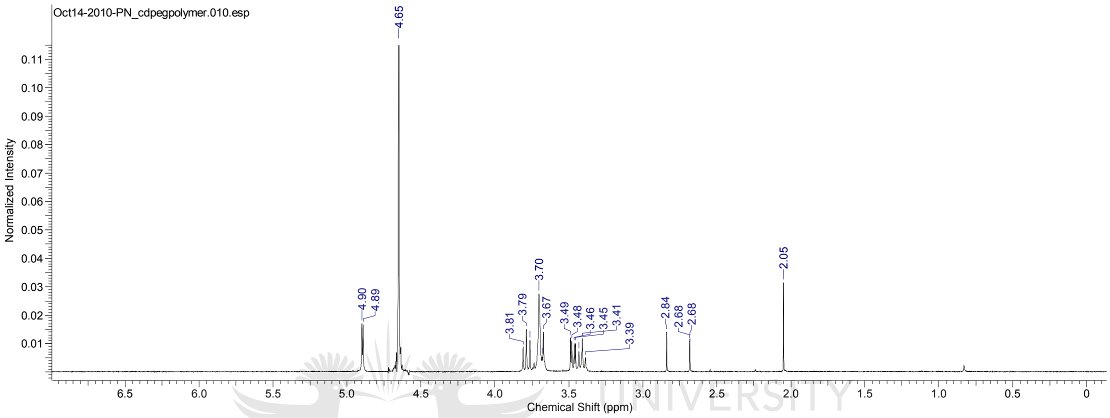

Figure 4A.7: NMR spectrum of β-CD-PEG polymer (no dye)

For the sensor material the ^{1}H-NMR spectrum clearly shows the presence of the dye protons at δ = 7.16 – 7.18; δ = 7.49 – 7.52 and δ = 7.75. The spectrum showed no triplet suggesting the structure of the dye-modified β-CD as shown in **Scheme 4A.1**. Also clearly seen are the ethylene glycol linker protons CH_2 (O) in the region δ = 2.0 – 3.5.

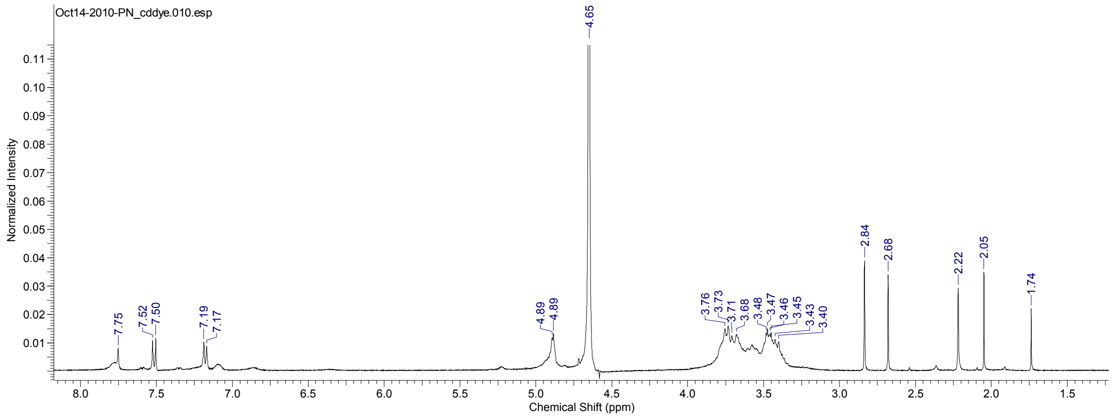

Figure 4A.8: NMR spectrum of azo dye-modified β-CD-PEG polymer

^{1}H-NMR spectroscopy confirmed the presence of aromatic protons (δ = 7 – 8) and the methyl protons (δ = 2 – 3). The dye was then attached to the β-CD by replacing the good leaving tosyl group through the phenoxy group of the dye to form the ether linked dye-modified β-CD **3**.

Through NMR spectroscopy it was clearly seen that the azo dye-modified β-CD units were linked by ethylene glycol bridges to form the new sensor molecule which was used for the detection of chlorophenols in water. The sensor molecule was water soluble and therefore easily applied for the detection of the sparingly soluble chlorinated organic compounds.

4.3.3 Detection of chlorophenols

4.3.3.1 Effect of solvent on fluorescence

The encapsulation of the dye moiety was also confirmed by investigating the effect of different solvents on the fluorescence of the azo dye β-CD polymer (**Figure 4A.9).**

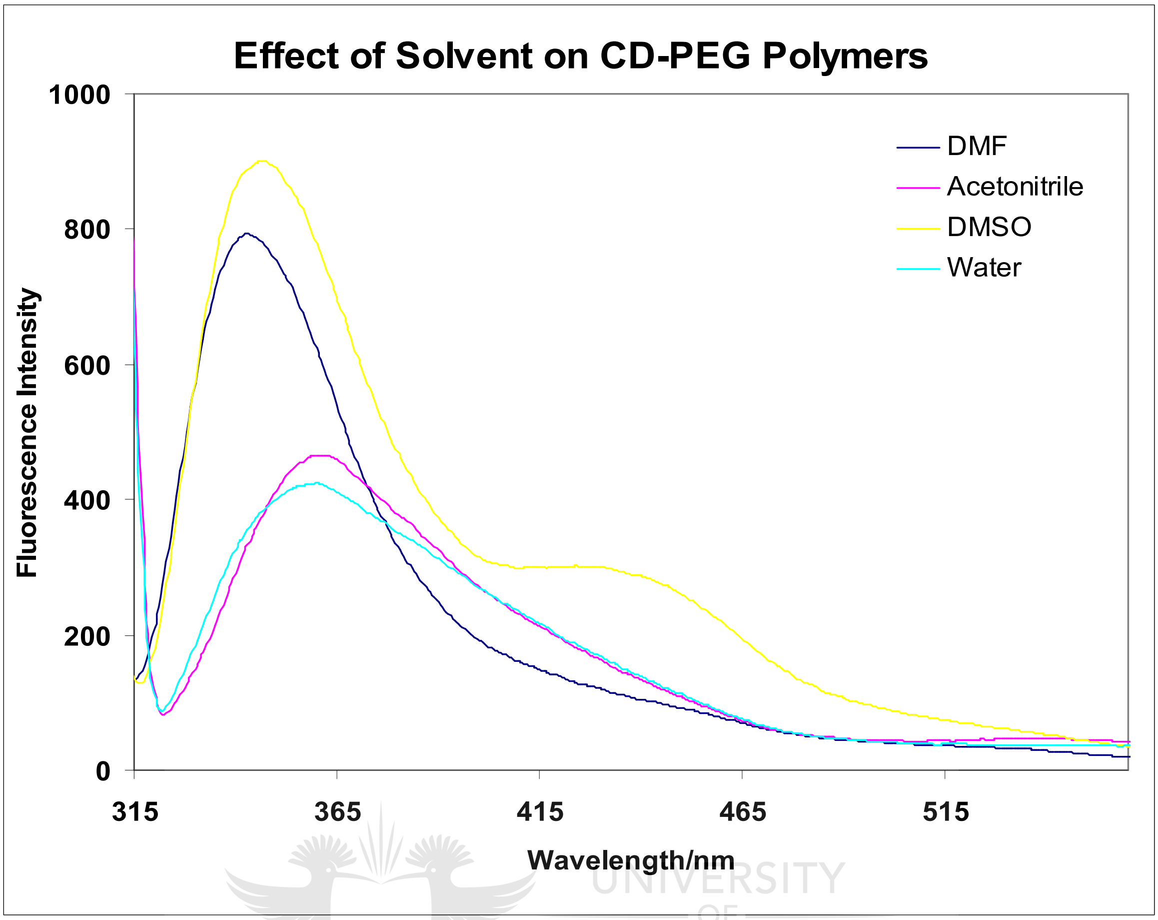

Figure 4A.9: Fluorescence spectra of the azo dye CD polymer in different solvents (λ_{exc} = 305 nm)

The fluorescence intensity of the polymer is greatly enhanced in DMSO and in DMF as compared to acetonitrile and water. A blue shift is also observed with the former solvents, with the fluorescence being shifted from around 370 nm for acetonitrile and water to around 350 nm for DMSO and DMF. The polarity of the solvents used is in the order H_2O > DMSO > CH_3CN > DMF. Since there is no correlation between the polarity and the observed effect on fluorescence, a possible explanation can come from the fact that both DMF and DMSO have bulkier methyl groups as compared to the other two solvents and therefore similar effects.

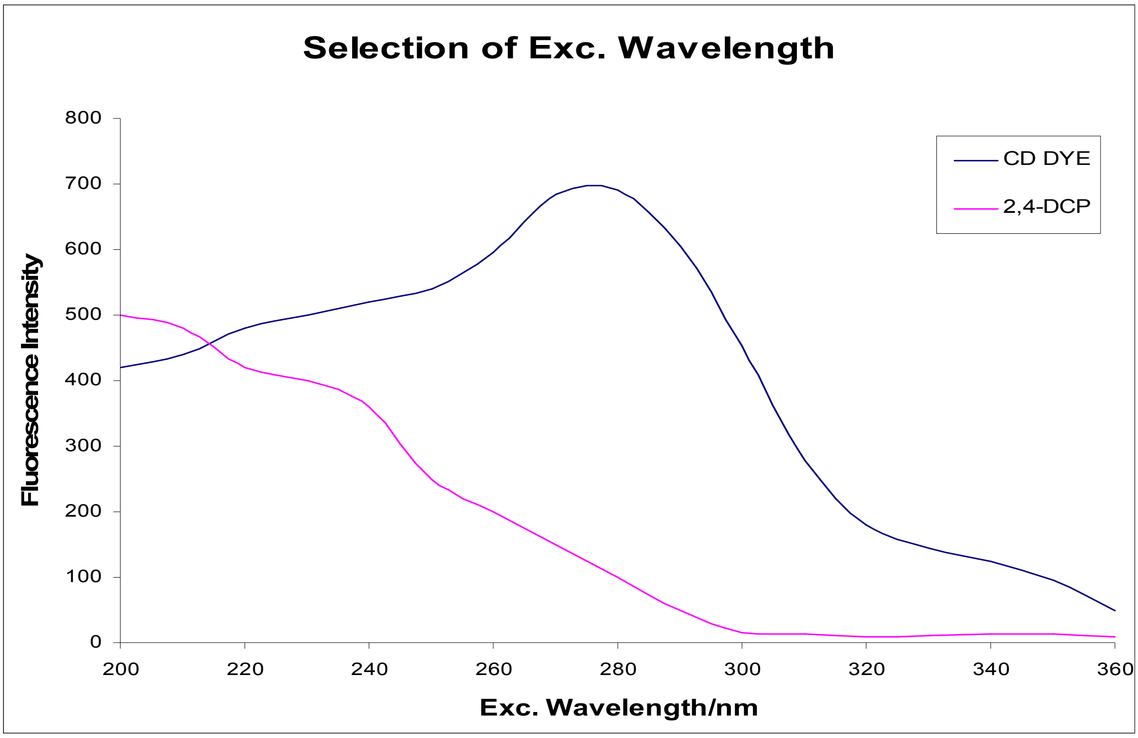

Figure 4A.10: Variation of fluorescence emission at different excitation wavelengths

4.3.3.2 Sensing properties

The response of the azo dye β-CD polymer towards CBPs was investigated by determining the sensitivity of the polymer towards the selected CBPs and binding constants of the sensor/CBP inclusion complexes using fluorescence spectroscopy (Liu et al., 2007; Becuwe et al., 2008).

4.3.3.3 Sensitivity factors

To calculate the sensitivity of the azo dye-modified cyclodextrin polymer towards the pollutants, the same amount of pollutant (2 mM) was added to separate aqueous solutions (50 ppm) of the polymer (**Figure 4A.11**). The fluorescence intensity of the polymer solution was greatly quenched by addition of 2,4-dichlorophenol as compared to phenol and 4-chlorophenol.

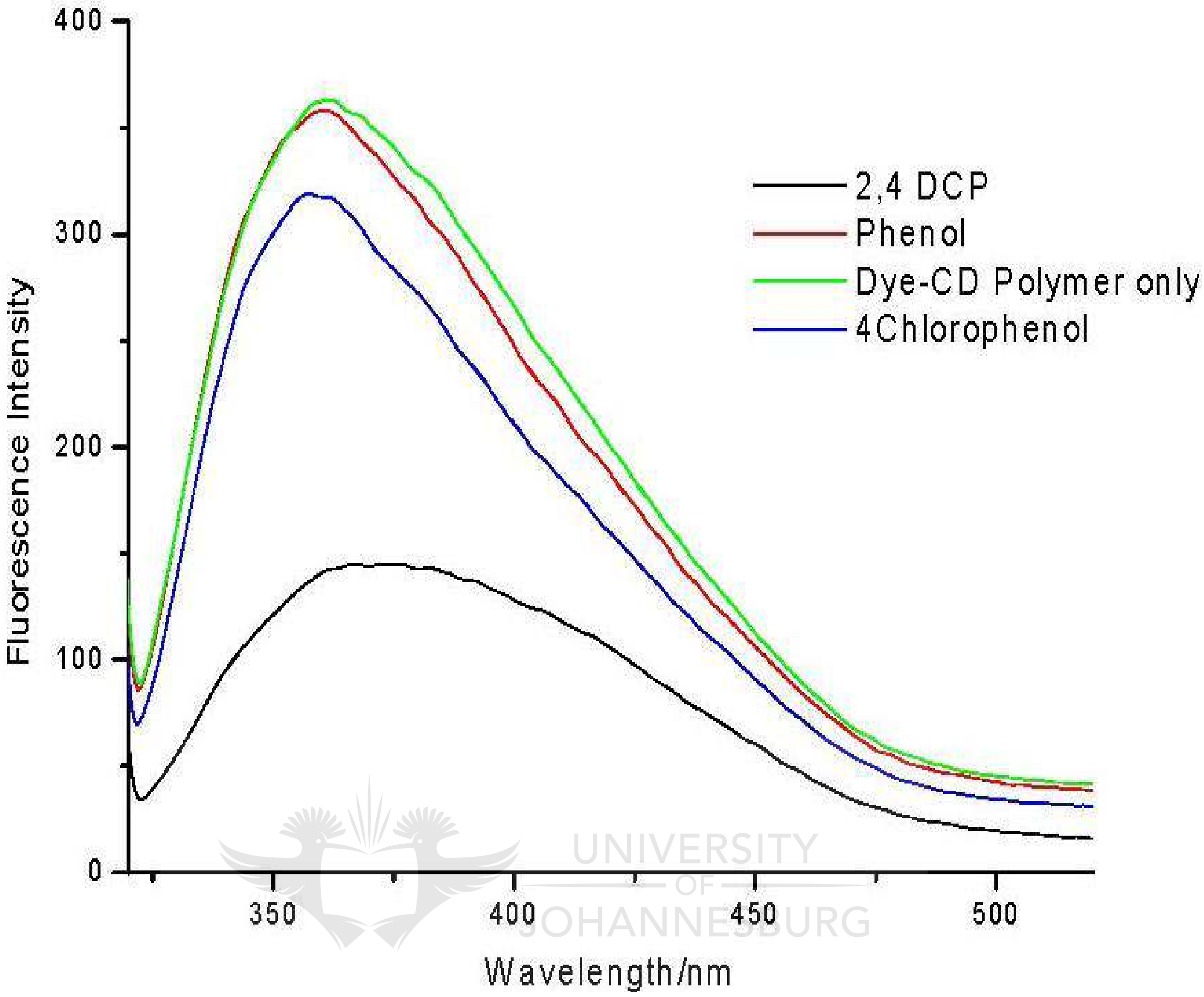

Figure 4A.11: Fluorescence spectra of dye-modified CD polymer on addition of different pollutants {[dye-CD-polymer] = 50 ppm; [pollutant] = 2.0 mM}

The sensitivity towards different pollutants is then estimated by calculating sensitivity factors (SF) as:

$$SF = \Delta I / I_o$$

where:

$\Delta I = I_o - I$

I_o is the fluorescence intensity in the absence of pollutant

I is the fluorescence intensity in the presence of pollutant (Surpateanu et al., 2007)

The sensitivity factors for phenol, 4-chlorophenol and 2,4-dichlorophenol are shown in **Table 4A.1**.

Table 4A.1: Sensitivity factors

Pollutant	CD dye	CD dye polymer
Phenol	$< 1 \times 10^{-4}$	0.05
4-Chlorophenol	$< 1 \times 10^{-4}$	0.12
2,4-Dichlorophenol	$< 1 \times 10^{-4}$	0.35

The sensitivity factors show that the polymer has greater sensitivity towards the chlorinated phenols as compared to phenol. Among the chlorophenols this polymer is more sensitive towards 2,4-dichlorophenol. This result means that the synthesised polymer can be used for molecular recognition of chlorophenols.

4.3.3.4 Titration experiments

To closely investigate the molecular recognition of the pollutants in aqueous solution by the dye-modified polymer, titration experiments were carried out. **Figure 4A.12** shows the effect of adding 2,4-dichlorophenol to a 50 ppm aqueous solution of the polymer. On adding small amounts of the pollutant (0 µℓ to 350 µℓ) the fluorescence intensity was quenched (very small volumes of pollutant are added in such experiments to ensure that any observed change is not due to dilution effects).

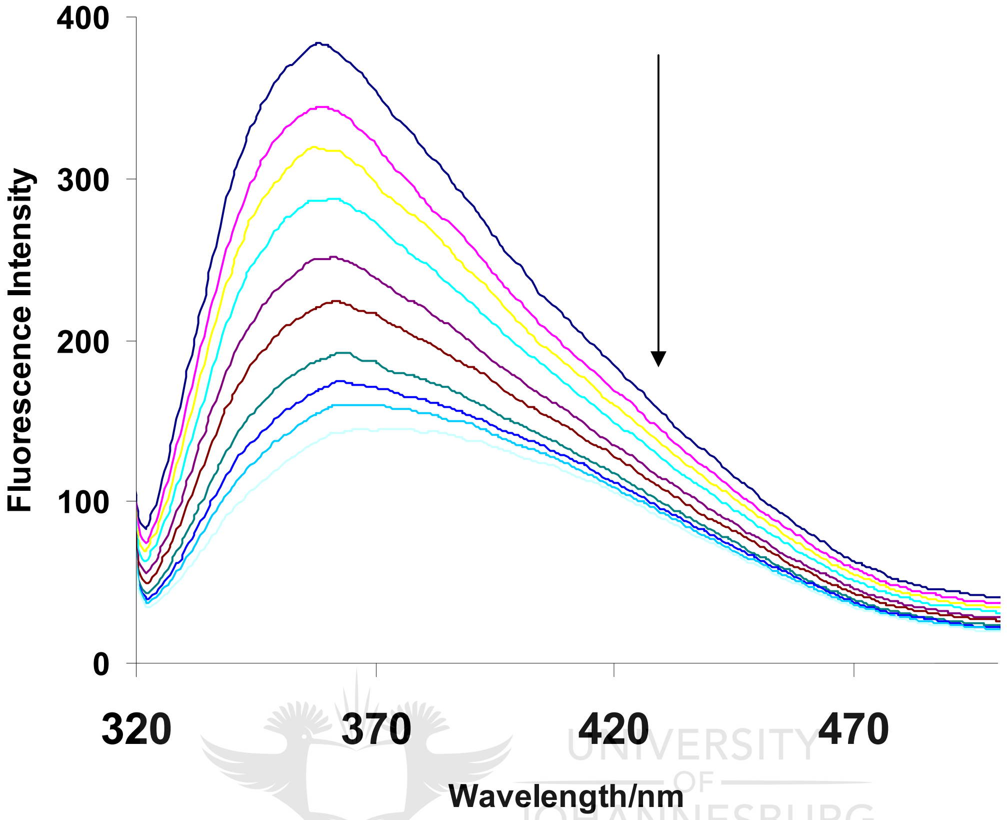

Figure 4A.12: Fluorescence quenching by addition of increasing amounts of 2,4-DCP {[dye-CD-polymer] = 50 ppm; [2,4-DCP] = 0 mM to 2.7 mM}

Figure 4A.13 shows a plot of Δ*I* vs. the concentration of pollutant added, where:

$$\Delta I = I_o - I$$

where:

I_o is the fluorescence intensity in the absence of pollutant

I is the fluorescence intensity in the presence of pollutant

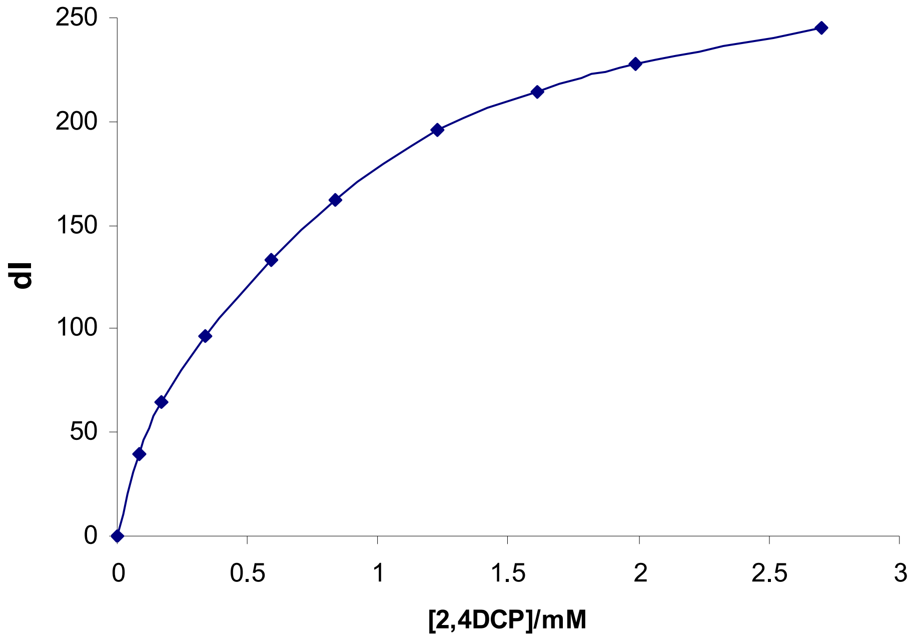

Figure 4A.13: Plot of concentration of 2,4-DCP vs. the change in fluorescence intensity (Δ*I*) with each addition of 2,4-DCP

As the concentration of the pollutant increases, the change in fluorescence intensity gradually becomes small indicating that the change observed is due to the interaction between the cyclodextrin and the pollutant. As the concentration increases the cyclodextrin cavities become saturated and therefore no further change in fluorescence is observed.

In general, fluorescence intensity of a substituted cyclodextrin decreases when a guest molecule is added because of competitive inclusion, that is, the preferred binding of the guest molecule into the cyclodextrin cavity excludes the fluorescent substituent out of the cavity into the hydrophilic aqueous environment, thereby quenching its fluorescence (Ogoshi and Harada, 2008). In a similar way, for our case, it can be inferred that the encapsulated azo dye group is excluded from the cyclodextrin cavity on addition of the chlorophenols, into the aqueous environment, thus the observed fluorescence quenching. The 2,4-dichlorophenol guest molecule displaces most of the azo dye moiety, hence the greater quenching of fluorescence. This implies that the 2,4-dichlorophenol guest molecule complexes most strongly with the cyclodextrin cavity and this is validated by calculating stability constants.

4.3.3.5 Stability constants

Stability constants, K_s also referred to as binding constants or association constants were determined from Benesi-Hildebrand plots (Benesi and Hildebrand, 1949; Al-Shihry, 2005). These plots are linear for a 1:1 stoichiometry. **Figure 4A.14** below shows a Benesi-Hildebrand plot for the CD dye polymer in the presence of increasing amounts of 2,4-dichlorophenol.

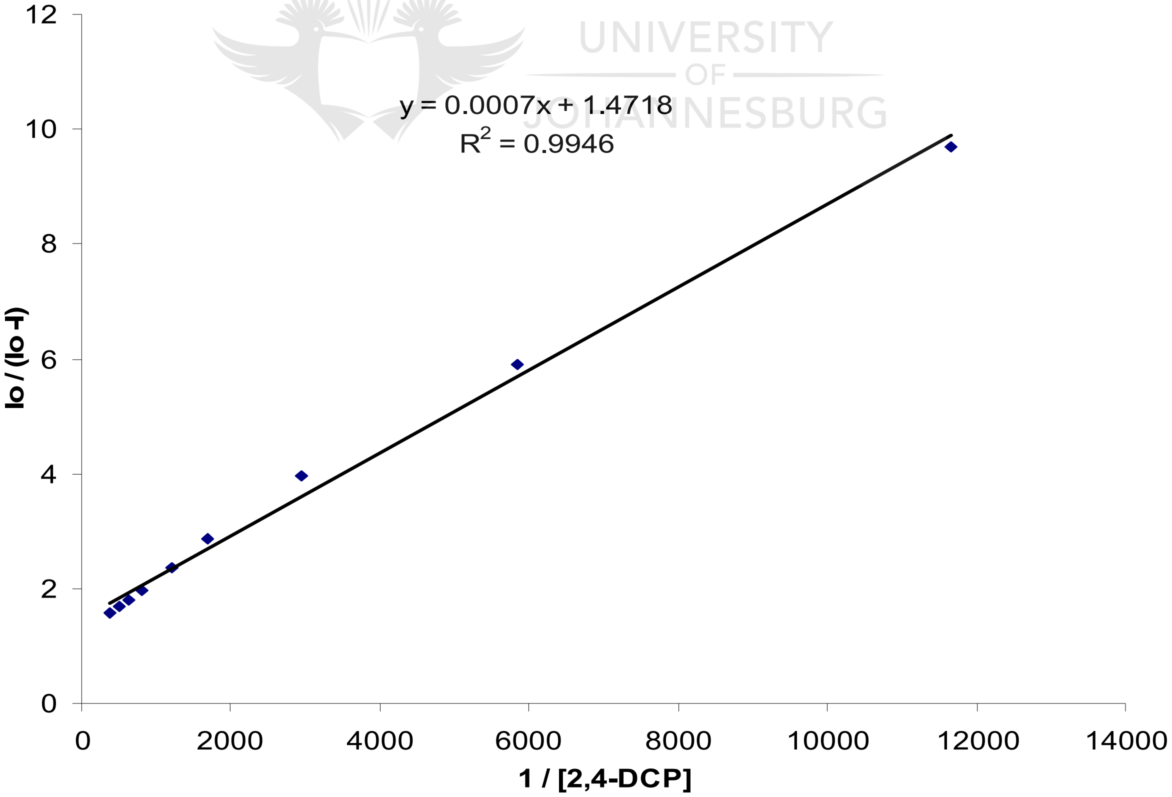

Figure 4A.14: Benesi-Hildebrand plot of CD dye polymer in presence of 2,4-DCP (0 mM to 2.7 mM)

A very good correlation coefficient of 0.9946 was seen for the plot, showing that the possible complex formed between the cyclodextrin and the pollutant is of a 1:1 stoichiometry. From the plot, the stability constant (K_s) was calculated by taking the intercept to slope ratio (Móczár et al., 2010),

$$K_s = \text{y-intercept/slope}$$

which for 2,4-DCP from **Figure 4A.14** was found to be 2104. Similar plots were made for the other pollutants and are summarised in **Table 4A.2**.

Table 4A.2: Stability constants

Pollutant	**K_s (fluorescence)***	**Literature *K* values (Leyva et al., 2001)**	
		K_s(UV-Vis)	**K_s (^{1}H-NMR)**
4-Chlorophenol	112	427	420
2,4-Dichlorophenol	2104	350	556

* K_s value for phenol could not be calculated as the fluorescence quenching was very small on addition of phenol.

Inclusion complexes formed between β-cyclodextrins and chlorophenols have been studied by several other researchers (Cserhati et al., 1988; & 1990; Leyva et al., 2001). The general trend seen is that the stability constants increase with the number and position of chloro-substituents, which is in agreement with our results. **Table 4A.2** also shows stability constants obtained by Leyva et al. (2001) using different methods. The stability constant obtained with our β-cyclodextrin derivative with 2,4-dichlorophenol is higher than obtained previously while that for 4-chlorophenol is lower. This may be good in the selectivity towards 2,4-dichlorophenol over 4-chlorophenol. The fluorescence difference on adding phenol was so insignificant that it was not possible to calculate stability constants, since the difference fell well within the error margin of the fluorescence spectrometer used (~ ±20 a.u. fluorescence intensity). However, from the literature, values of K_s for phenol have been calculated to be around 100 using similar β-CD dye derivatives (Becuwe et al., 2008). This means that our β-CD dye polymer forms very stable complexes with 2,4-dichlorophenol (K_s = 2104 M^{-1}) and can be a good probe for the molecular recognition of chlorinated products in water.

4.4 CONCLUSIONS

A new ethylene glycol linked azo dye-modified β-cyclodextrin polymer was synthesised and characterised. The fluorescence of the polymer was quenched by the addition of the chlorophenols studied with sensitivity towards 2,4-dichlorophenol being the greatest among the studied phenols. The stability constant, K_s for 2,4-dichlorophenol was calculated to be 2.104 x 10^3 M^{-1} which indicated that the inclusion complex formed with this pollutant was the most stable.

The fact that there was enhanced host-guest interaction between the chlorophenols and CD unit in the synthesised sensor as compared to native CD has implications on the application of the sensor. Such a polymer has the potential to be used as a probe for the molecular recognition of guests in molecular sensors for the detection of chlorinated organic molecules in drinking water. This fluorometric detection of non-fluorescent molecules can easily be used as a simple means of testing water quality.

4.5 REFERENCES

Al-Shihry, S.S. (2005). Spectroscopic studies of inclusion complexes of 1-naphthol-4-sulfonate with β-cyclodextrin in aqueous solution. *Spectrochim. Acta Mol. Biomol. Spectros.* **61**, 2439-2443.

Becuwe, M., Landy, D., Delattre, F., Czier, F. and Fourmentin, S. (2008). Fluorescent indolizine-β-cyclodextrin derivatives for the detection of volatile organic compounds. *Sensors* **8**, 3689-3705.

Benesi, H. A. and J. H. Hildebrand (1949). A Spectrophotometric Investigation of the Interaction of Iodine with Aromatic Hydrocarbons. *J. Am. Chem. Soc.* **71**(8): 2703-2707.

Casas-Solvas, J.M., Martos-Maldonado, M.C. and Vargas-Berenguel, A. (2008). Synthesis of β-cyclodextrin derivatives functionalised with azobenzene. *Tetrahedron* **64**, 10919-10923.

Cserhati, T., Szejtli, J. and Fenyvesi, E. (1988). Reversed-phase thin-layer chromatography of some chlorophenols in the presence of a soluble β-cyclodextrin polymer. *J. Chromatogr.* **439**, 393-403.

Cserhati, T., Szejtli, J. and Szogyi, M. (1990). Charge-transfer chromatographic study on inclusion complex formation between two hydroxypropyl- β-cyclodextrins and some chlorophenols. *J. Chromatogr.* **509**, 255-262.

Hamon, F., Djedaini-Pilard, F., Barbot, F. and Len, C. (2009). Azobenzenes: Synthesis and carbohydrate applications. *Tetrahedron* **65**, 10105-10123.

Leyva, E., Moctezuma, E., Strouse, J. and García-Garibay, M.A. (2001). Spectrometric and 2D NMR studies on the complexation of chlorophenols with cyclodextrins. *J. Incl. Phenom. Macrocycl. Chem*. **39**, 41-46.

Liu, Y., Shi, J. and Guo, D.H. (2007). Novel permethylated β-cyclodextrin derivatives appended with chromophores as efficient fluorescent sensors for the molecular recognition of bile salts. *J. Org. Chem.* ***72***, 8227-8234.

Móczár, I., Huszthy, P., Mezei, A., Kádár, M., Nyitrai, J. and Tóth, K. (2010). Synthesis and optical characterization of novel aza crown ethers containing an acridinone or an N-methylacridinone unit as a potential fluorescent chemosensor. *Tetrahedron* **66**, 350-358.

Muderawan, I.W., Ong, T.T., Lee, T.C., Young, D.J., Ching, C.B. and Ng, S.C. (2005). A reliable synthesis of 2- and 6-amino-β-cyclodextrin and permethylated-β-cyclodextrin. *Tetrahedron Lett.* **46**, 7905-7907.

Ogoshi, T. and Harada, A. (2008). Chemical sensors based on cyclodextrin derivatives. *Sensors* **8**, 4961-4982.

Surpateanu, G.G., Becuwe, M., Lungu, N.C., Dron, P.I., Fourmentin, S., Landy, D. and Surpateanu, G. (2007). Photochemical behaviour upon the inclusion for some volatile organic compounds in new fluorescent indolizine β-cyclodextrin sensors. *J. Photochem. Photobiol. A-Chem.* **185**, 312-320.

Zhong, N., Byun, H.S. and Bittman, R. (1998). An improved synthesis of 6-o-monotosyl-6-deoxy-β- cyclodextrin. *Tetrahedron Lett.* **39**, 2919-2920.

CHAPTER 4B

FLUOROMETRIC SENSING OF CHLOROFORM IN WATER USING AN AZO DYE-MODIFIED β-CD – EPICHLOROHYDRIN POLYMER

4.6 INTRODUCTION

Halogenated organic compounds are one of the largest groups of organic pollutants in water and of these trihalomethanes (THMs) are generally the most common. These small chlorinated organic molecules have been detected in drinking water despite their low solubility in water (WHO, 2004). Sources of these THMs are the use of chlorine, chlorine dioxide and chloramines in the disinfection of drinking water and many industrial chemical processes. Disinfection using chlorine and its compounds results in the formation of disinfection by-products (DBPs). The chlorine reacts with natural organic matter in the water to form these DBPs (Xie, 2004). Trihalomethanes (THMs) are the most common DBPs, with haloacetic acids (HAAs), trihaloacetaldehydes, haloacetonitriles, haloacetones, and trihalonitromethanes being the other organic DBPs that have been detected in chlorinated drinking water. Among the THMs, chloroform is the most commonly occurring and most harmful to health. The *South African Water Quality Guidelines*, for example, stipulate that prolonged long-term exposure to dose levels greater than 15 mg/kg of chloroform leads to pathological changes in the liver, kidney and thyroid gland (DWAF, 1996).

Many other industrial chemical processes result in the release of other small chlorinated organic molecules into water sources. These include molecules like dichloromethane, CH_2Cl_2 (DCM), 1,2-dichloroethane, CH_2ClCH_2Cl (1,2-DCE), 1,2-dichloropropane (1,2-DCP) and 1,3-dichloropropane (1,3-DCP). Concern over these small chlorinated compounds in drinking water has been necessitated by their suspected carcinogenic effects (Lawrence et al., 1984; King and Marrett,

---

The work presented in this chapter has been accepted for publication in the journal: *Physics and Chemistry of the Earth*, 2013, **In Press**.

1996), liver and kidney damage and spontaneous abortion (Gopal et al., 2007), among other health affects that have been linked to these chemicals. Local and international organisations such as the World Health Organization (WHO) have regulated these chemicals, together with many others, because of the health concerns associated with them. The WHO guideline concentration limit for chloroform is given as 0.3 mg/ℓ (WHO, 1996).

In this work an azo dye-modified β-CD was copolymerised with epichlorohydrin and used as a molecular sensor for the detection of chloroform as a model disinfection by-product. It is anticipated that such a molecular sensing probe can be incorporated into a simple hand-held gadget that could be used by small communities to determine the water quality and its suitability for drinking in line with the goals of the Integrated Water Resources Management (IWRM) (Mazvimavi et al., 2008) and the UN Millennium Development Goals (Nhapi et al., 2005).

4.7 EXPERIMENTAL

The synthetic procedures and characterisation techniques are given in **Chapter 3.**

4.8 RESULTS AND DISCUSSION

4.8.1 Synthesis and characterisation of copolymers

The copolymers of native β-CD with epichlorohydrin (EPC) have previously been synthesised (Renard et al., 1997). In our work, in addition to the polymerisation of native β-CD, an azo dye-modified β-CD was also used to yield the dye-modified sensor copolymer **3** (**Scheme 4B.1**). The azo dye-modified β-CD used had been synthesised as described in our previous work (Ncube et al., 2011).

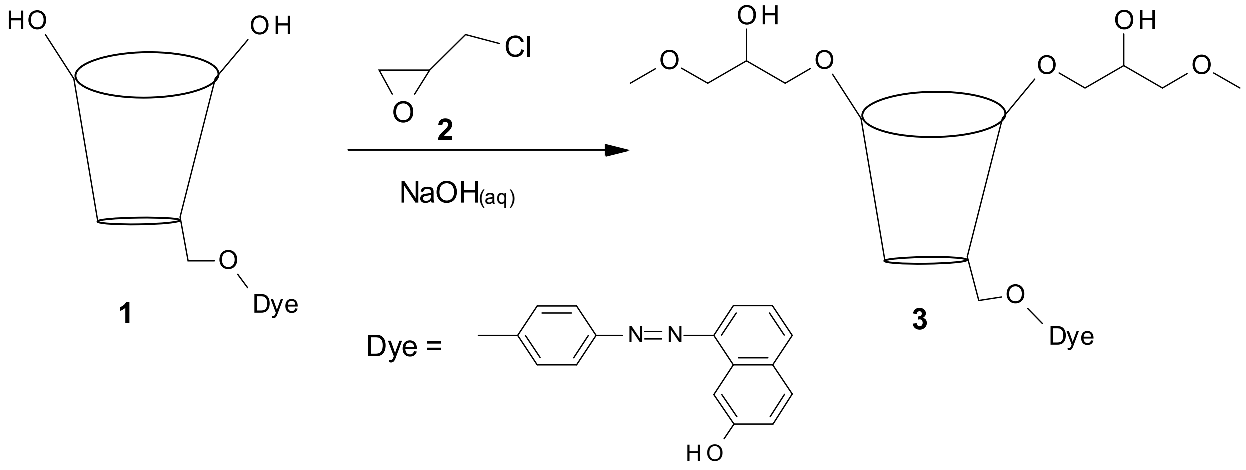

Scheme 4B.1: Synthesis of dye-modified β-CD-epichlorohydrin copolymer

The ratio EPH/β-CD, reaction time and temperature are important factors influencing the properties of the final product. In this work, a ratio of EPC/ β-CD = 15, a reaction time of 4 h and a reaction temperature of 60^{o}C was selected as these conditions produce water-soluble polymers. According to the work reported by Renard et al. (1997), EPC/β-CD ratios of between 4 and 20 result in water-soluble polymers while ratios 20 yield hard, water-insoluble copolymers. A water-soluble sensing material was desirable in our work for ease of analysis of the chlorinated aliphatic compounds which are not completely soluble in water.

4.8.1.1 UV-Vis and fluorescence characterisation

The UV-Vis absorption spectra of the EPC-CD copolymers with and without the dye attached are shown in **Figure 4B.1(a).** In absence of the dye there is no absorption peak observed, while two peaks, one at 404 nm and the other at 485 nm, are observed for the dye-modified copolymer. The first peak at 404 nm may be attributed to the absorption due to the phenyl part of the azo dye while the peak at 485 nm is due to the naphthyl moiety (see **Scheme 4B.1**).

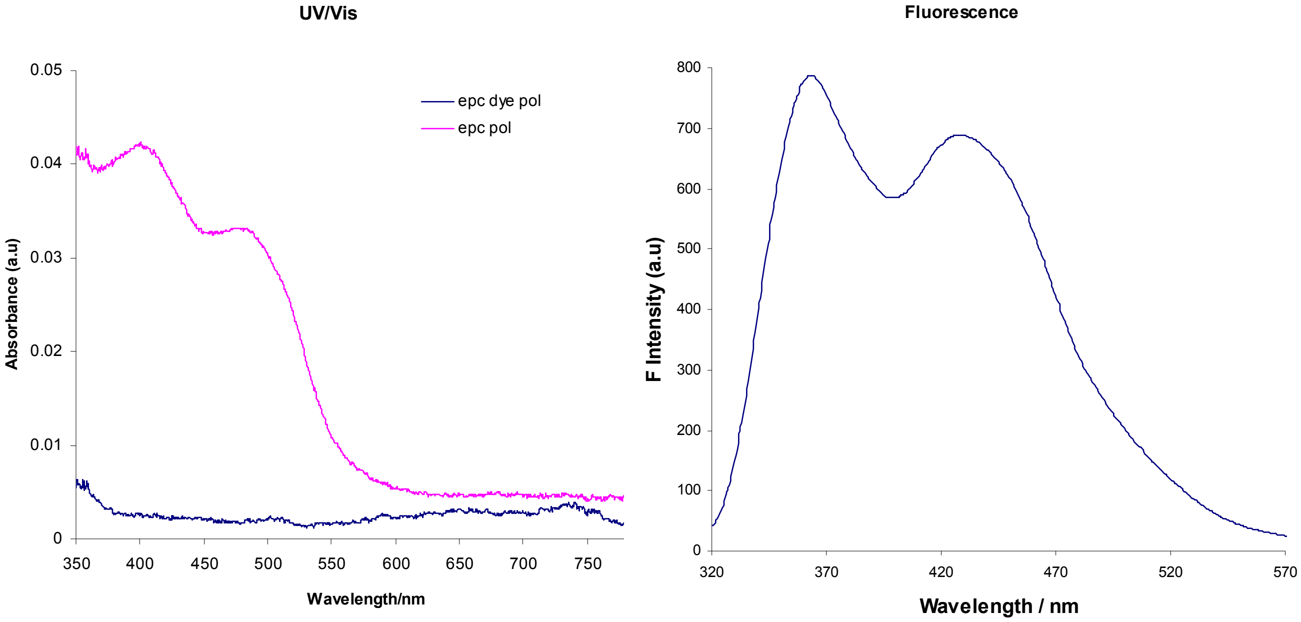

(a) **(b)**

Figure 4B.1: Absorption (a) and fluorescence (b) spectra of the β-CD-epichlorohydrin copolymer

The fluorescence spectrum [**Figure 4B.1(b)**] of the dye-modified copolymer shows two emission peaks, one at 364 nm and the other at 429 nm. Similarly, the first peak (364 nm) is due to excitation of the phenyl electrons while the second (429 nm) is due to the naphthyl group of the dye. Similar spectra were obtained for 2-naphthol containing EPC-CD copolymers synthesised by Zohrehvand and Evans (2005). This was, in part, a confirmation that we had indeed managed to copolymerise the azo dye-modified CD with epichlorohydrin.

4.8.1.2 FT-IR spectroscopic characterization

The FTIR spectra of native β-CD, dye-modified-β-CD (cd-dye), and the copolymer (epc-cd dye copoly) are shown in **Figure 4B.2**.

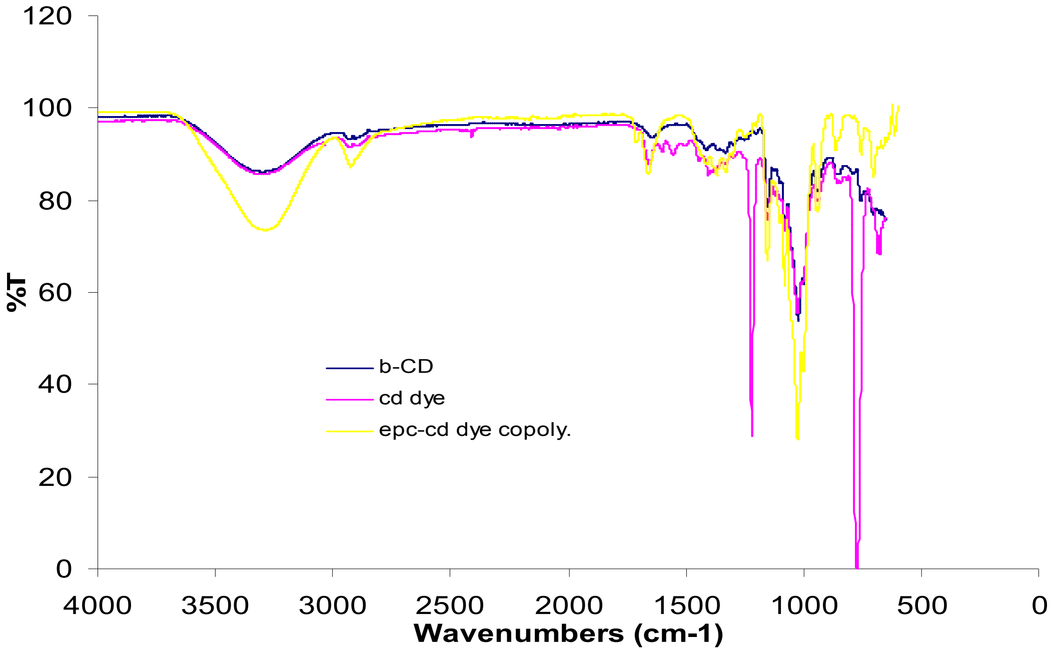

Figure 4B.2: FT-IR spectra of native β-CD, β-CD-dye and the copolymer sensor (epc-cd dye copoly)

All three compounds and derivatives showed a broad band around 3 280 cm^{-1} to 3 300 cm^{-1} due the presence of hydroxyl (OH) groups. However, the intensity of the peak was greatest for the copolymer as a result of the additional OH groups formed during the polymerisation reaction. Similarly, an increase in the intensity of the peak at 1 023 nm which is due to C – O – C stretch was observed as a result of the additional ester linkages due to polymerisation. Similar observations were noted in the work by Casas-Solvas and co-workers (2008) and this confirmed that indeed polymerisation had taken place.

4.8.1.3 ^{1}H-NMR spectroscopic characterisation

Proton nuclear magnetic resonance spectroscopy (^{1}H-NMR) was also used to characterise the sensor material. Comparing the ^{1}H-NMR spectrum of native cyclodextrin (**Figure 4B.3**) with that of the copolymerised CD without dye (**Figure 4B.4**), it is observed that there was an appearance of two peaks at δ = 2.70 [CH(OH)] and δ = 2.85 (CH_2). These were attributed to the alky protons from the linkage of epichlorohydrin and CD, further confirming that the polymerisation reaction had occurred. Protons due to the dye were observed further downfield in the aromatic region and only the OH group was likely to overlap with the excess CD OH groups not involved in the polymerisation reaction.

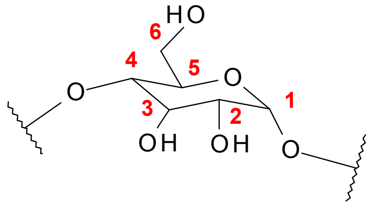

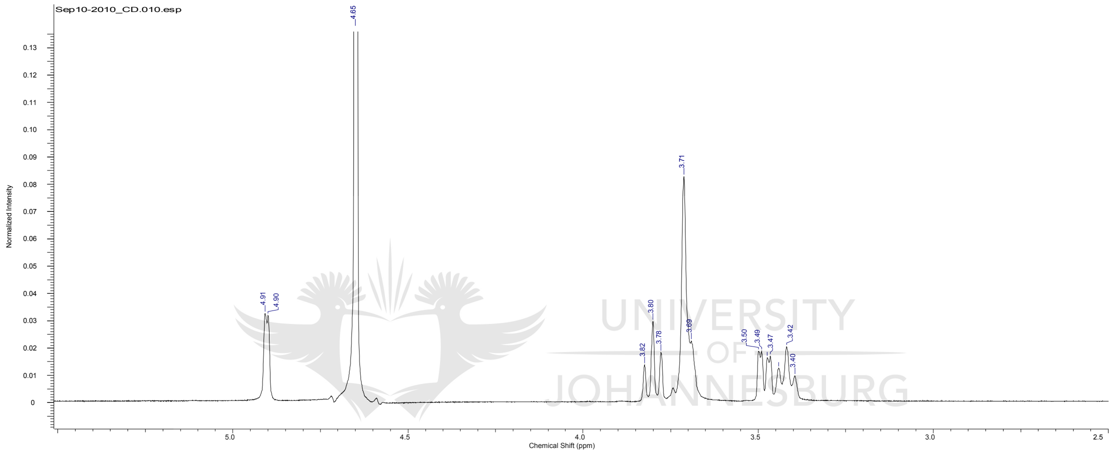

Figure 4B.3: ^{1}H-NMR spectrum of native β-CD (solvent D_2O)

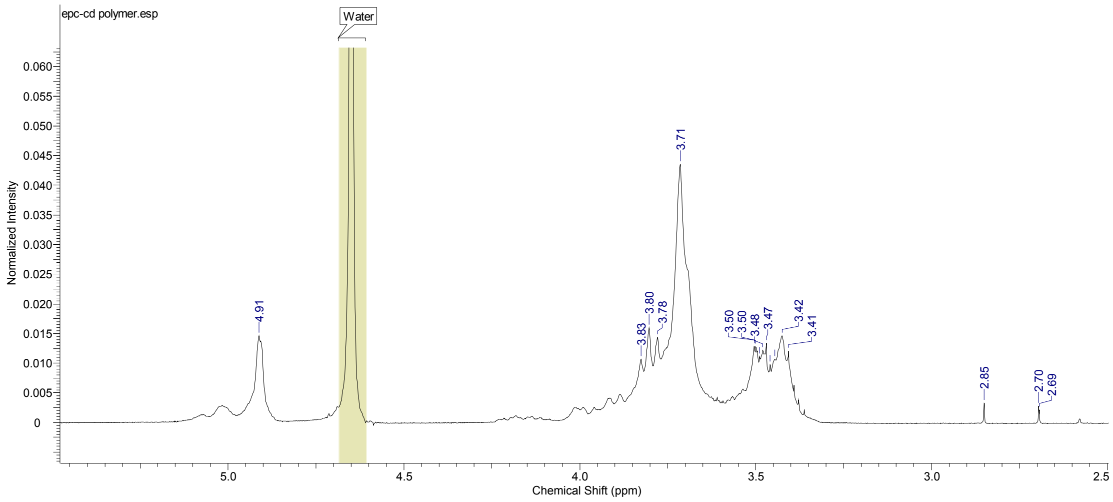

Figure 4B.4: ^{1}H-NMR spectrum of EPC-β-CD copolymer without dye (solvent D_2O)

2-D NMR correlation spectroscopy (COSY) was also done on the synthesised material and is shown in **Figure 4B.5**.

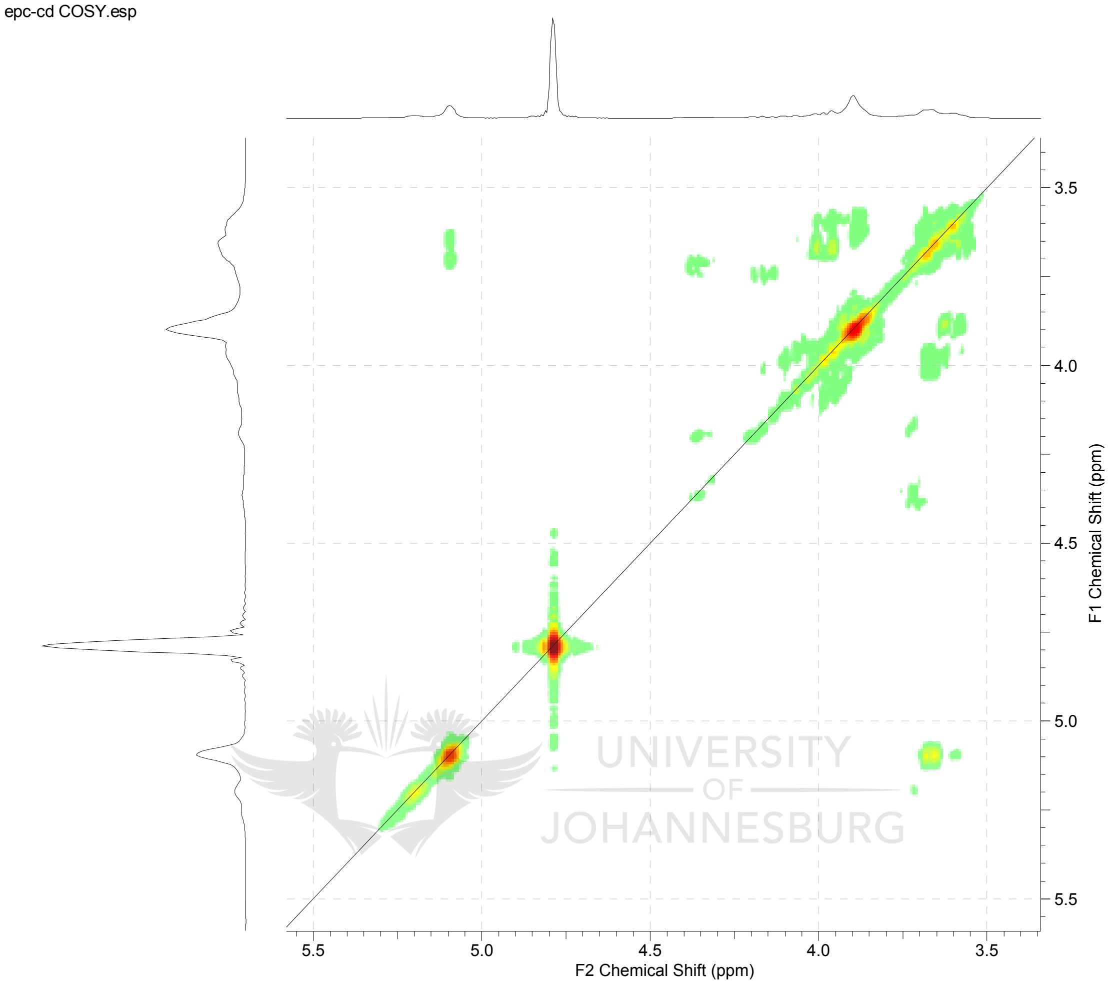

Figure 4B.5: 2D-NMR COSY spectrum EPC-β-CD copolymer

COSY spectral analysis gives insight into the protons that are coupled. As observed there are diagonal spots in the spectrum and off-diagonal spots. It is the off-diagonal spots that give an insight into the structure of molecule. The off-diagonal spot linking the OH protons (δ = 5.05 ppm) and protons around δ = 3.5 – 3.6 ppm show that there is extensive hydrogen bonding in the molecule between the OH and the H atoms of the cyclodextrin.

4.8.2 Quantification of cyclodextrin in EPC-CD polymer

4.8.2.1 NMR quantification

To further characterise the synthesised material, the amount of cyclodextrin was quantified by NMR measurements and by the anthrone method (**Loewus, 1952)**. This was achieved by doping a known amount of the polymer material with a known amount of p-nitrophenol (PNP) and measuring the ^{1}H-NMR spectra. All NMR measurements were done in a Bruker Avance II 400 NMR spectrometer with broad band inverse (BBI) magnet. Solvents used were D_2O. Spectra for the polymer, PNP and the mixture are given in **Figure 4B.6**.

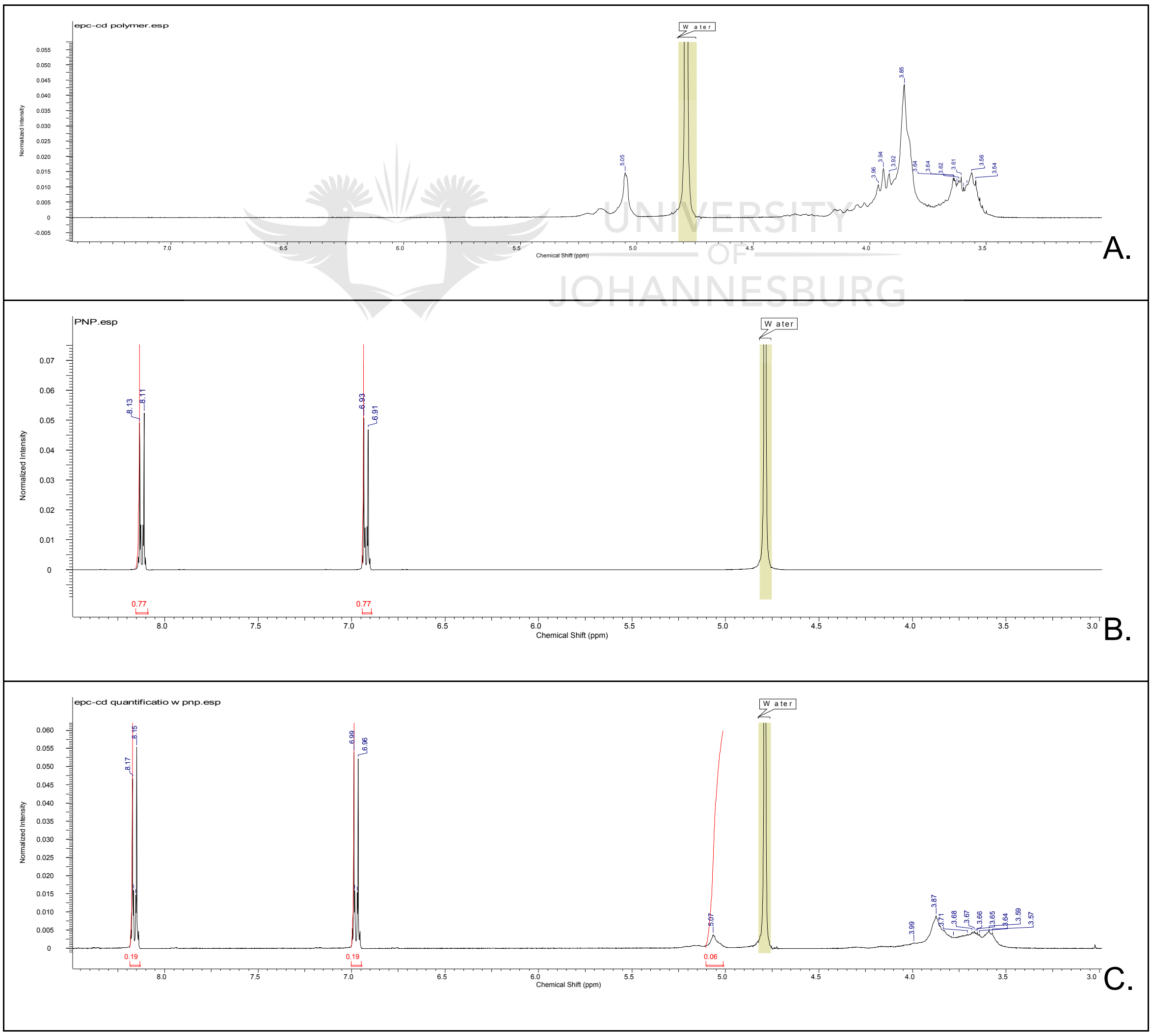

Figure 4B.6: ^{1}H-NMR spectra of polymer (A), PNP (B) and the mixture (B)

From the integration of the peak at δ = 5.05 which is due to the anomeric protons of the β-CD and the peaks for the PNP proton and the concentrations used, the percentage of cyclodextrin was estimated at 72% in the polymer material. The amount of cyclodextrin was also quantified using the anthrone method.

4.8.2.2 Anthrone reaction (Loewus, 1952)

Table 4B.1: Anthrone quantification of cyclodextrin in EPC-CD polymer

	Vol. β-CD stock soln. /mℓ	**Water added /mℓ**	**Anthrone soln. /mℓ**	**Final vol. /mℓ**	**[β-CD] /10^{-6} M**	**Absorbance at 620 nm**
Blank	-	1.60	8.0	9.6	0	0
Std 1	0.05	0.75	4.0	4.8	1.211	0.031
Std 2	0.10	0.70	4.0	4.8	2.423	0.084
Std 3	0.20	0.60	4.0	4.8	4.846	0.155
Std 4	0.40	0.40	4.0	4.8	9.692	0.265
Std 5	0.60	0.20	4.0	4.8	14.54	0.431
Sample	0.20 (sample)	0.60	4.0	4.8	3.591	0.105
Sample	0.20 (sample)	0.60	4.0	4.8	3.318	0.097
Sample	0.20 (sample)	0.60	4.0	4.8	3.079	0.090

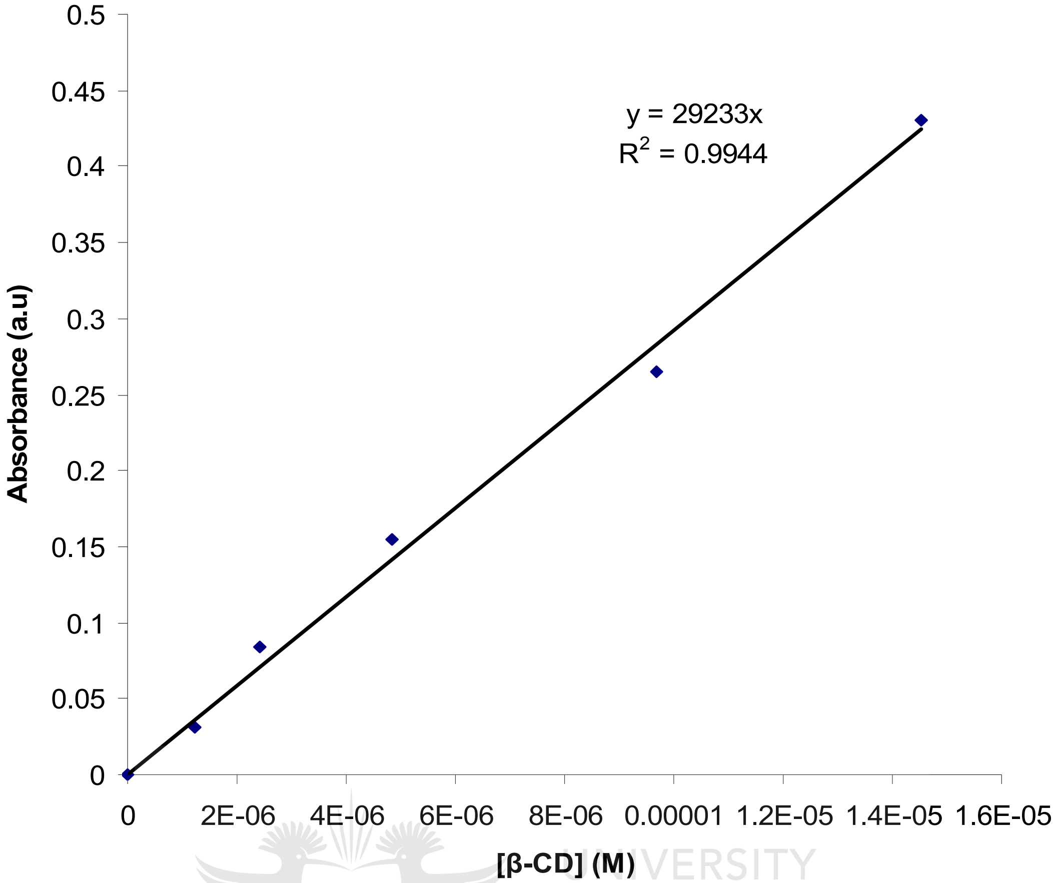

Figure 4B.6: Standard curve for quantification of cyclodextrin in EPC-CD polymer

From the standard curve the concentrations of cyclodextrin was calculated from the measured absorbance for each sample run and are shown in Table 4B.1. From the average concentration of cyclodextrin (3.329 x 10^{-6} M), the percentage in the sample was calculated to be 66.7% which is in good agreement with NMR quantification.

4.8.3 Thermodynamics of binding of guest molecules to EPC-CD polymer by ITC

4.8.3.1 Complexation with amantadine

The interaction of the synthesized EPC-CD polymer with organic guests was studied first with amantadine. Adamantine derivatives are known to form very stable complexes with both native cyclodextrin and modified cyclodextrin [Gomez et al., 2006]. The ITC results for the interaction of amantadine with native β-CD are shown in **Figure 4B.7** and those for EPC- β-CD polymer are shown in **Figure 4B.8**.

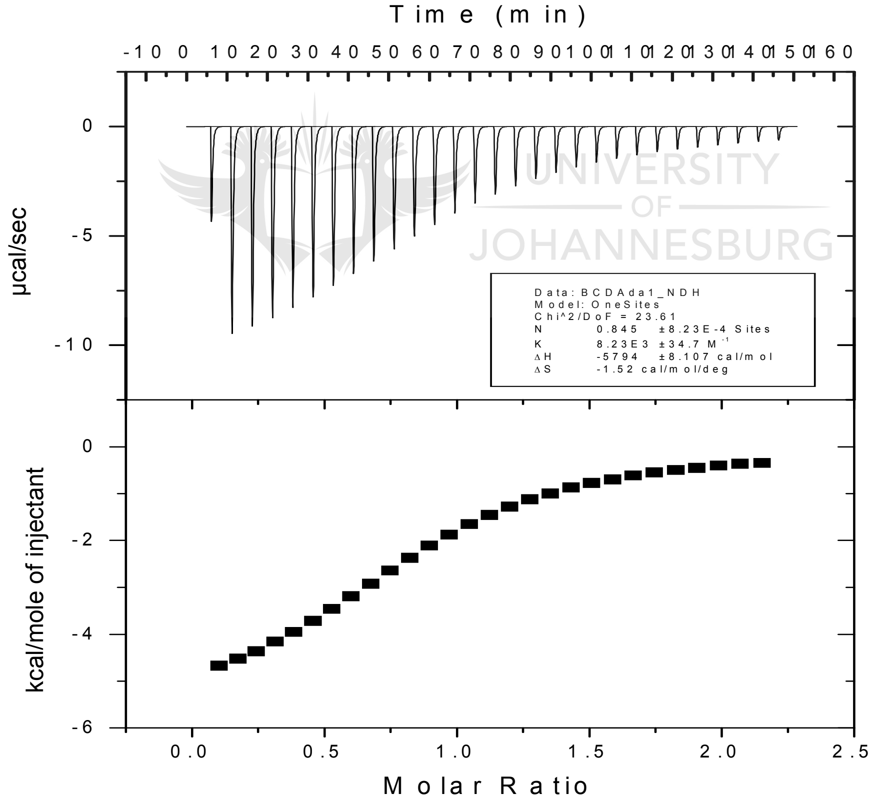

Figure 4B.7: ITC results for native β-CD complexation with amantadine

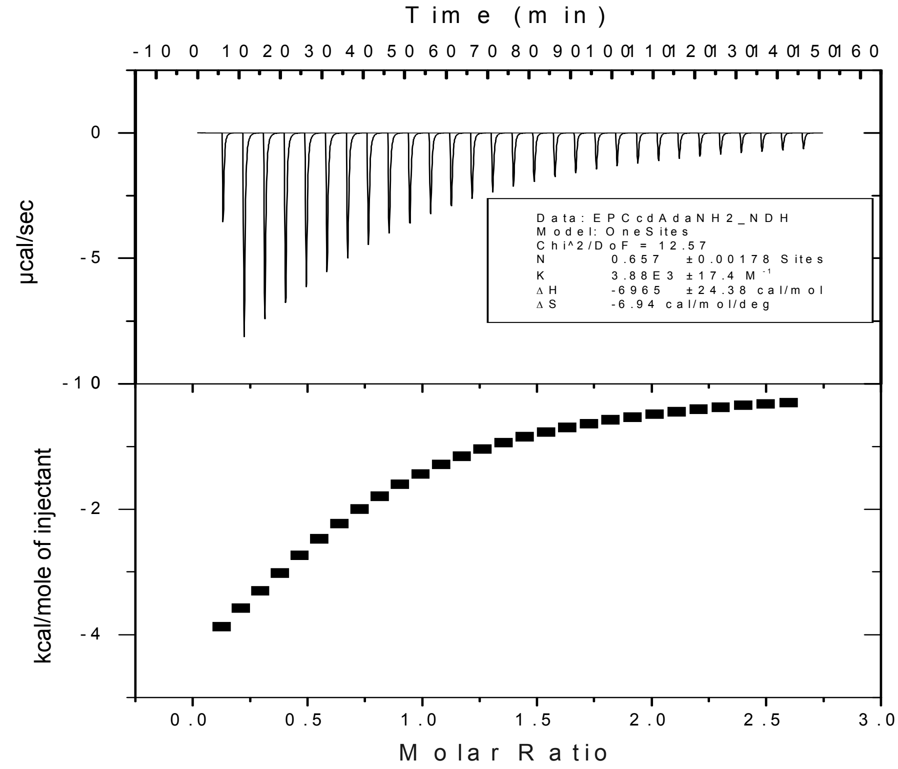

Figure 4B.8: ITC results for EPC-CD polymer complexation with amantadine

The stoichiometries for both native β-CD (n = 0.845) and for EPC-CD (n = 0.655), were found to be consistent with the 1:1 stoichiometry characteristic of cyclodextrin-adamantine complexes. The enthalpy change was negative ($\Delta H < 0$) for both the native and the modified β-CD, and were close in value meaning that the binding mechanism is the same. The association constant K, was slightly lower for the modified cyclodextrin ($K = 3.88 \times 10^{-3}\ M^{-1}$) as compared to the native β-CD ($K = 8.23 \times 10^{-3}\ M^{-1}$), but are both in the same order of magnitude ($10^{3}\ M^{-1}$). The entropy change, ΔS is more negative for the EPC-CD polymer (ΔS = - 6. 94 cal/mol/deg) than for the native β-CD (ΔS = - 1. 52 cal/mol/deg), meaning that the interaction is less favourable. This less favourable entropy explains the lower K value and is as a result of the polymerisation process which reduces the translational and conformational freedom of the EPC-CD polymer. For both processes, $|\Delta H| > |T\Delta S|$, which means that the interaction is through Van der Waals forces and is enthalpy driven. Also for both cases $\Delta G < 0$ which means that the complex formation process occurs spontaneously. The similar complex formation parameters for the native and polymerised β-CD show that the cyclodextrin cavities are available for interacting with guests even after the polymerisation process. The complex formation of the EPC-CD polymer with two guest molecules was investigated by ITC.

4.8.3.2 Complexation with p-chlorophenol and 1-chloronaphthalene

The ITC raw data and integrated peak areas for para-chlorophenol are shown in **Figure 4B.9** and that for 1-chloronaphthalene is shown in **Figure 4B.10**.

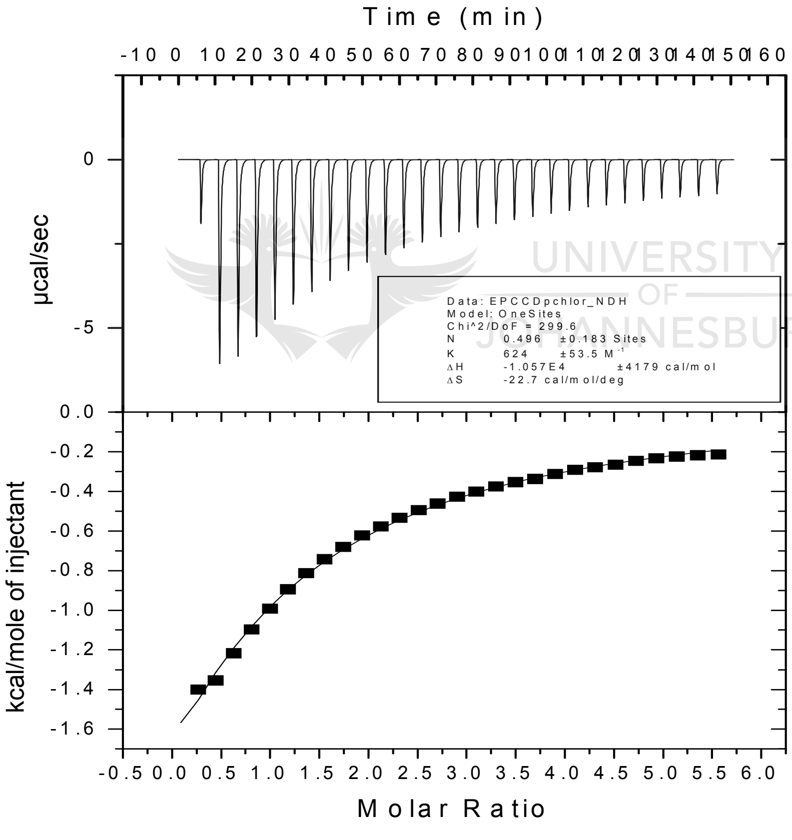

Figure 4B.9: ITC results for EPC-CD polymer complexation with p-chlorophenol

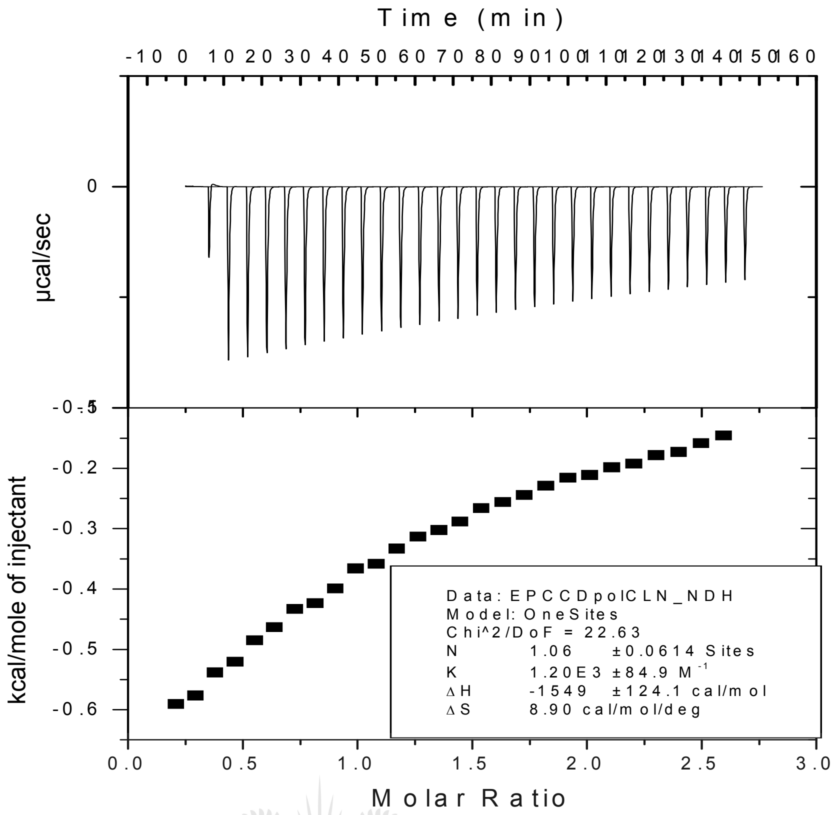

Figure 4B.10: ITC results for EPC-CD polymer complexation with 1-chloronaphthalene

The complex formation processes indicated a 1:1 stoichiometry. The association constant *K* (*K* = 624 M^{-1}) for the p-nitrophenol : EPC-CD complex was in the same order of magnitude with the literature value for β-CD (*K* = 407 M^{-1}) [Rekharsky and Inoue, 1998). A slightly higher association constant for the polymer material may be desirable for use of the material for complex formation with similar guest molecules. The entropy change was negative (Δ*S* = - 22.7 cal/mol·deg) whereas the literature value for β-CD is slightly positive (Δ*S* = +2.4 cal/mol·deg), a result of the reduced conformational freedom due to polymerisation. Also |Δ*H*| > |*T*Δ*S*| and as in the case for amantadine, the process is enthalpy driven with no contribution from entropy effects. In the case of 1-chloronaphthalene the *K* value is the same for the native CD as for the polymer. However, Δ*S* for the polymer is much more positive while Δ*H* is small meaning that the process is entropy driven (|Δ*H*| >

|*T*Δ*S*|). The interaction is therefore by hydrophobic interactions between the 1-chloro-naphthalene guest and the cyclodextrin cavities. The Gibbs free energy (Δ*G*) is negative for all interactions meaning that the processes occur spontaneously.

4.9 Fluorometric detection of chloroform

In addition to chloroform **1**, five other chloroalkanes were investigated for comparison. The chloroalkanes were dichloromethane **2**; 1,2-dichloroethane **3**; 1,1,2-trichloroethane **4**; 1,2-dichloropropane **5;** and 1,3-dichloropropane **6** (**Scheme 4B.2**).

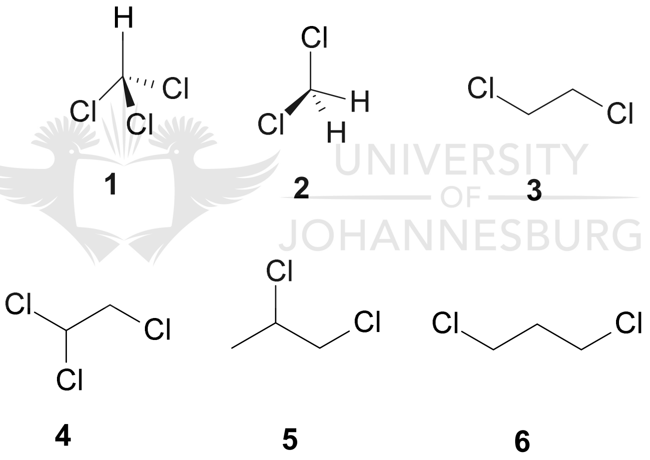

Scheme 4B.2: Structures of studied molecules

Since there was no observed change in the UV-Vis spectrum upon addition of all of the pollutants, fluorescence spectroscopy was selected for the study of host-guest interaction of the polymer sensor with the pollutants. Interaction of such small organic molecules with β-cyclodextrin and their subsequent fluorescent detection has been demonstrated in previous work by Nakashima and Yoshida, (2006) in which small acyclic and cyclic alcohols were investigated. In order to ascertain optimum conditions for the performance of the sensor, fluorescence behaviour was first investigated at various pH values.

4.9.1 Optimisation of pH conditions

To attain the optimum pH for the sensing by the polymer probe, fluorescence intensities, at the emission peak at λ = 429 nm, were measured at different pH values (**Figure 4B.11**). The maximum fluorescence was obtained at pH = 7.03. The maximum at this pH could be due to the fact that the sensor has high fluorescence when it is not charged whereas at low pH and high pH when it is cationic and anionic due to protonation and deprotonation of hydroxyl groups respectively, the fluorescence emission is reduced. A buffer solution (Titrisol® buffer at pH 7) was therefore selected for all subsequent fluorescence measurements.

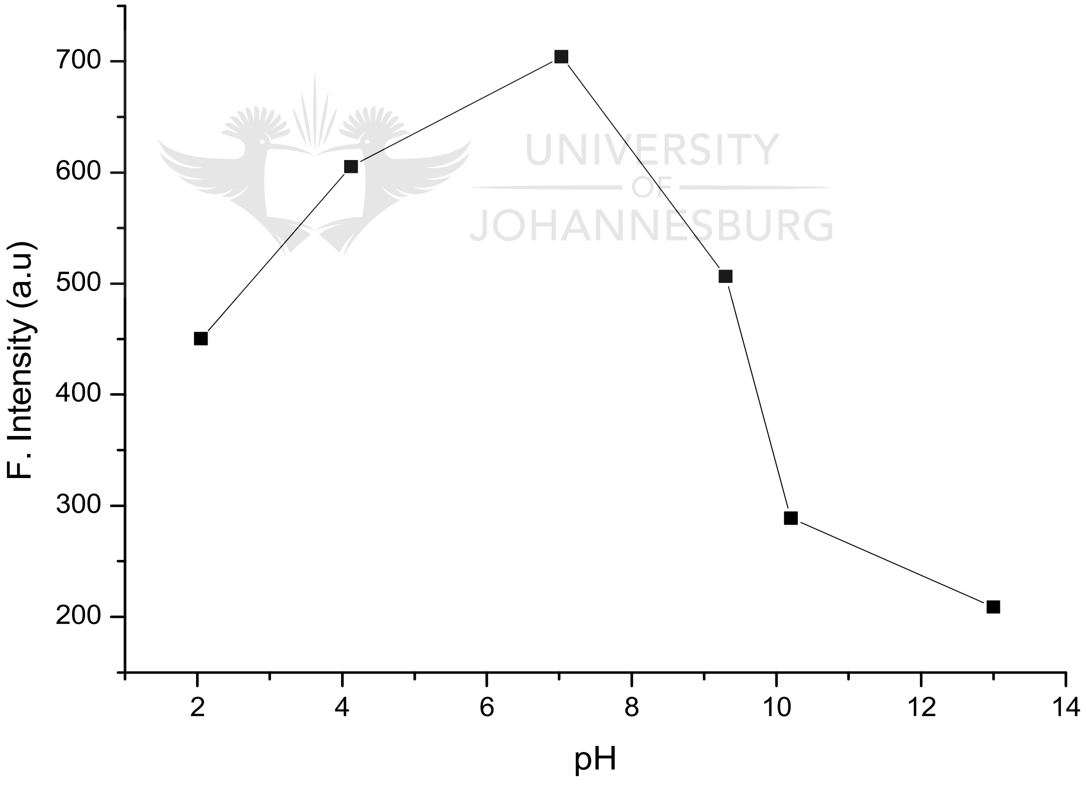

Figure 4B.11: Optimisation of pH for maximum fluorescence emission of the β-CD-epichlorohydrin-dye copolymer ([Dye] = 1ppm; $\lambda_{exc.}$ = 305 nm; F. Intensity at λ = 429 nm)

4.9.2 Fluorescent recognition of chlorinated compounds

The six different chlorinated compounds were each added separately to the EPC-CD dye copolymer solution (1.0 ppm) and the fluorescence spectrum for each solution recorded and plotted on the same axes (**Figure 4B.12**). The concentration of chloroform added was 15 μM while the concentrations of other pollutants were maintained at 150 μM. The addition of chloroform resulted in a significant quenching of the fluorescence, particularly the emission at 429 nm. While the concentration of the other pollutants was ten times more (150 μM compared to 15 μM) than that of chloroform their presence did not alter the fluorescence intensity of the sensor much. The **inset** in **Figure 4B.12** illustrates the greater quenching efficiency of chloroform as compared to the other studied molecules.

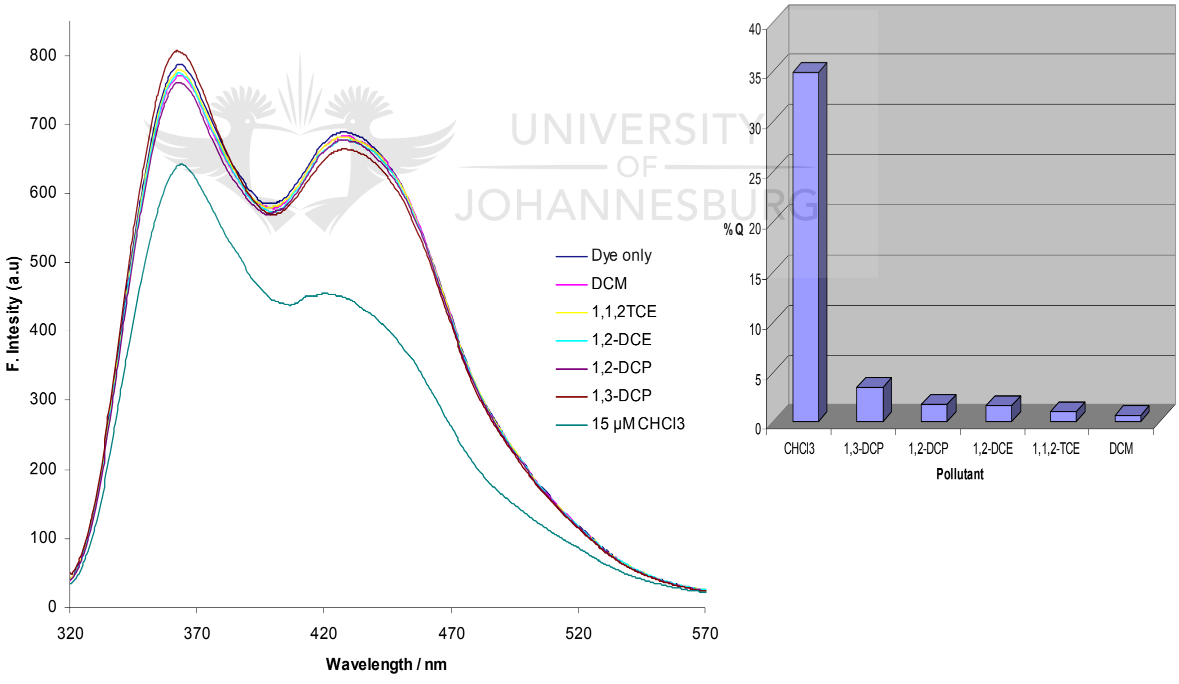

Figure 4B.12: Effect of adding chlorinated compounds on the fluorescence of the dye-modified β-CD-epichlorohydrin copolymer (EPH-CD dye); [dye] = 1 ppm, $[CHCl_3]$ = 15 μM; [1,2-DCE] = [1,2-DCP] = [1,3-DCP] = 150 μM; $\lambda_{exc.}$ = 305 nm. ***Inset:*** **Quenching efficiency (%Q) of each pollutant (λ = 429 nm)**

4.9.2.1 Sensing factors

To quantify the sensitivity of the probe towards the different chlorinated compounds, sensing factors were calculated (Narita et al., 1999). The higher the sensing factor for a molecule, the more sensitive the probe is to that molecule. The sensing factor (SF) for each pollutant was calculated as:

$$SF = \Delta I / I_o \qquad \textbf{9}$$

where:

$\Delta I = I_o - I$

I_o is the fluorescence intensity in the absence of the pollutant

I is the fluorescence intensity in the presence of pollutant (Yorozu et al. 1982)

The sensitivity factors are summarised in **Table 4B.2**. The sensitivity towards chloroform is ten times more than that of the next molecule, namely 1,3-dichloropropane and is about 50 times greater than for dichloromethane, towards which the probe was least sensitive. The chlorinated compounds in **Table 4B.2** represent typical pollutants often found in disinfected water.

Table 4B.2: Sensitivity factors

Chlorinated compound	Sensing factor
Chloroform	0.35
1,3 Dichloropropane	0.035
1,2-Dichloroethane	0.017
1,2-Dichloropropane	0.017
1,1,2-Trichloroethane	0.011
Dichloromethane	0.0073

4.9.2.2 Stability constant of the EPC-CD-dye:$CHCl_3$ inclusion complex

To gain further insight into the interaction of the guest chlorinated compounds with the cyclodextrin polymer, titration experiments were carried out (**Figure 4B.13)**. The concentration of chloroform was gradually increased and each emission spectrum was recorded.

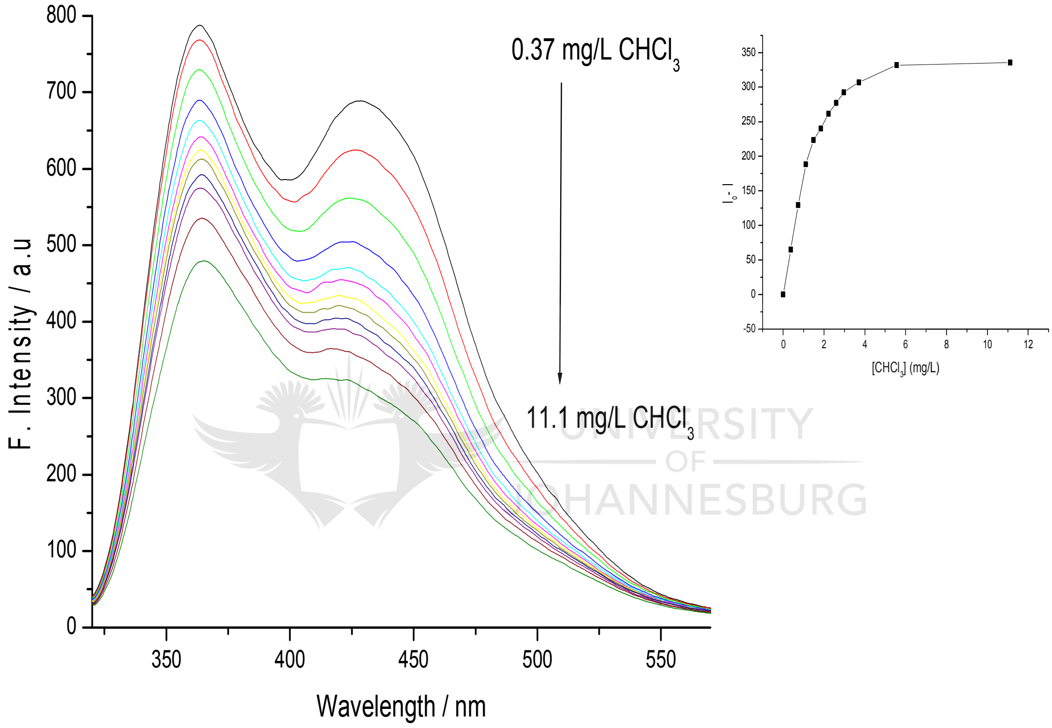

Figure 4B.13: Fluorescence quenching by addition of increasing amounts of chloroform {[dye-CD-polymer] 1 ppm; [chloroform] = 0 to 11.1 mg/ℓ; $\lambda_{exc.}$ = 305 nm}. *Inset*: Plot of concentration of chloroform vs. the change in fluorescence intensity (Δ*I*) with each addition of chloroform.

With an increase in the concentration of chloroform, it is observed that the emission intensity was reduced in a linear fashion initially, but then a plateau was reached at high concentrations (**Figure 4B.13 *Inset***). This supports the assertion that the fluorescence quenching is due to host-guest interaction between cyclodextrin and chloroform, with a plateau being reached because of the saturation of the host cavities (Park et al., 1994; Al-Shihry, 2005).

From the titration experiments, the Benesi-Hildebrand plot (Benesi and Hildebrand, 1945) (**Figure 4B.14**) was drawn in order to obtain the stability constant for the cyclodextrin-guest molecule inclusion complex formed. The stability constant (K_s) for chloroform was calculated from the plot and was found to be 5.00 x 10^4 M^{-1}.

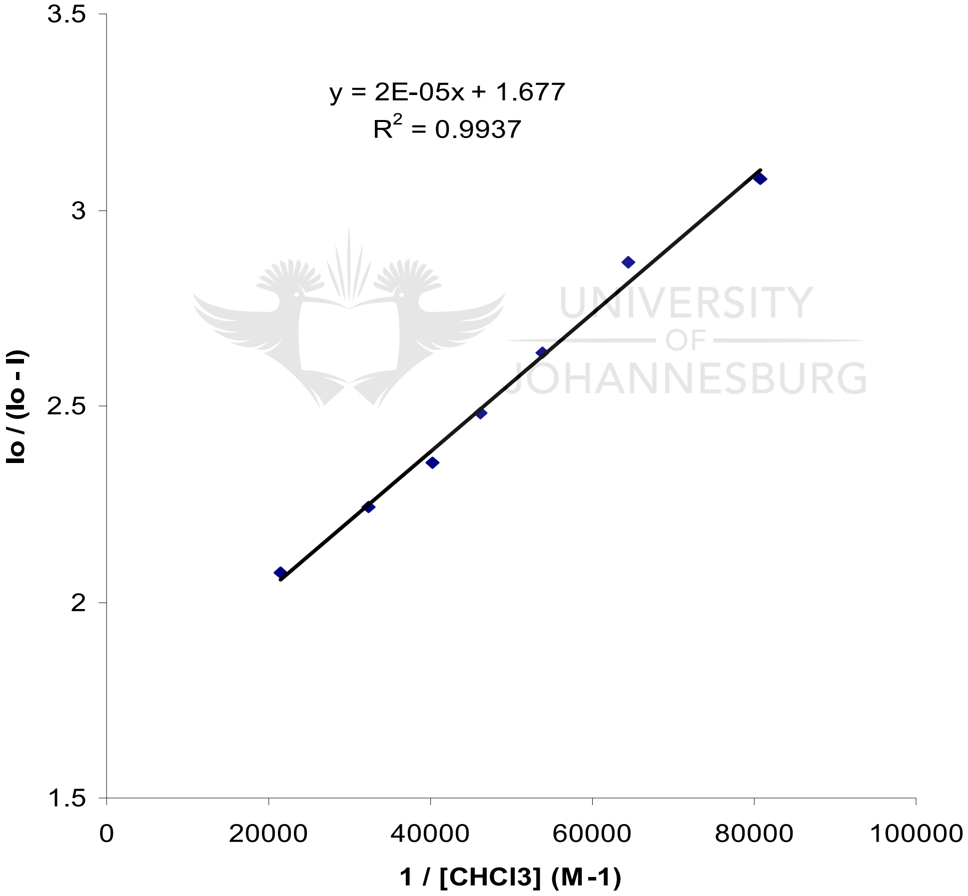

Figure 4B.14: Benesi-Hildebrand plot ([$CHCl_3$] = 1.23 x 10^{-5}M to 4.65 x 10^{-5}M)

4.9.2.3 Interference studies

Since all or some of the chloroalkanes may be present in a typical water sample together with chloroform, it was important to investigate their effect on the fluorescence quenching of the sensor.

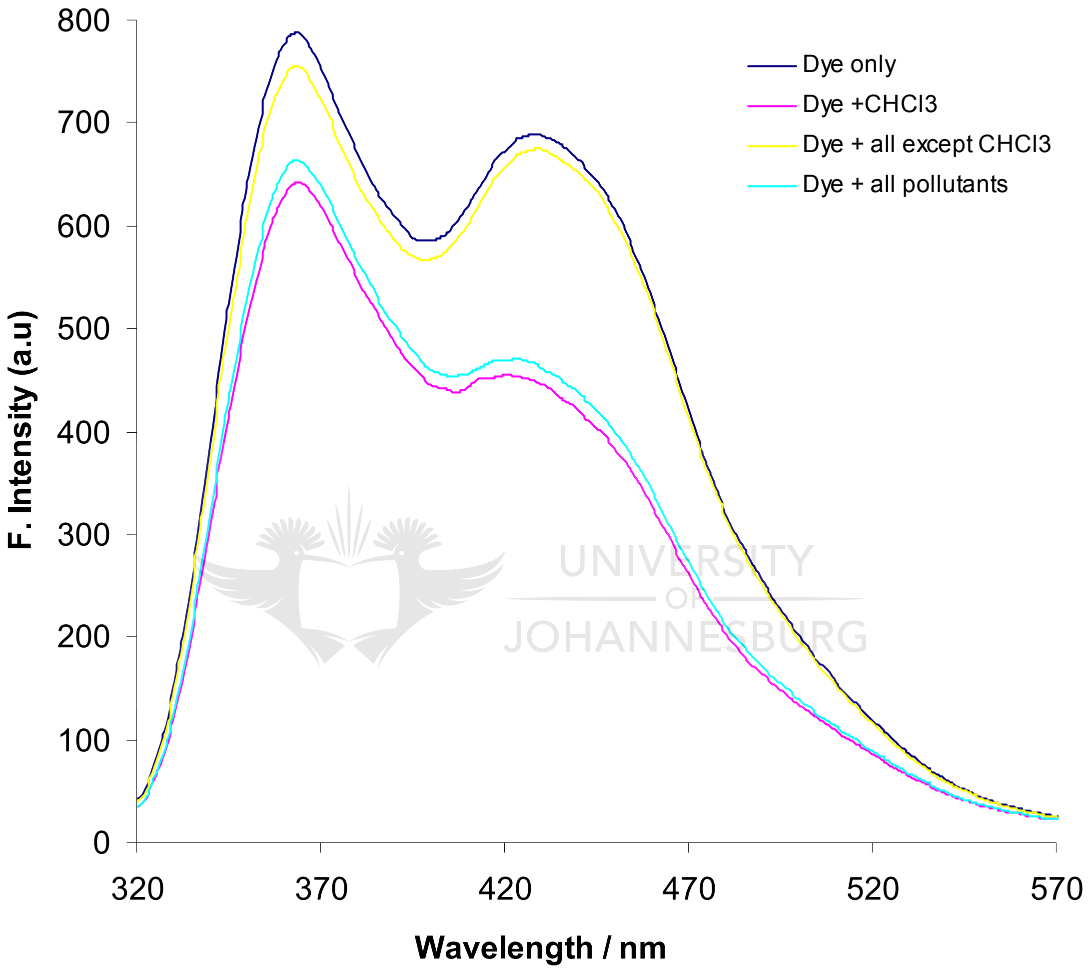

Figure 4B.15: Effect of the presence of other pollutants in water on the fluorescence quenching EPC-CD dye by chloroform; [dye] = 1 ppm; [$CHCl_3$] = 15 μM and [other pollutants] = 0.15 mM; $\lambda_{exc.}$ = 305 nm.

As seen in **Figure 4B.15,** the presence of all pollutants including chloroform results in the same quenching of the sensor. When there was no chloroform added (dye + all except $CHCl_3$) the fluorescence changes observed were insignificant. This demonstrates that the observed fluorescence quenching was due to chloroform and that the presence of other pollutants in the solution had no effect. This suggests that the detection of chloroform by the sensor was not interfered with by the presence of similar chlorinated molecules.

4.9.3 Analysis of real water samples

In investigating the possibility of using the proposed probe in the detection of chloroform in real water samples, two samples were obtained; one from a dam (Sample 1) and the other from a local bottled water (Sample 2). A calibration curve (**Figure 4B.16)** in the linear chloroform concentration range of 0 mg/ℓ to 1.48 mg/ℓ was constructed by plotting the quenching efficiency vs. the concentration (Hu et al., 2010) of chloroform in order to determine the concentrations of chloroform in the water samples.

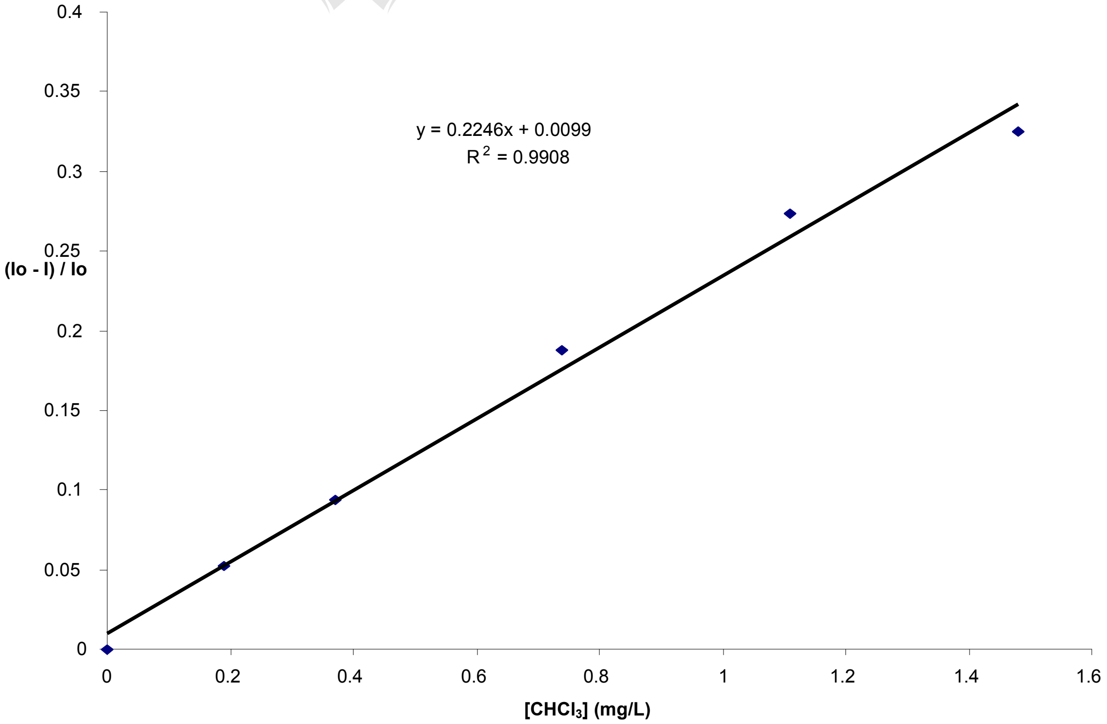

Figure 4B.16: Calibration curve for $CHCl_3$ determination

No chloroform was detected in either of the water samples, so they were spiked with known amounts of chloroform and the sensing polymer probe solution was used to determine the percentage recovery of chloroform.

Table 4B.3: Detection of chloroform in spiked actual water samples

Water sample	Spike level (mg/ℓ)	Detected by polymer sensor (mg/ℓ)	% Recovery
Sample 1	1) 0.50 2) 1.10	1) 0.41 ± 0.01 2) 1.01 ± 0.05	1) 82.0 2) 91.8
Sample 2	1) 0.50 2) 1.10	1) 0.49 ± 0,005 2) 1.07 ± 0.02	1) 98.0 2) 97.3

The percentage recoveries were fairly high for both water samples. Because of the high volatility of chloroform, 100% recoveries are virtually not possible. The slightly lower values for Sample 1 may be due to the fact that the dam water may contain some interfering organic species which are not present in the bottled water sample. The high recoveries for the bottled water (Sample 2) is also indicative of the fact that mineral ions which are usually present in water resources will not affect the functioning of the probe material in detecting chloroform.

4.10 CONCLUSIONS

A simple fluorescent probe for the detection of chloroform was successfully synthesised, characterised and shown to be sensitive and selective towards chloroform. The visual decrease in fluorescence intensity of the probe as a means of detecting chloroform means that the probe can easily be used in the field with a simple hand-held light source. For this reason, the probe can be used in remote rural communities to detect chlorinated compounds and ensure that the quality of water is adequately safe for drinking. The probe was able to detect concentrations in the range of the WHO limit of 0.3 mg/ℓ, which makes it suitable for use in ensuring that the water quality is within world standards. In this way the quality of life of these communities can be greatly improved with less risk of suffering from health effects associated with chlorinated compounds.

REFERENCES

Al-Shihry, S.S. (2005). Spectroscopic studies of inclusion complexes of 1-naphthol-4-sulfonate with β-cyclodextrin in aqueous solution. *Spectrochim. Acta Mol. Biomol. Spectros.* **61**, 2439-2443.

Benesi, H. A. and Hildebrand, J.H. (1949). A spectrophotometric investigation of the interaction of iodine with aromatic hydrocarbons. *J. Am. Chem. Soc.* **71**(8), 2703-2707.

Casas-Solvas, J.M., Martos-Maldonado, M.C., and Vargas-Berenguel, A. (2008). Synthesis of [beta]-cyclodextrin derivatives functionalized with azobenzene. *Tetrahedron* **64**(48), 10919-10923.

Department of Water Affairs and Forestry (DWAF) (1996). *South African Water Quality Guidelines* (2nd edition). **Volume 1**: *Domestic Use*. pp.163 – 166. <http://www.dwaf.gov.za/IWQS/wq_guide/domestic.pdf> (Accessed on 12-02-2013).

Gomez, C. G. and Chambat, G., Heyraud, A., Villar, M. and Auzely-Velty, R. (2006). Synthesis and characterization of a β-CD-alginate conjugate. *Polymer* **47**(26), 8509-8516.

Gopal, K., Tripathy, S.S., Bersillon, J.L. and Dubey, S.P. (2007). Chlorination byproducts, their toxicodynamics and removal from drinking water. *J. Hazard. Mater.* **140**(1-2), 1-6.

Hu, D., Sheng, Z., Gong, P., Zhang, P. and Cai, L. (2010). Highly selective fluorescent sensors for Hg^{2+} based on bovine serum albumin-capped gold nanoclusters. *Analyst* **135**, 1411-1416.

King, W.D. and Marrett, L.D. (1996). Case-control study of bladder cancer and chlorination by-products in treated water (Ontario, Canada). *Cancer Causes and Control* **7**, 596-604.

Lawrence, C.E. Taylor, P.R., Trock, B.J. and Reilly, A.A. (1984). Trihalomethanes in drinking water and colorectal cancer. *J. Nat. Cancer Inst.* **72**, 563-568.

Loewus, F. A. (1952). Improvement in Anthrone Method for Determination of Carbohydrates. *Anal. Chem.* **24**(1), 219-219.

Mazvimavi, D. Hoko, Z., Jonker, L., Nhapi, I., and Senzanje, A. (2008). Integrated water resources management (IWRM) – from concept to practice. *Phys. Chem. Earth*. **33**, 609-613.

Nakashima, H. and Yoshida, N. (2006). Fluorescent detection for cyclic and acyclic alcohol guests by naphthalene-appended amino-β-cyclodextrins. *Org. Lett.* **8**(22), 4997-5000.

Narita, M., Koshizaka, S., and Hamada, F. (1999). Fluorescent pyrrolinone-modified cyclodextrins as a chemo-sensor for organic guests. *J. Incl. Phenom. Macro*. *Chem*. **35**(4), 605-619.

Ncube, P., Krause, R.W. and Mamba B.B. (2011**).** Fluorescent sensing of chlorophenols in water using an azo dye modified β-cyclodextrin polymer. *Sensors* **11**, 4598-4608.

Nhapi, I., Holchi, W., Mazvimavi, D., Mashauri, D.A., Jewitt, G., Mudege, N., Swatuk, L.A. and Benkman, R. (2005). Integrated water resources management (IWRM) and the Millennium Development Goals: Managing water for peace and prosperity. *Phys. Chem. Earth*. **30**, 623-624.

Park, H.-R., Mayer, B., Wolschann, P. and Koehler, G. (1994). Excited-state proton transfer of 2-naphthol inclusion complexes with cyclodextrins. *J. Phys. Chem.* **98**(24), 6158-6166.

Rekharsky, M.V. and Inoue, Y. (1998). Complexation thermodynamics of cyclodextrins. *Chem. Rev.* **98**(5), 1875-1918.

Renard, E., Deratani, A. Volet, G. and Sebille, B. (1997). Preparation and characterization of water soluble high molecular weight β-cyclodextrin-epichlorohydrin polymers. *Europ. Polym. J.* **33**(1), 49-57.

World Health Organization (WHO) (1996). *Guidelines for Drinking-Water Quality* (2nd edn.) **Vol.2**. *Health Criteria and other Supporting Information.* World Health Organization, Geneva, Switzerland.

World Health Organization (WHO) (2004). *Trihalomethanes in Drinking Water*. WHO/SDE/WSH/03.04/64. Background document for development of WHO *Guidelines for Drinking Water Quality,* World Health Organization, Geneva, Switzerland pp. 1-39.

Xie, Y.F. (2004). *Disinfection Byproducts in Drinking Water: Formation, Analysis and Control.* Lewis Publishers: Florida, USA. pp 1-10.

Yorozu, T., Hoshino, M., Imamura, M. and Shizuka, H. (1982). Photoexcited inclusion complexes of beta.-naphthol with .alpha.-, .beta.-, and .gamma.-cyclodextrins in aqueous solutions. *J.Phys. Chem.* **86**(22), 4422-4426.

Zohrehvand, S. and Evans C.H. (2005). 2-Naphthol-containing β-cyclodextrin–epichlorohydrin copolymers: synthesis, characterization and fluorescence studies. *Polym. Int.* **54**(5), 744-753.

CHAPTER 4C

FLUOROMETRIC DETECTION OF HEAVY METALS IN WATER USING DYE-MODIFIED CROWN ETHERS

4.11 INTRODUCTION

The detection of heavy metals in polluted environments is an ever-growing concern and is the subject of current ongoing research in various research groups. Of the toxic heavy metals, mercury is one of the highly toxic metals leading to diseases such as acrodynia (‘pink disease’), Hunter-Russell syndrome and Minamata disease (Fujiki and Tajima, 1992; Kudo et al., 1988; He et al., 2009). Health problems associated with mercury are made worse due to its accumulative and persistent nature in the environment and in living organisms. Mercury is released into water by industrial processes such as coal burning and natural causes like volcanic eruptions (Yari and Papi, 2009).

South Africa has been reported as the second highest emitter of Hg (50 t/yr) in the world after China (Pacyna et al., 2006), even though later estimates dispute this high emission and put Hg emissions in the range of 2.6 t/yr to 17.6 t/yr (Dabrowski et al., 2008). South Africa is the third largest coal producer in the world, with coal accounting for 64% of SA’s energy supply. Electricity generation takes up 61% of the total coal combustion. About 93% of SA’s electricity is produced from coal-fired power plants (Dabrowski et al., 2008). South African coal Hg content ranges from 0.04 to 0.25 ppm. This extensive use of coal in electricity generation means large amounts of mercury are released annually into South African water and the atmosphere.

The work presented in this chapter has been accepted for publication in the journal, *Water SA*; 2013, **In Press.**

The detection of these heavy metals in water resources, therefore, remains a challenge. In this work we report on a naphthyl azo dye-modified dibenzo-18-crown-6 ether as a potential fluorescent probe for the selective detection of mercury (II) in water. Samples were collected near a South African coal-fired power station where mercury is likely to be released in large quantities from the burning of coal for power generation.

4.12 EXPERIMENTAL

The synthetic procedures and characterisation techniques used are as described in Chapter **3,** along with the procedure for the fluorometric detection of heavy metals.

4.13 RESULTS AND DISCUSSION

4.13.1 Synthesis

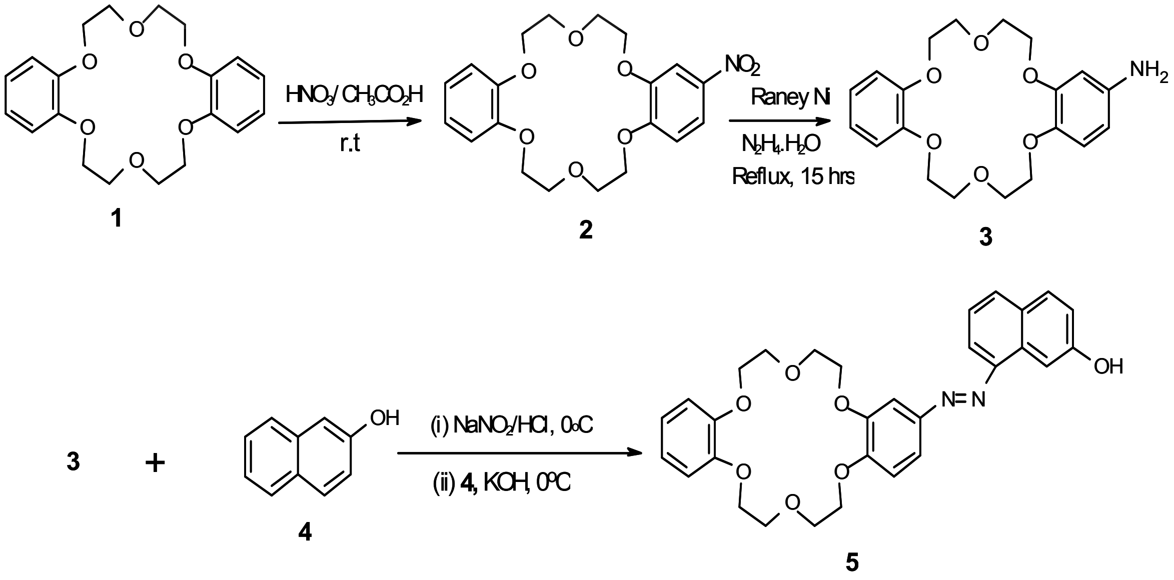

Scheme 4C.1: Synthetic pathway to crown ether 5

4.13.2 FT-IR characterisation

The FT-IR spectra of the starting material, DB18C6, the intermediates and that of the sensor molecule, azo dye DB18C6 are shown in **Figure 4C.1.** The stretching frequencies for the starting material were as follows: v (cm^{-1}): 3 065 (CH stretch); 1 595 (C-N stretch); 1 254 (Ar-O stretch); 1 227 (C-O-C stretch). For the final product the stretching frequencies were as follows: v (cm^{-1}): 3 265 (OH stretch); 3 053 (CH stretch); 1 629 (C=C stretch); 1 600 (N-H bending); 1 275 (Ar-O stretch); 1 241 (C-O-C stretch). The obvious appearance of the OH stretch at 3 265 cm^{-1} and the similarities of the other parts of the spectrum gave a clear indication that the product formed was the azo dye-modified DB18C6 sensor molecule.

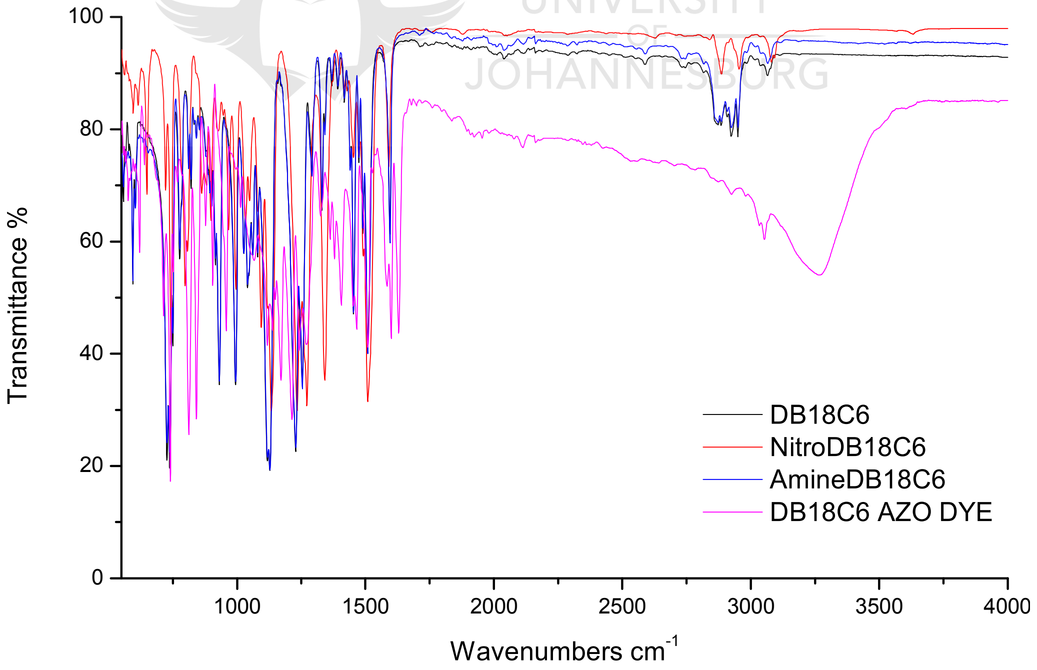

Figure 4C.1: FT-IR spectra of DB18C6, the intermediates and DB18C6 azo dye sensor molecule

4.13.3 NMR characterisation

The ^{1}H-NMR spectrum of the starting DB18C6 had the following chemical shifts: δ (ppm) 7.85 (1H, dd, 5'-H); 7.64 (1H, d, 3'-H); 6.81 (5H, s, 6'-, 3''- , 4''-, 5''-, and 6''-H); 4.05 – 4.37 (8H, m, 4α-OCH$_2$) 3.67 – 4.07 (8H, m, 4β-OCH$_2$). The ^{1}H-NMR spectrum for the synthesised sensor molecule is shown in **Figure 4C.3.**

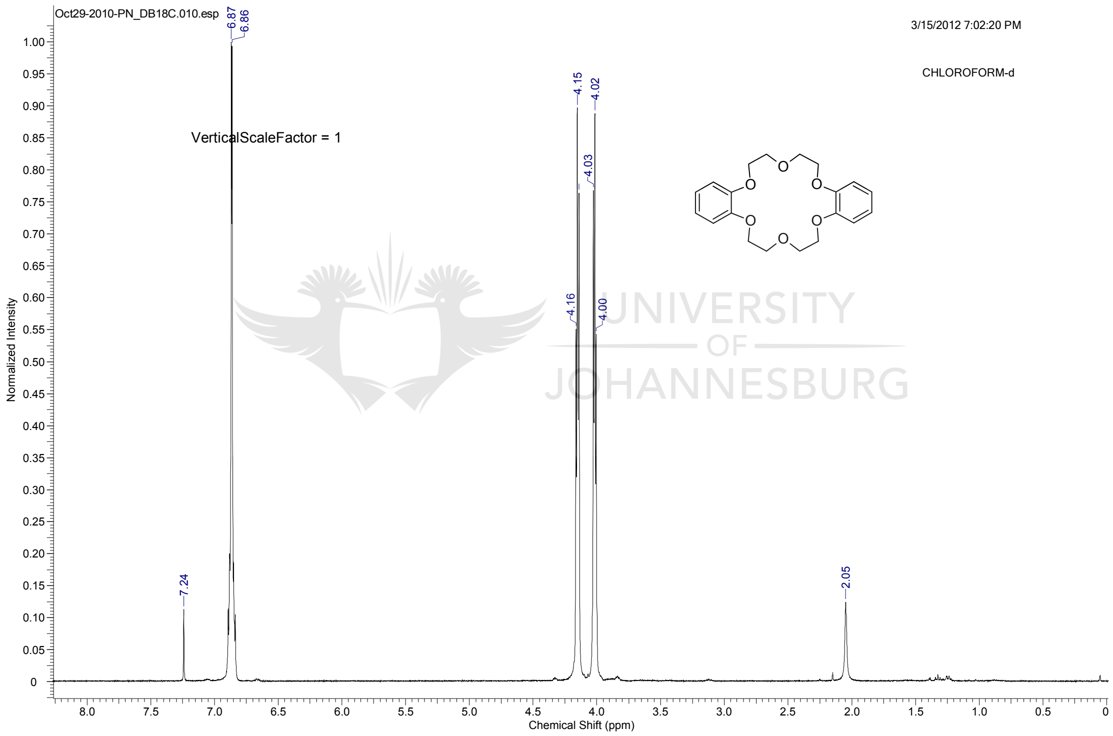

Figure 4C.2: ^{1}H-NMR spectrum of unmodified DB18C6 (solvent: CDCl$_3$).

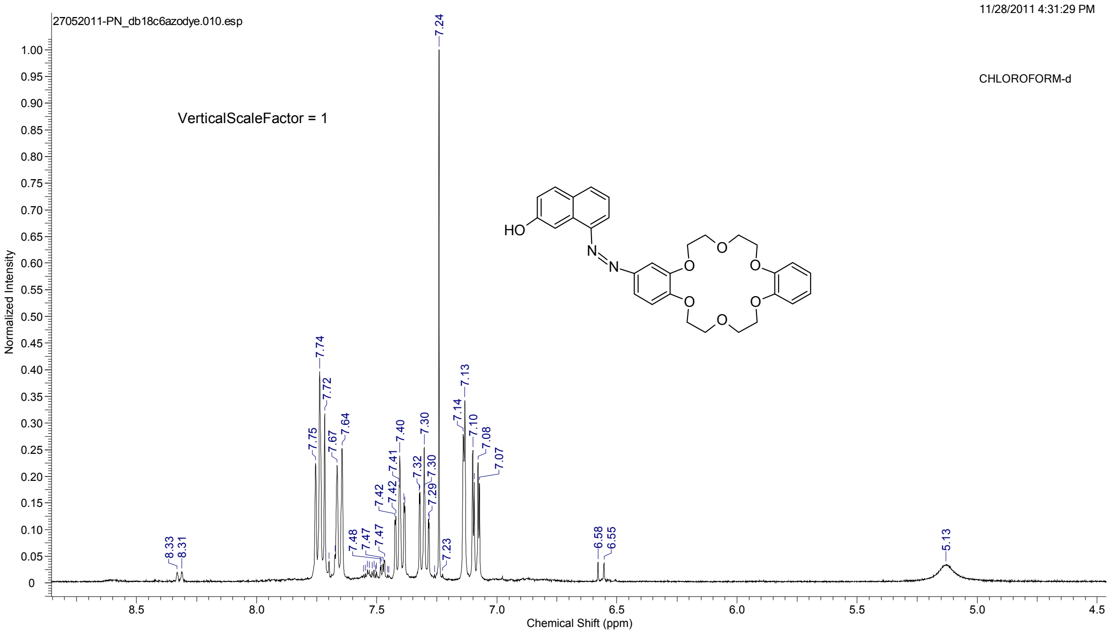

Figure 4C.3: ^{1}H-NMR spectrum of the sensor molecule; azo dye-modified DB18C6 (solvent: $CDCl_3$).

Upon modification to the sensor molecule, the spectrum obtained clearly showed the additional aromatic peaks as shown in **Figure 4C.3**. The ^{13}C-NMR showed the following shifts: δ (ppm): 144.84; 133.65; 132.40; 129.80; 129.32; 128.49; 128.07; 127.69; 127.50; 126.99; 126.59; 123.58; 121.30; 119.51; 118.33; 113.97; 68.10; 70.50. The aromatic peaks are from 113 to 144 (**Figure 4C.4**) while the methylene carbon peak in the crown ring appear at 68.10 and 70.50. The several aromatic peaks were consisted with the suggested structure of the sensor molecule.

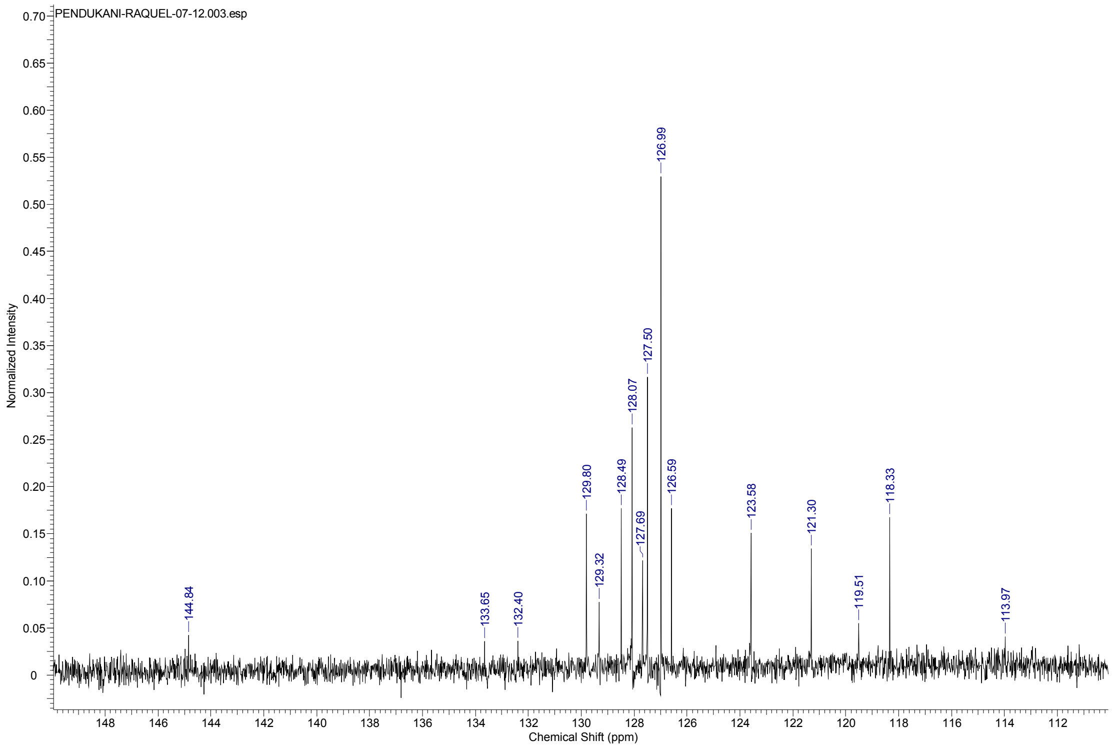

Figure 4C.4: ^{13}C-NMR spectrum of the dye sensor molecule (solvent: $CDCl_3$)

4.13.4 Mass spectrometric characterisation

Electrospray ionisation – mass spectrometry (ESI-MS) was another technique used to characterise the synthesised sensor material. The spectrum is shown in **Figure 4C.5**.

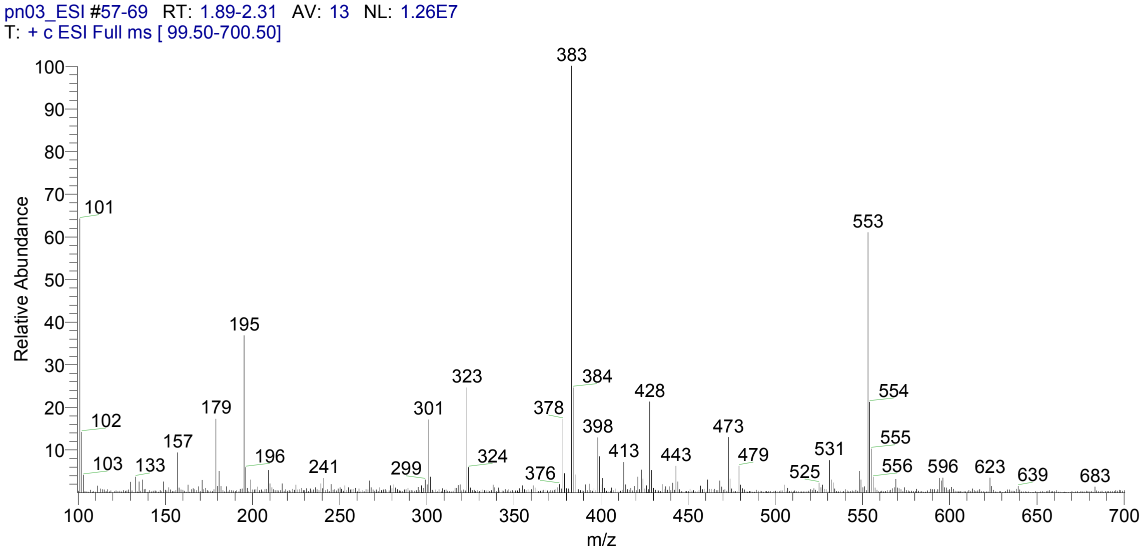

Figure 4C.5: ESI-mass spectrum of the sensor molecule, azo dye-modified DB18C6

The calculated molecular mass of the dye sensor from the proposed structure in Figure 4C.1 is 530.58 g/mol. This was confirmed from the mass spectrum of the product (**Figure 4C.5**) with the appearance of peaks at m/z = 531 corresponding to the $[M + 1]^+$ ion as well as the peak at m/z = 553 due to the $[M + Na]^+$ ion as a result of the sodium used in the electrospray ionization (ESI) mass spectrometry method used in obtaining the spectrum. The fragmentation pattern seen in the spectrum was also consistent with the proposed structure notably the peak at m/z = 383 corresponding to the fragment $[DB18C6 + Na]^+$ ion.

4.13.5 Elemental analysis characterisation

The elemental composition of the synthesised sensor molecule was carried out by CHNS elemental analysis. The calculated percentage composition from the molecular formula of the sensor molecule is; C: 67.91%; H: 5.70%; N: 5.28%. This was confirmed from the results of elemental analysis of the product which were close to the calculated values (C: 67.20%; H: 5.81%; N: 5.40%).

4.14 Hg^{2+} ion recognition by fluorescence emission spectroscopy

The absorption spectrum of the dye-modified DB18C6 ether (1.0 mM) in ethanol/water (1:1) mixture is shown in **Figure 4C.6 (a)** and **Figure 4C.6 (b)** shows the fluorescence emission spectrum of the dye.

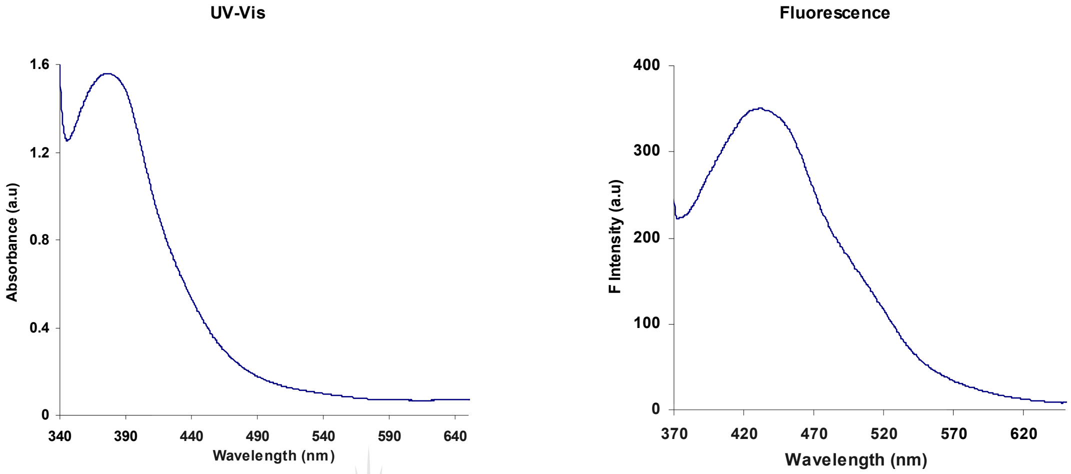

Figure 4C.6 (a) UV-Vis spectrum (1:1 MeOH/H_2O); and (b) fluorescence spectrum (λ_{exc} = 355 nm) of the dye-modified DB18C6

The dye had a maximum absorbance at 380 nm and a fluorescence emission maximum at 432 nm. The absorption spectrum of the DB18C6-dye was not changed by the addition of metal ions. The sensing of metals ions by the dye was therefore studied by fluorescence spectroscopy.

The emission spectra of the DB18C6-dye in the absence and presence of 14 different metal ions (Ag^{+}, Ca^{2+}, Cu^{2+}, Hg^{2+}, K^{+}, La^{3+}, Li^{+}, Mg^{2+}, Na^{+}, Ni^{2+}, Pb^{2+}, Sr^{2+}, Zn^{2+} and Cd^{2+}) were recorded separately and are plotted on the same axes (**Figure 4C.7**). Addition of Hg^{2+} ions (1.0 mM) resulted in the greatest quenching of fluorescence of the DB18C6-dye (75%) while other metal ions resulted in only slight quenching or slight fluorescence enhancement except for Cu^{2+} (45%) and Pb^{2+} (30%) (**Figure 4C.8**). Changes resulting from all other metals were insignificant (all < 6%) compared to 75% quenching for Hg^{2+} ions. Interference in the sensing of Hg^{2+} ions could therefore only be expected from Cu^{2+} and Pb^{2+}

when using the proposed sensing probe and similar observations have been previously reported for similar types of sensing materials (Hsieh et al., 2009; Hu et al., 2010). It is therefore important to ensure that levels of Cu^{2+} and Pb^{2+} are low in a water sample when applying this sensing method.

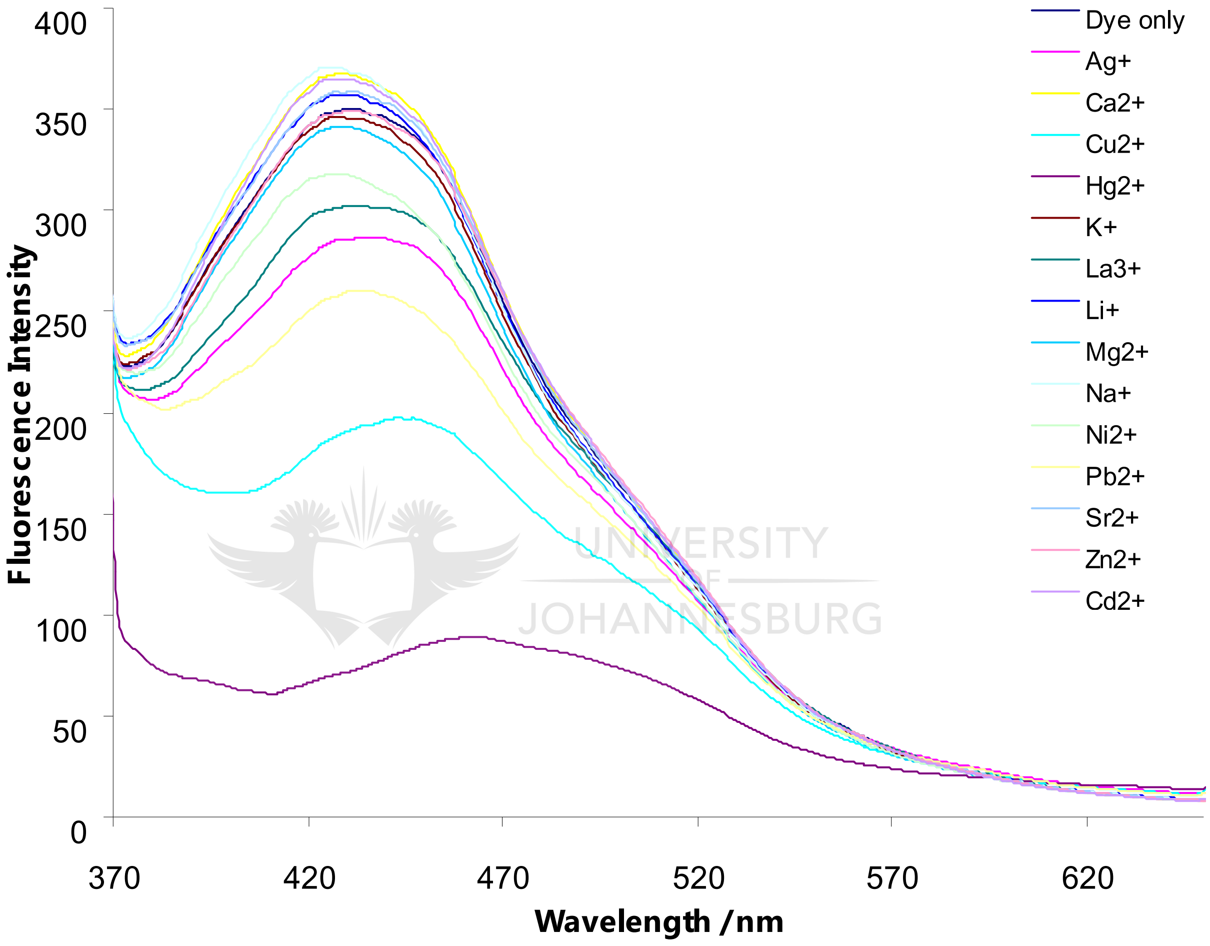

Figure 4C.7: Effect of adding various metal ions (M^{n+}) on fluorescence of DB18C6 azo dye. [M^{n+}] = 1.0 mM; [DB18C6 dye] = 10^{-4} M.

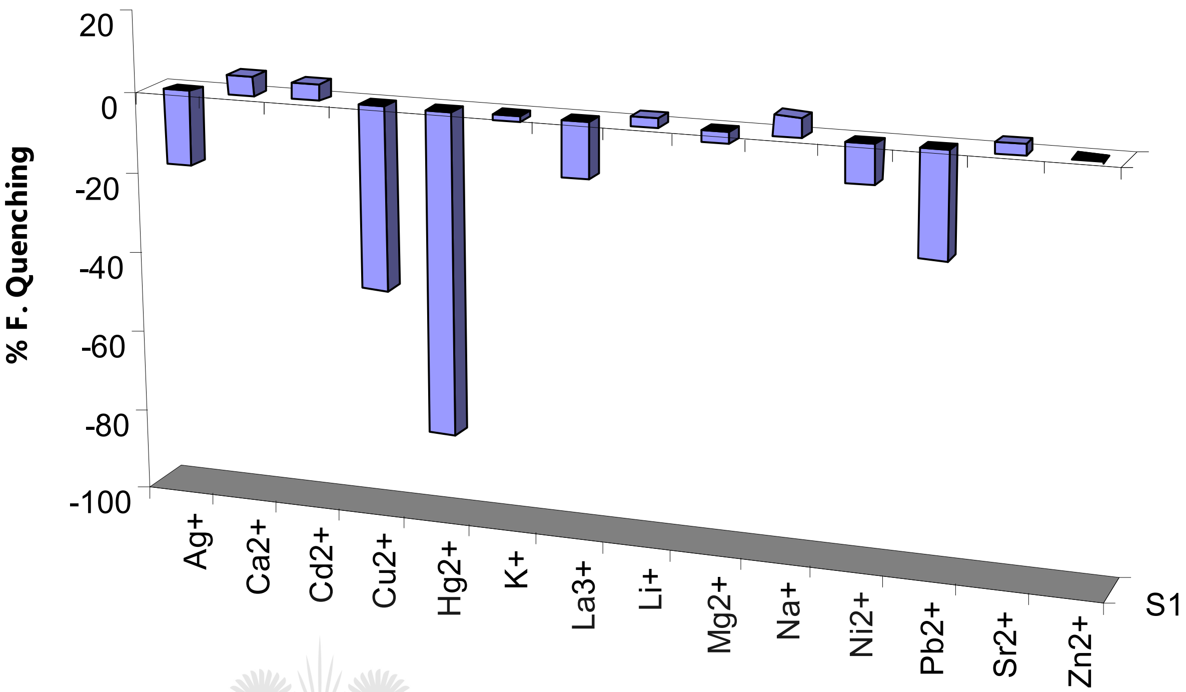

Figure 4C.8: Percentage fluorescence quenching of DB18C6 azo dye due to addition of various metal ions

In **Figure 4C.7** it can be seen that in the presence of Hg^{2+} ion, in addition to fluorescence quenching, there was also a red shift of 29 nm from 432 nm in the absence of Hg^{2+} to 461 nm after 1.0 mM Hg^{2+} was added. This shift can be attributed to the effective change in the conjugation of the crown ether as a result of its complexation with the Hg^{2+} ion (Yari and Papi, 2009). The shift suggests that the interaction between Hg^{2+} and the dye involves the transfer of electrons between the excited naphthyl fluorophore and the metal ion-crown ether complex (Hsieh et al., 2009). For all the other metal ions only insignificant shifts ($\pm$ 3 nm) were observed except for Cu^{2+} which resulted in 15 nm red shift (see **Figure 4C.7**) confirming significant complexation of Cu^{2+} with the probe and therefore possible interference.

4.14.1 Titration experiments

To have further insight into the interaction of the dye with the metal ions, titration experiments were carried out. Hg^{2+} and Cu^{2+} were selected as they gave the highest fluorescence quenching.

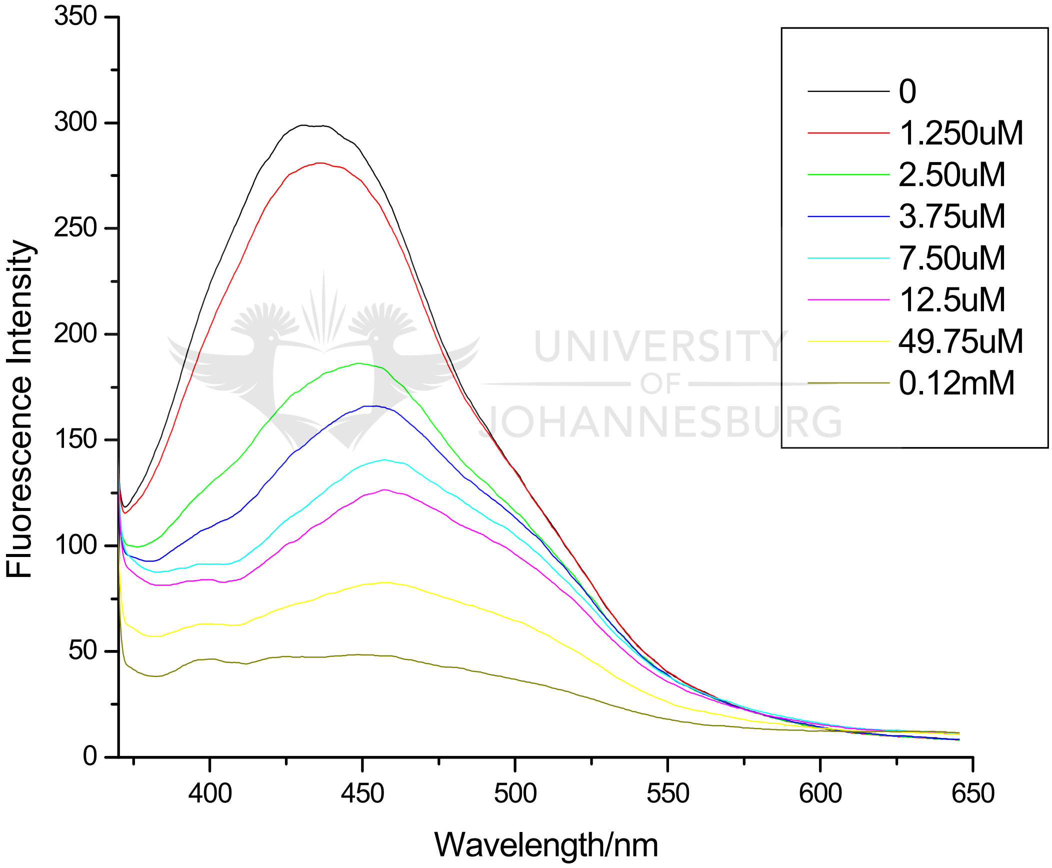

Figure 4C.9: Hg^{2+} titration (λ_{exc} = 355 nm; [Hg^{2+}] = 1.25 μM to 0.12 mM)

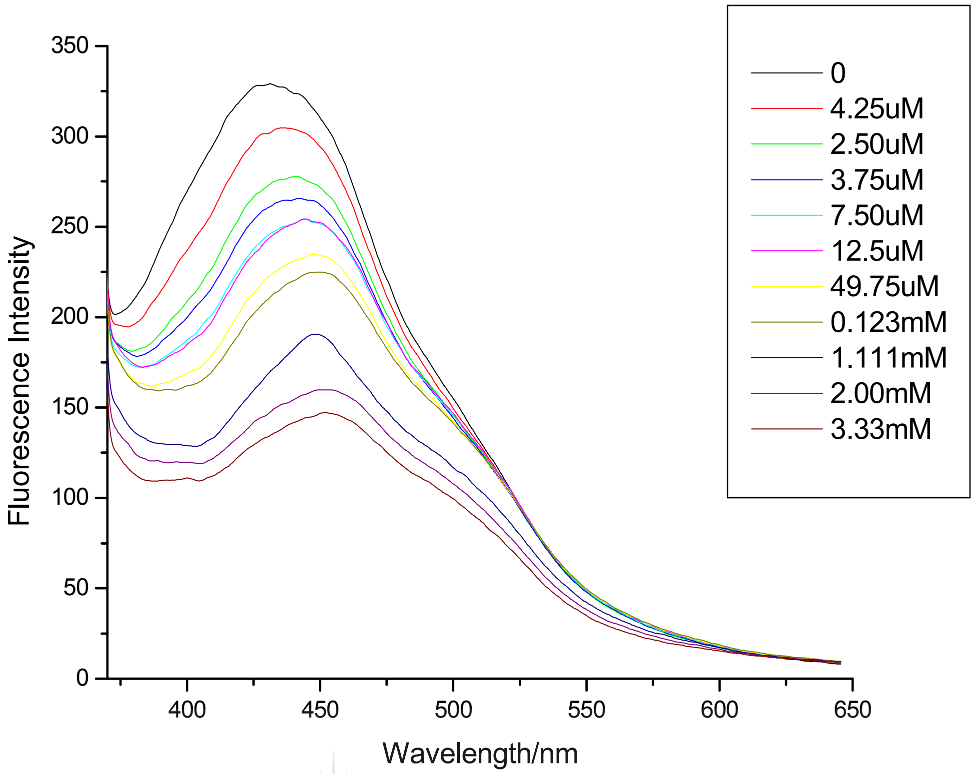

Figure 4C.10: Cu^{2+} titration (λ_{exc} = 355 nm; [Cu^{2+}] = 4.25 μM to 3.3 mM)

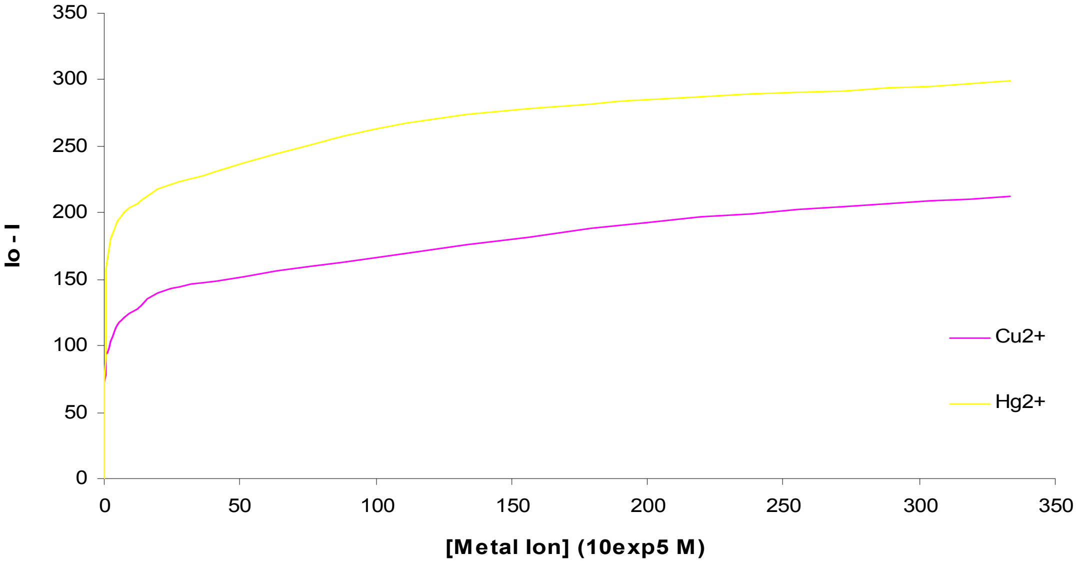

Figure 4C.11: Fluorescence change ($I_o - I$) as a function of metal-ion concentration

Figures 4C.9 and **4C.10** show the titration results for Hg^{2+} and Cu^{2+}, respectively. Increasing the concentration of Hg^{2+} resulted in an increase in the fluorescence quenching. The fluorescence is quenched to the instrument noise level (I = 40) after adding 1.2 x 10^{-4} M Hg^{2+}, while even after adding a 30-fold concentration of Cu^{2+} (3.33 x 10^{-3} M) there was only 50% fluorescence quenching. This shows great sensitivity of the dye towards Hg^{2+} ions. **Figure 4C.11** shows that for mercury a very high level of quenching is reached at very low concentrations of Hg^{2+} compared to Cu^{2+}, demonstrating greater sensitivity towards the former. The lowest detectable amount of Hg^{2+} ion was determined from the titration plots to be 1.25 x 10^{-8} M. This limit compared favourably to other similar types of sensing materials (**Table 4C.1**).

4.14.2 Determination of Binding constants

The quenching constants (K_{sv}) for the interaction of the Hg^{2+} and Cu^{2+} with the dye material were determined from Stern-Volmer plots. The constants were determined using the Stern-Volmer equation (Keizer, 1983):

$$I_o / I = K_{sv} [Q] + 1 \quad \ldots\ldots\ldots\ldots\ldots\ldots\ldots\ldots\ldots\ldots\ldots\ldots \mathbf{10}$$

where:

I_o = fluorescence intensity in absence of added quencher

I = fluorescence intensity in presence of added quencher

$[Q]$ = concentration of quencher

K_{sv} = quenching constant

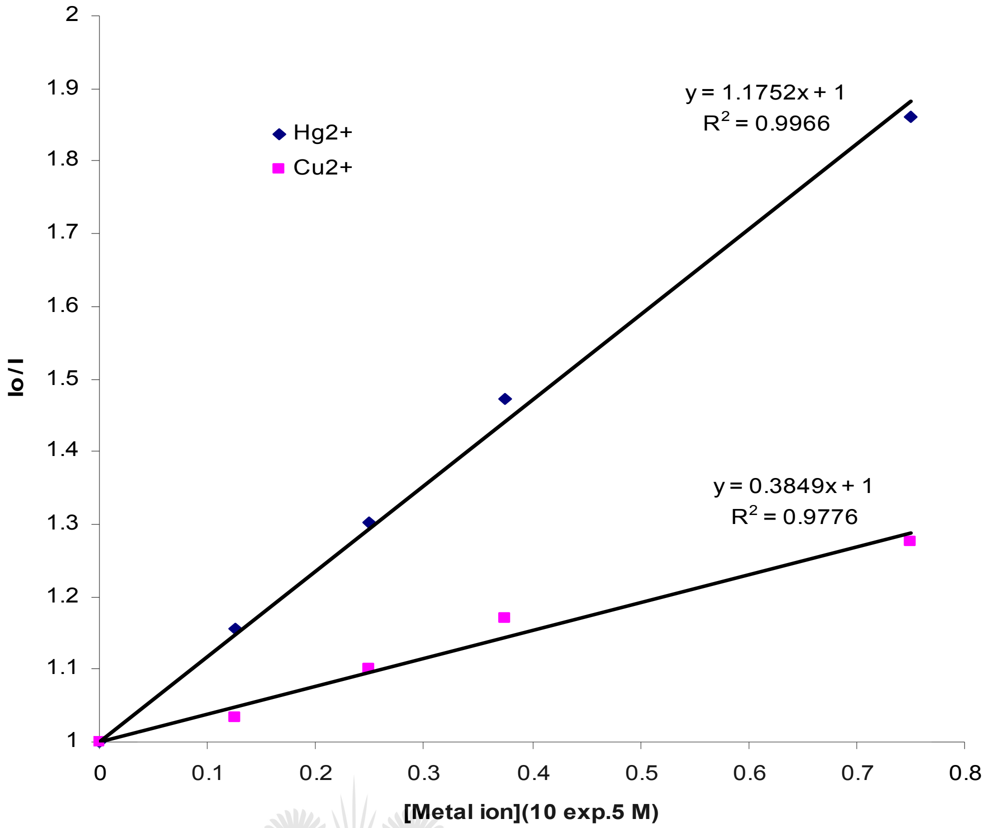

Figure 4C.12: Stern-Volmer plots

From the plot (**Figure 4C.12**) the slopes of the linear fits gave the Stern-Volmer quenching constants of 1.18 x 10^5 M^{-1} and 3.85 x 10^4 M^{-1} for Hg^{2+} and Cu^{2+}, respectively. The three-fold higher constant for Hg^{2+} suggests that a much stronger complex is formed between the Hg^{2+} ion and the crown moiety of the DB18C6 dye as compared to the Cu^{2+} complex. The binding constants are comparable to those reported elsewhere (Hsieh et al., 2009; Hu et al., 2010) confirming that indeed an Hg^{2+}.DB18C6-dye complex had been formed (**Table 4C.1**).

Table 4C.1: Comparison of proposed method of Hg (II) detection with other fluorescent methods reported in literature

Sensing material	Medium	pH	Detection limit (M)	Binding constant (M^{-1})	Major interferences	Ref.
Sugar-azo-crown ether	Methanol	nr	1.39×10^{-5}	4.0×10^{5}	Cu^{2+}	Hsieh et al., 2009
Bovine serum albumin capped gold nanoparticles	water	7.4	7.90×10^{-8}	nr	Cd^{2+}, Zn^{2+}, Cu^{2+}, Ni^{+}	Hu et al., 2010
p-Dimethylamino benzaldehyde thiosemicarbazone	Ethanol/ water	4.6	7.7×10^{-7}	7.48×10^{6}	Cu^{2+}	Yu et al., 2010
Dibenzo-18-crown-6 ether azo dye	Water	4	1.25×10^{-8}	1.0×10^{5}	Cu^{2+}	This work

Dibenzo-18-crown-6-ethers have been shown in earlier work to form complexes with Hg^{2+} ions (Williams et al., 2009). The quenching of fluorescence observed upon addition of Hg^{2+} ions can be attributed to the reverse photo-induced electron transfer (PET) mechanism involving electron donation from the excited naphthyl azo fluorophore part to the metal-ion complexed crown-ether receptor part [16], as illustrated in **Scheme 4C.2**. Before the addition of Hg^{2+} ion, excitation of the fluorophore with UV radiation (355 nm) resulted in the emission of red light (432 nm). After the metal ion had been added, the excited electron from the fluorophore was transferred to the metal bound crown-ether part which acted as an electron acceptor resulting in no fluorescence being observed (**Scheme 4C.2**). This mechanism was further supported by the fact that no change in the absorption spectra was observed meaning that the quenching could only be due to the interaction between the fluorophore in the excited state as the donor and the bound metal ion as the acceptor (Motoyoshiya et al., 2008).

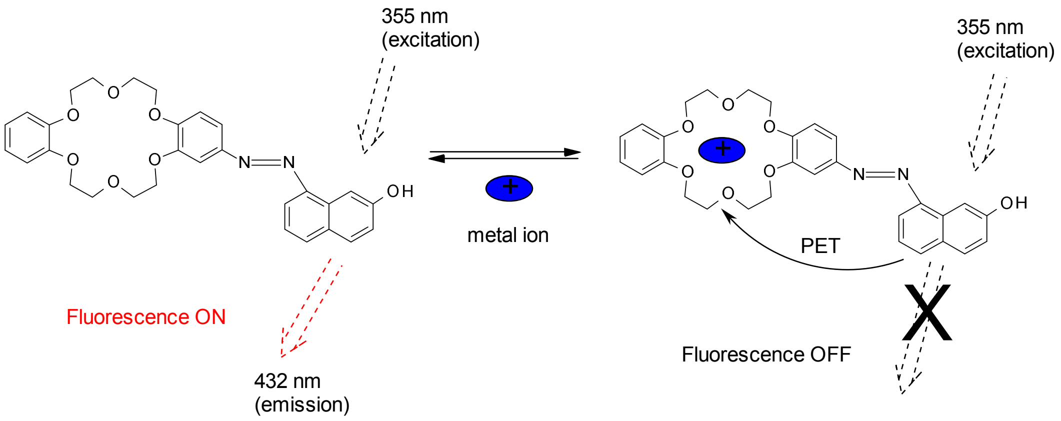

Scheme 4C.2: Proposed mechanism for fluorescence quenching

4.14.3 Interference from other metal ions

To investigate interference from other metals on the fluorescence quenching of the dye by Hg^{2+}, all metal ions were added to the dye solution except Hg^{2+}. In the absence of Hg^{2+} fluorescence quenching was only about 40% (**Figure 4C.13**) most of which could be attributed to Cu^{2+} ions. In the presence of Hg^{2+}, however, a significant quenching was observed, even in the presence of the other metals. This should provide a means for detecting Hg^{2+} in solution, based on the decrease in fluorescence even in the presence of other interfering ions.

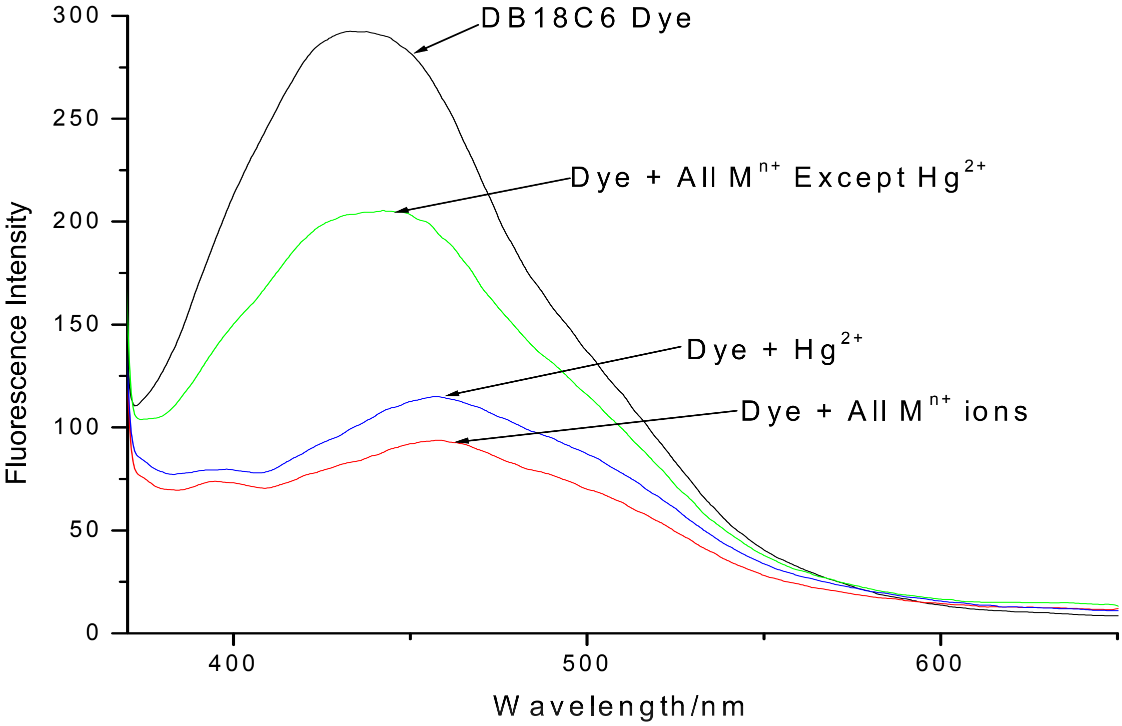

Figure 4C.13: Effect of other metals on Hg^{2+} fluorescence quenching of DB18C6 azo dye. $[Hg^{2+}] = 1 \times 10^{-4}$ M; [other metal ions] = 3.0×10^{-3} M

4.14.4 Analysis of real water sample

The proposed sensing probe was tested on an industrial water sample obtained from a power generation plant that uses coal with a high probability of mercury release into both the atmosphere and water. The physical properties and concentrations of selected metal ions in the water sample as collected are shown in Table 4C.2.

Table 4C.2: Physical and chemical properties of the water sample

Property	**Value**
pH	6.7
Conductivity (mS/cm)	0.1
Dissolved Organic Content (DOC) (mg/ ℓ^{-1})	4.82
Hg^{2+} (mol ℓ^{-1})	$1.65 \times 10^{-6} \pm 0.01$
Cu^{2+} (mol ℓ^{-1})	$6.83 \times 10^{-5} \pm 0.05$
Na^{+} (mol ℓ^{-1})	$7.50 \times 10^{-3} \pm 0.01$
K^{+} (mol ℓ^{-1})	$1.05 \times 10^{-4} \pm 0.04$
Ca^{2+} (mol ℓ^{-1})	$2.65 \times 10^{-5} \pm 0.01$
Mg^{2+} (mol ℓ^{-1})	$7.06 \times 10^{-5} \pm 0.01$
Ag^{+} (mol ℓ^{-1})	$7.22 \times 10^{-5} \pm 0.01$
Pb^{2+} (mol ℓ^{-1})	$5.35 \times 10^{-6} \pm 0.02$

Dissolved organic content was found to be 4.82 mg/ ℓ^{-1} (**Table 4C.2**) and so the water sample was first digested with concentrated HNO_3 to remove any organic species that could interfere with the fluorescence analysis. The concentration of metal ions in the water sample were so low that they would not be expected to interfere with the method since from Figure 4C.7, concentrations as high as 1.0×10^{-3} M showed no significant quenching of fluorescence of the dye sensor. Notably the concentration of Cu^{2+}, a likely interference, was very low (6.83×10^{-5} M) and therefore the sample was analysed with the proposed method without any further treatment. A portion of the industrial water sample was also spiked with a known amount of Hg^{2+} along with two tap water samples. The concentration of Hg^{2+} in the four water samples was determined from a calibration curve, plotting quenching efficiency, $(I_o - I) / I_o$ vs. $[Hg^{2+}]$ (Hu et al., 2010). The results obtained were confirmed by inductively coupled plasma optical emission spectrometry (ICP-OES) (**Table 4C.3**).

Table 4C.3: Determination of Hg^{2+} in real water samples

Water sample	Spike level (10^6 M)	[Hg^{2+}] (10^6 M) by proposed method	[Hg^{2+}] (10^6 M) by ICP-OES
Un-spiked tap water	-	-	-
Tap water A	2.0	1.95 ± 0.03	2.03 ± 0.02
Tap water B	5.0	4.89 ± 0.05	5.00 ± 0.03
Industrial water	-	1.64 ± 0.05	1.65 ± 0.01
Industrial water	2.0	3.64 ± 0.03	3.65 ± 0.02

The concentration of mercury (II) in the industrial sample was found to be 1.64 x 10^{-6} M (0.33 mg/ℓ) and this was confirmed by ICP-OES. Furthermore the determination of spiked water samples produced results which were in agreement with the well-established ICP method (**Table 4C.2**).

4.15 CONCLUSION

A simple sensor molecule was synthesised, characterised and used for the fluorescent detection of Hg^{2+} ions. Its applicability in actual samples showed that the molecule can be used for the detection of Hg^{2+} as a simple measure for determining water quality. The results reported in this chapter show the photo-induced electron transfer (PET) resulting from the complexation of Hg^{2+} with a crown moiety of a crown-ether modified azo dye. The dye can be used as a probe for selective mercury (II) ion detection in water samples. The dye is easily prepared, shows a low detection limit, is sensitive and has a rapid response time. No interference effects of other metal ions commonly found in water were observed in the response of the dye to mercury (II) ions. The dye was successfully used to detect Hg^{2+} ions in an industrial water sample and to determine the amount of mercury in the samples. The probe dye material can be attached or mixed with other materials for incorporation into sensing devices and its response to Hg^{2+} ions in these materials is currently being investigated.

4.16 REFERENCES

Dabrowski, J.M., Ashton, P.J., Murray, K., Leaner, J.J. and Mason, R.P. (2008). Anthropogenic mercury emissions in South Africa: Coal combustion in power plants. *Atm.Chem.* **42**(27), 6620-6626.

Fujiki, M. and Tajima, S. (1992). The pollution of Minamata Bay by mercury. *Water Sci. & Technol.* **25**(11), 133-140.

He, C., Zhu, W., Xu, Y., and Qian, X. (2009). Trace mercury (II) detection and separation in serum and water samples using a reusable bifunctional fluorescent sensor. *Anal. Chim. Acta* **651**, 227-233.

Hsieh, Y-C., Chir, J-L., Wu, H-H., Chang, P-S. and Wu, A-T. (2009). A sugar-aza-crown ether-based fluorescent sensor for Hg^{2+} and Cu^{2+}. *Carbohydr. Res.* **344**, 2236-2239.

Hu, D., Sheng, Z., Gong, P., Zhang, P. and Cai, L. (2010). Highly selective fluorescent sensors for Hg^{2+} based on bovine serum albumin-capped gold nanoclusters. *Analyst* **135**, 1411-1416.

Keizer, J. (1983). Nonlinear fluorescence quenching and the origin of positive curvature in Stern-Volmer plots. *J. Am. Chem. Soc.* **105**, 1494-1498.

Kudo, A., Fujikawa, Y., Miyahara, S., Zheng, J., Takigami, H., Sugahara, M. and Muramatsu, T. (1998). Lessons from Minamata mercury pollution, Japan - after a continuous 22 years of observation. *Water Sci. & Technol.* **38**(7), 187-193.

Martinis, E.M., Bertón, P., Olsina, R.A., Altamirano, J.C. and Wuilloud, R.G., (2009). Trace mercury determination in drinking and natural water samples by room temperature ionic liquid based-preconcentration and flow injection-cold vapor atomic absorption spectrometry. *J. Hazard. Mater.* **167**, 475-481.

Motoyoshiya, J., Fengqiang, Z., Nishii, Y. and Aoyama, H., (2008). Fluorescence quenching of versatile fluorescent probes on strongly electron-donating distyrylbenzenes responsive to aromatic chlorinated and nitro compounds, boronic and Ca^{2+}. *Spectrochim. Acta: A*. **69**, 167-173.

Pacyna, E.G., Pacyna, J.M., Steenhuisen, F. and Wilson, S. (2006). Global anthropogenic mercury emission inventory for 2000. *Atmospheric Environment* **40**, 4048-4063

Williams, N. J., Hancock, R. D., Riebenspies, J.H., Fernandes, M. and de Sousa, A.S. (2009). Complexation of mercury (I) and mercury (II) by 18-crown-6: Hydrothermal synthesis of the mercuric nitrite complex. *Inorg. Chem.* **48**(24), 11724-11733.

Yari, A. and Papi, F. (2009). Highly selective sensing of mercury (II) by development and characterization of a PVC-based optical sensor. *Sensors and Actuators B: Chem.* **138**, 467-473.

Yu, Y., Lin, L-H., Yang, K-B., Zhong, X., Huang, R-B. and Zheng, L-S. (2006). *p*-Dimethylaminobenzaldehyde thiosemicarbazone: A simple novel selective and sensitive fluorescent sensor for mercury (II) in aqueous solution. *Talanta* **69**(1), 103-106.

CHAPTER 5

CONCLUSIONS AND RECOMMENDATIONS

5.1 Conclusions

The aim of the research work presented in this thesis was to design, synthesise, characterise and test fluorescent-based molecular sensors for the detection of organic and inorganic pollutants in water. This was achieved by the successful synthesis of two sets of molecular sensors; one for the detection of chlorinated organic compounds in water and the other for the detection of Hg^{2+} as a typical heavy-metal pollutant in water.

- Synthesis and characterisation of a novel ethylene glycol linked azo dye-modified β-CD sensor molecule.

- The detection of chlorophenols in water using the synthesised sensor.

- The synthesised sensor showed greater sensitivity and selectivity and had superior interaction (measured by binding constants) with chlorophenols compared to unmodified β-CD and other fluorophore-modified β-CD.

- Synthesis and characterisation of a novel epichlorohydrin-linked azo dye-modified β-CD sensor consisting of 67% to 72% β-CD.

- Thermodynamic measurements by ITC showed that the host-guest chemistry of β-CD was not altered by modification and polymerisation processes.

- The detection of chloroform in water using the synthesised sensor, showing great selectivity and sensitivity as well as applicability to real water samples.

- Synthesis and characterisation of azo dye-modified crown ether.

- The detection of Hg^{2+} in water by the synthesised sensor.

- Applicability of the sensor molecule to detect Hg^{2+} in real water samples was demonstrated.

The use of an optical method such as fluorescence in the detection of non-optical analytes was demonstrated in this research work. Optical methods are advantageous in that light is easily available, meaning that these sensor molecules can easily be incorporated into simple gadgets that can be carried around and used for real-time monitoring of water pollution in remote communities. Also the disappearance of fluorescence as a signal indicating the presence of a pollutant is an easily observable change that can be understood by everyone regardless of their literacy level. This means that these molecular sensors can be vital in ensuring that small communities receive clean and safe water in line with the IWRM and the UN Millennium Development Goals (MDGs).

5.2 Recommendations

The work carried out as part of this project stimulated interest in further research that can be done as an extension to the current work. The following are some of the areas that can be explored in line with or as an extension of this work:

- The use of inorganic signalling units such as nanoparticles (NPs) in place of organic dyes.

Metal NPs such as silver and gold exhibit what is known as surface plasmon resonance (SPR) which is the collective oscillation of the conducting electrons when their frequency matches that of the incident electromagnetic radiation (Vilela et al. 2012). As a result of this phenomenon strong absorption bands or increased scattering intensity of the radiation occurs at certain wavelengths. SPR is related to the NP size, shape, composition, interparticle distance and the refractive index of the medium (Vilela et al. 2012). The shorter the distance between particles, the stronger the overlap between the plasmon fields causing a red shift in the SPR bands with an increased intensity and an observable colour change. This is the basis of metal NP-based colorimetric sensors.

So the extension of the work reported in this thesis can be the replacement of the azo dye with metal nanoparticles whose extinction coefficients are several orders of magnitude higher than those of organic chromophores. Examples of such NP based sensors include unmodified nanoparticles (Wang et al., 2010, Ravindran et al., 2012) as well as functionalized nanoparticles (Yao et al., 2010; Zhou et al. 2011) for the colorimetric detection of various metal ions.

- The synthesised molecular sensors can be cast into films and their sensing abilities tested.

- The use of different host units can be explored. For example, α- and γ- CDs as well as different sized crown ethers can be used.

References

1. Ravindran, A., M. Elavarasi, et al. (2012). "Selective colorimetric detection of nanomolar Cr (VI) in aqueous solutions using unmodified silver nanoparticles." *Sensors and Actuators B: Chem.*, **166–167**, 365-371.

2. Vilela, D., M. C. González, et al. (2012). "Sensing colorimetric approaches based on gold and silver nanoparticles aggregation: Chemical creativity behind the assay. A review. *Anal. Chim. Acta* **751**, 24-43.

3. Yao, Y., D. Tian, et al. (2010). "Cooperative Binding of Bifunctionalized and Click-Synthesized Silver Nanoparticles for Colorimetric Co2+ Sensing." *ACS App. Mat. & Interf.,* **2**(3): 684-690.

4. Zhou, Y., H. Zhao, et al. (2012). "Colorimetric detection of Mn^{2+} using silver nanoparticles cofunctionalized with 4-mercaptobenzoic acid and melamine as a probe." *Talanta*, **97**(0): 331-335.

APPENDIX 1

Table A2.1 Guideline values for chemicals that are of health significance in drinking-water

Chemical	Guideline value (mg/ℓ)	Remarks
Acrylamide	0.0005b	
Alachlor	0.02b	
Antimony	0.02	
Arsenic	0.01 (P)	
Atrazine	0.002	
Barium	0.7	
Benzene	0.01b	
Benzo[*a*]pyrene	0.0007b	
Boron	0.5 (T)	
Bromate	0.01b (A, T)	
Bromodichloromethane	0.06b	
Bromoform	0.1	
Cadmium	0.003	
Carbofuran	0.007	
Carbon tetrachloride	0.004	
Chlorate	0.7 (D)	
Chlordane	0.0002	
Chlorite	0.7 (D)	
Chloroform	0.3	
Chlorotoluron	0.03	
Chlorpyrifos	0.03	
Chromium	0.05 (P)	For total chromium;
Copper	2	staining of laundry and sanitary ware may occur below guideline value
Cyanazine	0.0006	
Cyanide	0.07	
Cyanogen chloride	0.07	For cyanide as total
Dibromoacetonitrile	0.07	
Dibromochloromethane	0.1	
1,2-Dibromo-3-chloropropane	0.001b	
1,2-Dibromoethane	0.0004b (P)	
Dichloroacetate	0.05b (T, D)	
Dichloroacetonitrile	0.02 (P)	
Dichlorobenzene, 1,2-	1 (C)	
Dichlorobenzene, 1,4-	0.3 (C)	
Dichloroethane, 1,2-	0.03b	
Dichloroethene, 1,2-	0.05	

Dichloromethane	0.02	
1,2-Dichloropropane (1,2-DCP)	0.04 (P)	
1,3-Dichloropropene	0.02b	
Dichlorprop	0.1	
Dimethoate	0.006	
Dioxane, 1,4-	0.05b	
Hexachlorobutadiene	0.0006	
Isoproturon	0.009	
Lead	0.01	
Lindane	0.002	
Manganese	0.4 (C)	
MCPA	0.002	
Mecoprop	0.01	
Mercury	0.006	For inorganic mercury
Methoxychlor	0.02	
Metolachlor	0.01	
Molybdenum	0.07	
Monochloramine	3	
Monochloroacetate	0.02	
Nickel	0.07	
N-Nitrosodimethylamine (NDMA)	0.1	
Pendimethalin	0.02	
Pentachlorophenol	0.009b (P)	
Selenium	0.01	

Table A2.2: EPA Guideline values for selected inorganic contaminants in water

Inorganic Chemicals

Contaminant	MCLG[1] (mg/L)[2]	MCL or TT[1] (mg/L)[2]	Potential health effects from long-term exposure above the MCL (unless specified as short-term)	Sources of contaminant in drinking water
Antimony	0.006	0.006	Increase in blood cholesterol; decrease in blood sugar	Discharge from petroleum refineries; fire retardants; ceramics; electronics solder
Arsenic	0[7]	0.010 as of 01/23/06	Skin damage or problems with circulatory systems, and may have increased risk of getting cancer	Erosion of natural deposits; runoff from orchards, runoff from glass and electronics production wastes
Asbestos (fibre >10 µm)	7 million fibres/ℓ	7 MFL	Increased risk of developing benign intestinal polyps	Decay of asbestos cement in water mains; erosion of natural deposits

Inorganic Chemicals

Contaminant	MCLG[1] (mg/L)[2]	MCL or TT[1] (mg/L)[2]	Potential health effects from long-term exposure above the MCL (unless specified as short-term)	Sources of contaminant in drinking water
Barium	2	2	Increase in blood pressure	Discharge of drilling wastes; discharge from metal refineries; erosion of natural deposits
Beryllium	0.004	0.004	Intestinal lesions	Discharge from metal refineries and coal-burning factories; discharge fro electrical, aerospace, and defence industries
Cadmium	0.005	0.005	Kidney damage	Corrosion of galvanized pipes; erosion of natural deposits; discharg from metal refineries; runoff from waste batteries and paints
Chromium (total)	0.1	0.1	Allergic dermatitis	Discharge from steel and pulp mills; erosion of natural deposits
Copper	1.3	TT[7]; Action Level=1.3	Short term exposure: Gastrointestinal distress Long term exposure: Liver or kidney damage People with Wilson's Disease should consult their personal doctor if the amount of copper in their water exceeds the action level	Corrosion of household plumbing systems; erosion of natural deposits
Cyanide (as free cyanide)	0.2	0.2	Nerve damage or thyroid problems	Discharge from steel/metal factories discharge from plastic and fertilizer factories
Fluoride	4.0	4.0	Bone disease (pain and tenderness of the bones);	Water additive which promotes stron teeth; erosion of natural deposits;

Inorganic Chemicals

Contaminant	MCLG[1] (mg/L)[2]	MCL or TT[1] (mg/L)[2]	Potential health effects from long-term exposure above the MCL (unless specified as short-term)	Sources of contaminant in drinking water
			children may get mottled teeth	discharge from fertilizer and aluminium factories
Lead	zero	TT[7]; Action Level=0.015	Infants and children: Delays in physical or mental development; children could show slight deficits in attention span and learning abilities	Corrosion of household plumbing systems; erosion of natural deposits
			Adults: Kidney problems; high blood pressure	
Mercury (inorganic)	0.002	0.002	Kidney damage	Erosion of natural deposits; discharg from refineries and factories; runoff from landfills and croplands
Selenium	0.05	0.05	Hair or fingernail loss; numbness in fingers or toes; circulatory problems	Discharge from petroleum refineries; erosion of natural deposits; discharg from mines
Thallium	0.0005	0.002	Hair loss; changes in blood; kidney, intestine, or liver problems	Leaching from ore-processing sites; discharge from electronics, glass, ar drug factories

Table A2.3: EPA Guideline values for selected chlorinated organic contaminants in water

Organic Chemicals

Contaminant	MCLG[1] (mg/L)[2]	MCL or TT[1] (mg/L)[2]	Potential health effects from long-term exposure above the MCL (unless specified as short-term)	Sources of contaminant i drinking water
Carbon tetrachloride	zero	0.005	Liver problems; increased risk of cancer	Discharge from chemical plants and other industria

Organic Chemicals

Contaminant	MCLG[1] (mg/L)[2]	MCL or TT[1] (mg/L)[2]	Potential health effects from long-term exposure above the MCL (unless specified as short-term)	Sources of contaminant i drinking water
				activities
Chlorobenzene	0.1	0.1	Liver or kidney problems	Discharge from chemical and agricultural chemical factories
1,2-Dibromo-3-chloropropane (DBCP)	zero	0.0002	Reproductive difficulties; increased risk of cancer	Runoff/leaching from soil fumigant used on soybeans, cotton, pineapples, and orchards
o-Dichlorobenzene	0.6	0.6	Liver, kidney, or circulatory system problems	Discharge from industrial chemical factories
p-Dichlorobenzene	0.075	0.075	Anaemia; liver, kidney or spleen damage; changes in blood	Discharge from industrial chemical factories
1,2-Dichloroethane	zero	0.005	Increased risk of cancer	Discharge from industrial chemical factories
1,1-Dichloroethylene	0.007	0.007	Liver problems	Discharge from industrial chemical factories
cis-1,2-Dichloroethylene	0.07	0.07	Liver problems	Discharge from industrial chemical factories
trans-1,2-Dichloroethylene	0.1	0.1	Liver problems	Discharge from industrial chemical factories
Dichloromethane	zero	0.005	Liver problems; increased risk of cancer	Discharge from drug and chemical factories
1,2-Dichloropropane	zero	0.005	Increased risk of cancer	Discharge from industrial chemical factories
Hexachlorobenzene	zero	0.001	Liver or kidney problems; reproductive difficulties; increased risk of cancer	Discharge from metal refineries and agricultura chemical factories
Hexachlorocyclopentadiene	0.05	0.05	Kidney or stomach problems	Discharge from chemical factories

Organic Chemicals

Contaminant	MCLG[1] (mg/L)[2]	MCL or TT[1] (mg/L)[2]	Potential health effects from long-term exposure above the MCL (unless specified as short-term)	Sources of contaminant i drinking water
Methoxychlor	0.04	0.04	Reproductive difficulties	Runoff/leaching from insecticide used on fruits, vegetables, alfalfa, livestock
Polychlorinated biphenyls (PCBs)	zero	0.0005	Skin changes; thymus gland problems; immune deficiencies; reproductive or nervous system difficulties; increased risk of cancer	Runoff from landfills; discharge of waste chemicals
Pentachlorophenol	zero	0.001	Liver or kidney problems; increased cancer risk	Discharge from wood preserving factories
Tetrachloroethylene	zero	0.005	Liver problems; increased risk of cancer	Discharge from factories and dry cleaners
1,2,4-Trichlorobenzene	0.07	0.07	Changes in adrenal glands	Discharge from textile finishing factories
1,1,1-Trichloroethane	0.20	0.2	Liver, nervous system, or circulatory problems	Discharge from metal degreasing sites and othe factories
1,1,2-Trichloroethane	0.003	0.005	Liver, kidney, or immune system problems	Discharge from industrial chemical factories